ISEG2026

International Symposium on Epitaxial Graphene

21.09.-24.09.2026 in Chemnitz/Germany

Funded by
DFG Deutsche Forschungsgemeinschaft
German Research Foundation

DFG FOR 5242

Map

Schedule

Monday		Tuesday		Wednesday		Thursday	
Time	Event	Time	Event	Time	Event	Time	Event
9:00	Badge Pickup	9:00	**Norimatsu**	9:00	**Erhardt**	9:00	**Tegenkamp**
		9:40	Lara-Avila	9:40	Tilgner	9:40	Mamiyev
		10:00	Pradeepkumar	10:00	Kumpf	10:00	Yamane
10:30	Opening	10:20	Coffee	10:20	Coffee	10:20	Coffee
10:50	**Coletti**	10:50	**Benedek**	10:50	**Chae**	10:50	**Göhler**
11:30	Küster	11:30	Federl	11:30	Bothe	11:30	Datta
11:50	Rejhon	11:50	Kuzel	11:50	Fan	11:50	Schädlich
12:10	Yin	12:10	Gradl	12:10	Wang	12:10	Closing
12:30	Lunch	12:30	Lunch	12:30	Lunch	12:30	Lunch
14:00	**Bampoulis**	14:00	**Chagas**	14:00	**Kolmer**	14:00	
14:40	Matta	14:40	Forti	14:40	Dedkov		
15:00	Reddy	15:00	Höllmann	15:00	Pham		
15:20	Coffee	15:20	Coffee	15:20	Coffee		Ecxursion
15:50	**Bolotin**	15:50	**Möttönen**	15:50	**Voloshina**		
16:30	Kunc	16:30	Morzhuk	16:30	Henz		
16:50	Lüpke	16:50		16:50	Wundrack	17:00	
17:10	Meet		Poster				
	and	19:30				19:00	
21:00	Greet						Conference Dinner
						23:00	

Program

Monday, 21.09.2026, Location: Institute of Physics

9:00		Badge Pickup (Foyer)
10:30	T. Seyller	Opening
		Session Mo1 – Chair: P. Schädlich
10:50	**C. Coletti**	Graphene on SiC: Lessons Learned and Future Directions
11:30	K. Küster	Doping graphene up to and beyond the van Hove singularity by rare earth intercalation
11:50	M. Rejhon	Exploring and controlling ABC-stacked graphene domains in epitaxial graphene
12:10	H. Yin	30°-Twisted Bilayer Graphene by Hydrogen Intercalation
12:30		Lunch (Mensa)
		Session Mo2 – Chair: C. Kumpf
14:00	**P. Bampoulis**	Electric-Field Control of Topology in Germanene
14:40	B. Matta	Pb intercalation in epigraphene - Charge neutral graphene and 2D interlayer bands and spin textures
15:00	V. Reddy	Domain-resolved electronic structure of AgTe-intercalated graphene on SiC
15:20		Coffee (Foyer)
		Session Mo3 – Chair: F. Göhler
15:50	**K. Bolotin**	Turning new knobs on Hamiltonians of 2D materials
16:30	J. Kunc	Advanced Interfacial Engineering of Edge Contacted Graphene Devices
16:50	F. Lüpke	Giant orbital Zeeman effects at the interface of graphene and Fe_3GeTe_2
17:10 – 21:00		Meet and Greet (Foyer)

Tuesday, 22.09.2026, Location: Institute of Physics

		Session Tu1 – Chair: U. Starke
9:00	**W. Norimatsu**	Growth of hetero-epitaxial graphene and 2D materials on SiC
9:40	S. Lara-Avila	Delamination and transfer of wafer-scale single-crystalline monolayer graphene from SiC substrate
10:00	A. Pradeepkumar	Operando Monitoring of Epitaxial Graphene Growth using High Temperature Neutron Reflectometry
10:20		Coffee(Foyer)
		Session Tu2 – Chair: S. Gemming
10:50	**G. Benedek**	Dynamics and Electron-Phonon Coupling in Graphene Heterostructures from Helium Atom Scattering
11:30	M.-E. Federl	Ultrafast signatures of Dirac - flat-band hybrid states from time-resolved ARPES
11:50	P. Kuzel	Ultrafast dynamics of terahertz plasmons in in-plane periodic nanostructures of epitaxial graphene
12:10	J. Gradl	Influence of sulphur vacancies on ultrafast charge separation in WS_2-graphene heterostructures
12:30		Lunch (Mensa)
		Session Tu3 – Chair: S. Wolff
14:00	**T. Chagas**	Epitaxial growth of 2D Se-Ta-S Janus membranes on Au(111)
14:40	S. Forti	Surface reconstruction governs graphene epitaxy on sapphire
15:00	D. Höllmann	Controlled Partial Gallium Intercalation in Epitaxial Graphene Hall Bars - A 2D Normal-Superconductor Junction
15:20		Coffee (Foyer)
		Session Tu4 – Chair: Y. Dedkov
15:50	**M. Möttönen**	Graphene bolometers and calorimeters
16:30	B. Morzhuk	Quantitative Photocurrent Decomposition in Epitaxial Graphene 6H-SiC Photodetectors

16:50 – 19:30 Poster session (Foyer)

P01	S. Anchamkudy	Quantitative imaging of surface potential From molecules on metals towards charge density waves on 2D materials
P02	M. Gruschwitz	Towards enhanced spin-orbit coupling in epitaxial graphene via Pb intercalation
P03	J. K. Hofmann	Shear-resistant topology and electrical anisotropy in the quasi-one-dimensional van der Waals material α-Bi_4Br_4
P04	S. Inagaki	Growth of carbon nanotubes on the surface of SiC powder by controlling pressure and gas atmosphere
P05	T. Kamimura	Fabrication of graphene-Mo_2C-SiC heterostructure and its electrical states
P06	J. Koch	Functionalization of epitaxial graphene by proximity to heavy metals and TMDs
P07	K. Küster	Intercalation of graphene on SiC: tuning the electronic structure of graphene by proximity coupling and inducing novel 2D interlayer band structures
P08	W. Norimatsu	Polymer assisted sublimation graphene growth on 4-degree off SiC(0001)
P09	F. Onodera	Effect of gas flow on carbon nanotubes growth on SiC
P10	S. Sologub	Reversible transition between (10×10) and (11×11) phases of Pb intercalated EG on 6H-SiC(0001)
P11	S. Wolff	Selenium intercalation of graphene on SiC(0001)
P12	M. Yokose	Mechanism of step unbunching phenomenon on 4 degrees off-axis 4H-SiC (0001) surface
P13	Z. Zhang	Vapor-Controlled Growth of Semiconducting Epitaxial Graphene

Wednesday, 23.09.2026, Location: Institute of Physics

		Session We1 – Z. Mamijev
9:00	**J. Erhardt**	Beneath the Moiré - Decoupling Intrinsic and Graphene Induced Properties in Intercalated 2D Films
9:40	N. Tilgner	Engineering Bismuthene via Confinement Heteroepitaxy - H-Controlled Structure and Spin Texture
10:00	C. Kumpf	Solving the Phase Problem of Diffraction - X-Ray Standing Waves Imaging on Bismuthene on SiC(0001)
10:20		Coffee (Foyer)
		Session We2 – Chair: C. Tegenkamp
10:50	**D.-H. Chae**	Epitaxial Graphene Devices for Quantum Electrical Metrology
11:30	M. Bothe	Magneto-Transport Investigation of PASG-grown Graphene van der Waals Heterostructures
11:50	X. Fan	High-precision quantum resistance metrology based on epitaxial graphene and all-graphene-based multi-parameter quantum metrology devices
12:10	H. Wang	Pronounced scale-dependent charge carrier density in graphene quantum Hall devices
12:30		Lunch (Mensa)
		Session We3 – Chair: K. Küster
14:00	**M. Kolmer**	Understanding local electronic properties in epitaxial graphene heterostructures by scanning tunneling microscopy and spectroscopy
14:40	Y. Dedkov	Electronic properties of epitaxial graphene-Mn_5Ge_3-Ge interfaces
15:00	V. D. Pham	Reconstruction of 2D silver at the interface between graphene and SiC
15:20		Coffee (Foyer)
		Session We4 – Chair: B. Matta
15:50	**E. Voloshina**	Epitaxial Graphene Interfaces - From Atomistic Understanding to Band Structure Control
16:30	J. Henz	Investigation of the Heterogeneity and Temperature Dependence of Bilayer Gallium Intercalated at the Epitaxial Graphene/Silicon Carbide Interface with Cryogenic Spectroscopic Imaging Ellipsometry
16:50	S. Wundrack	Metals under confinement- Unlocking room temperature intercalation of indium in epitaxial graphene

Thursday, 24.09.2026. Location: eniProd-Building (C16)

		Session Th1 – Chair: F. Lüpke
9:00	**C. Tegenkamp**	The CISS effect: spin transport phenomena through chiral molecules proximitized to surfaces
9:40	Z. Mamiyev	Raman Spectroscopy of Intercalated Epitaxial Graphene on SiC(0001)
10:00	A. Yamane	Strain introduction into graphene and its electronic states via Pd intercalation
10:20		Coffee (Foyer)
		Session Th2 – Chair: W. Norimatsu
10:50	**F. Göhler**	Exploring the electronic structure of topology-protected surface states by advanced angle-resolved photoemission
11:30	S. Datta	Phase-controlled two-dimensional Ag intercalation at the graphene-SiC interface
11:50	P. Schädlich	Calcium intercalation of epitaxial graphene
12:10	T. Seyller	Closing
12:30		Lunch (Mensa)
14:00		Excursion (Chemnitz City, details will be provided)
19:00 – 23:00		Conference Dinner (Location: Restaurant Miramar, details will be provided)

Abstracts in chronological order

Graphene on SiC: Lessons Learned and Future Directions

C. Coletti[1]

[1] Center for Nanotechnology Innovation @NEST, Istituto Italiano di Tecnologia, Pisa, Italy

Graphene on SiC (epi-graphene) has represented the first truly scalable graphene platform explored by the scientific community, playing a pivotal role in shaping both fundamental understanding and technological perspectives of graphene-based systems. Since its early development, this material has provided key insights into the interplay between growth, interface physics, and electronic properties, many of which continue to guide current research.

In this talk, I will present a critical perspective on impactful discoveries enabled by epi-graphene and how they have shaped the broader field of graphene research. From the role of the graphene-substrate interface in guiding decoupling strategies [1], which remain central to ongoing efforts across different material platforms [2-4], to the possibility of obtaining multilayer graphene systems of interest such as rhombohedral graphene through substrate engineering [5, 6].

I will also discuss how early demonstrations of quantum Hall physics in epi-graphene [7], have contributed to establishing it as a model system for quantum transport and have inspired analogous studies in graphene on other substrates [8]. In addition, epi-graphene has proven to be a remarkable platform for the synthesis of van der Waals heterostructures with potential for applications [9].

Finally, I will highlight more recent advances, including the recognition of buffer layer graphene as an electronic material in its own right [10] and the development of novel characterization approaches, such as Raman spectroscopy combined with deep learning, enabling its rapid identification [11].

By bridging historical milestones with current developments, this talk aims to illustrate how epi-graphene continues not only to provide fundamental lessons, but also to open new directions for scalable, high-quality graphene and to inspire novel concepts and applications in the years to come.

References:

[1] C. Riedl et al., Phys. Rev. Lett. 103, 246804 (2009).
[2] N. Mishra et al., Small Methods 10, 5 (2026).
[3] Z. Gebeyehu et al., Adv. Mater. 36, 2404590 (2024).
[4] S. Forti et al., Nat. Commun. 11, 2236 (2020).
[5] C. Coletti et al., Phys. Rev. B 88, 155439 (2013).
[6] C. Bouhafs et al., Carbon 177, 282-290 (2021).
[7] J. Jobst et al., Phys. Rev. B 81, 195434 (2010).
[8] S. Pezzini et al., 2D Mater. 7, 041003 (2020).
[9] A. Rossi et al., 2D Mater. 3 031013 (2016).
[10] J. Zhao et al., Nature 625, 60–65 (2024).
[11] D. Poteryayev et al., arXiv:2601.04445 (2026).

Doping graphene up to and beyond the van Hove singularity by rare earth intercalation

K. Küster[1], P. Rosenzweig[1,2], B. Matta[1], U. Starke[1]

[1] Max-Planck-Institut für Festkörperforschung, 70569 Stuttgart, Germany
[2] Physikalisches Institut, Universität Stuttgart, 70569 Stuttgart, Germany

The intercalation of graphene on SiC(0001) is a versatile route to decouple graphene from the substrate and simultaneously tune its electronic properties. The electron doping of graphene can be steered by the intercalation of different atomic species. Theoretical work predicts correlated electron states such as charge or spin density waves and chiral superconductivity (SC) when the charge carrier concentration in graphene is high enough in the vicinity of the van Hove singularity (VHS) [1].

High electron doping can be realized by intercalation of rare earth elements like Gd [2], Yb [3,4] and Tb [5], which leads to a flat band scenario (extended VHS) exhibiting a high density of states along the $\overline{KMK'}$ direction of the Brillouin zone (BZ), as observed by angle-resolved photoelectron spectroscopy (ARPES). In the case of Yb the doping can be steered around the VHS: by diluting the amount of Yb underneath the graphene layer the VHS is moved into the unoccupied states [3], while additional adsorption of potassium on top of the graphene leads to a shift of the flat band below the Fermi level leading to a so-called overdoping of graphene [4]. Furthermore, hybridization of the graphene π^*-bands with the Yb 4f electron states leads to a strong renormalization of the band structure of graphene [3].

Intercalation of Tb leads to a doping beyond the VHS with the flat band residing 70 meV below the Fermi level (Fig 1). Based on the random phase approximation, we could show that the graphene hosts a SC state with a critical temperature in the regime of 300 to 600 mK [5]. A spectral function analysis of the π^*-bands in the Eliashberg framework indicates an electron-phonon coupling constant of ~0.49, which is below a theoretically estimated critical value of 0.56, indicative of a stable d-wave SC, in contrast to a conventional phonon-driven s-wave SC state.

Besides the strong doping phase, which does not show any additional diffraction spots in low-energy electron diffraction (LEED), we observed a new superstructure by LEED when depositing a higher amount of Tb and flash annealing to temperatures around 1200 °C. Our photoemission studies hint towards the formation of a Tb-carbide phase by reaction with the carbon atoms of the graphene layer.

References:
[1] M.L. Kiesel et al., Phys. Rev. B 86 (2012) 20507(R).
[2] S. Link et al., Phys. Rev. B 100, (2019) 121407(R).
[3] P. Rosenzweig et al., Phys. Rev. B 100 (2019) 035445.
[4] P. Rosenzweig et al., Phys. Rev. Lett. 125 (2020) 176403.
[5] S. A. Herrera et al., ACS Nano 18 (2024) 34842.

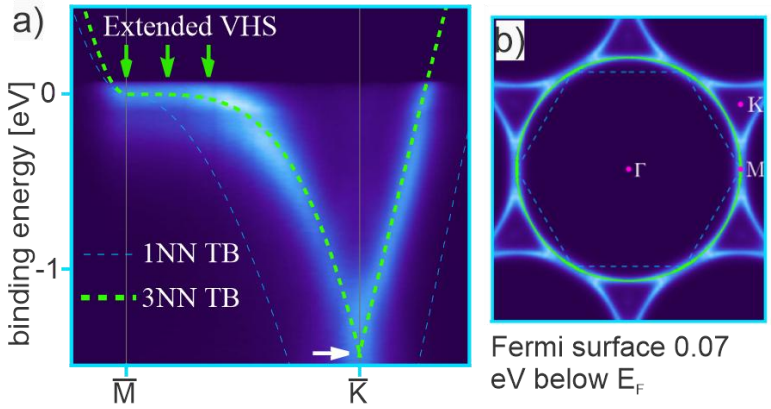

Fig. 1: Band structure of Tb intercalated graphene: (a) Extended VHS (green arrows) measured along the $\overline{MKΓ}$-direction. The Dirac point (white arrow) is at approx. −1.55 eV. The graphene band dispersion is well reproduced by the overlaid 3rd nearest neighbor tight binding (3NN TB) model (dashed green lines) while a 1st NN TB model (dashed blue lines) does not capture the experimental band structure. (b) Constant-energy surface measured at the VHS, 0.07 eV below the Fermi level; some high-symmetry points of the (1 × 1) BZ are indicated. (Adopted from Ref. [5]).

Exploring and controlling ABC-stacked graphene domains in epitaxial graphene

M. Baeva[1], M. Shestopalov[1], B. Morzhuk[1], J. Kunc[1], M. Rejhon[1]

[1] Charles University, Faculty of Mathematics and Physics, Institute of Physics

In graphene, emergent properties such as superconductivity and ferroelectricity have been observed in ABC-stacked domains, typically obtained through exfoliation followed by precise mechanical twisting and alignment with the desired orientation. This process is challenging and non-scalable.
Here, we demonstrate that ABC-stacked graphene can be obtained using a scalable growth technique, namely, the thermal decomposition of silicon carbide. Using conductive atomic force microscopy, we identified distinct conductivity patterns in untwisted trilayer epitaxial graphene on silicon carbide. These patterns revealed the presence of ABA and ABC domains, matching the conductivity differences observed in twisted exfoliated graphene and those predicted by density functional theory. The size and geometry of the stacking domains depend on the interplay between strain, solitons crossing, and the shape of the three-layer regions [1]. Furthermore, we showed that by controlling the strain of the graphene lattice, we can tune the dimension and geometry of moiré patterns (Fig. 1). This study demonstrates the potential of the thermal decomposition method for producing ABA/ABC domains, paving the way for future applications in electronic and optoelectronic devices.

References:
[1] M. Rejhon et al., Proc. Natl. Acad. Sci. U.S.A. 121 (50) e2408496121, (2024).

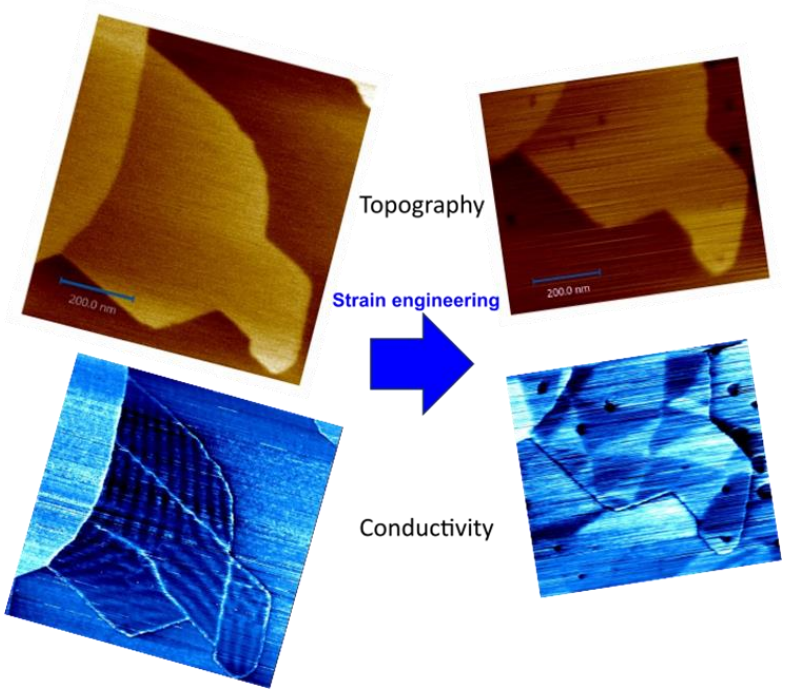

Fig. 1: Topography and local conductivity channel before and after strain engineering via hydrogen intercalation.

30°-Twisted Bilayer Graphene by Hydrogen Intercalation

H. Yin[1,2], S. Soubatch[1,2], F. S. Tautz[1,2,3], F. C. Bocquet[1,2], and C. Kumpf[1,2,3]

[1] Peter Grünberg Institute (PGI-3), Forschungszentrum Jülich, Jülich, Germany
[2] Jülich-Aachen Research Alliance (JARA), Fundamentals of Future Information Technology, Jülich, Germany
[3] Experimentalphysik IV A, RWTH Aachen University, Aachen, Germany

Quasi-free-standing twisted bilayer graphene (TBG) with a 30° twist angle is achieved on a 6H-SiC(0001) surface through hydrogen intercalation. Initially, 0°-rotated monolayer graphene is prepared on a zeroth layer graphene (ZLG) using the surfactant-mediated epitaxial growth method [1]. Then, the ZLG is physically and chemically decoupled from the SiC substrate by the intercalation of hydrogen atoms. Since the ZLG is 30°-rotated with respect to the substrate, this process results in a hydrogen-intercalated 30°-twisted bilayer graphene. We performed this process step by step, and investigated the intermediate stages using Low Energy Electron Microscopy and Diffraction (LEEM and LEED), and Angular Resolved Photo-Electron Spectroscopy (ARPES). The measurements confirm the 30°-rotation and the bilayer-stacking configuration of the graphene layers on the surface after the hydrogen intercalation.

For fully exploiting the instrument's spatial resolution, we applied a sophisticated, automatized approach for analyzing LEEM-*IV* data. Subsequent curve clustering allows the identification of homogenous domains on the surface and its illustration as a false-color image. LEED patterns, BF-LEEM images, LEEM-*IV* plots, and false-color images at different stages of intercalation are shown in Fig. 1. We found a continuous evolution of spectral shapes, which reflect the gradual structural transformation of stacked graphene layers at intermediate stages of the hydrogen intercalation.

References:
[1] F. C. Bocquet et al., Phys. Rev. Lett 125 (2020) 106102.

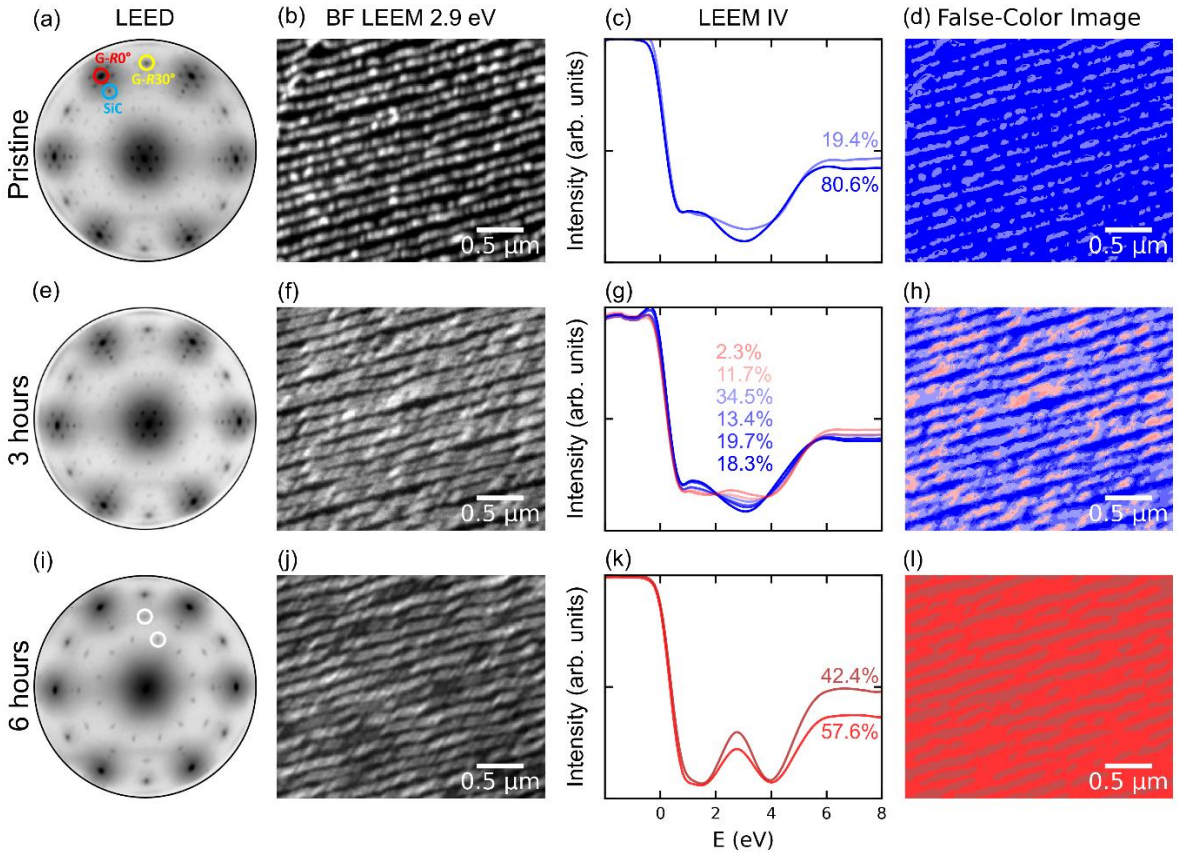

Fig. 1: LEED patterns, BF-LEEM images, average curves of sorted LEEM-*IV* spectra, and false-color images representing the clustering results, obtained from the sample surface at different stages of the hydrogen intercalation. (a,b,c,d) pristine surface, (e,f,g,h) after 3 hours, and (i,j,k,l) after 6 hours.

Electric-Field Control of Topology in Germanene

P. Bampoulis[1]

[1] Physics of Interfaces and Nanomaterials, MESA+ Institute, University of Twente, Drienerlolaan 5, 7522 NB Enschede, The Netherlands

Controlling topological quantum states with an external electric field is a central objective in the development of next-generation low-power electronics. Here, we demonstrate electric-field-driven topological phase transitions in germanene, the germanium analogue of graphene. In two-dimensional epitaxial films, germanene realizes a quantum spin Hall insulator with a sizable bulk bandgap and topologically protected edge states. A perpendicular electric field drives sequential transitions from the topological insulator phase to a Dirac semimetal and to a topologically trivial insulator [1]. Upon lateral confinement, we fabricate zigzag-terminated germanene nanoribbons and identify a critical width of approximately 2 nm below which the two-dimensional topological phase collapses due to edge-state hybridization, see Fig. 1. These ultra narrow nanoribbons are characterized by symmetry-protected end states [2]. In this limit, we achieve reversible all-electric switching of the zero-dimensional boundary modes, establishing atomic-scale control over topological states [3]. These results position germanene as a field-tunable platform for investigating dimensionality-driven topology and for realizing low-energy topological field-effect device concepts.

References:
[1] Bampoulis, P. et al. Phys. Rev. Lett. 130 (2023), 196401.

[2] Klaassen, D. J. et al. Nat. Commun. 16 (2025) 205.

[3] Eek, L. et al. Phys. Rev. Lett. 135 (2025) 206601.

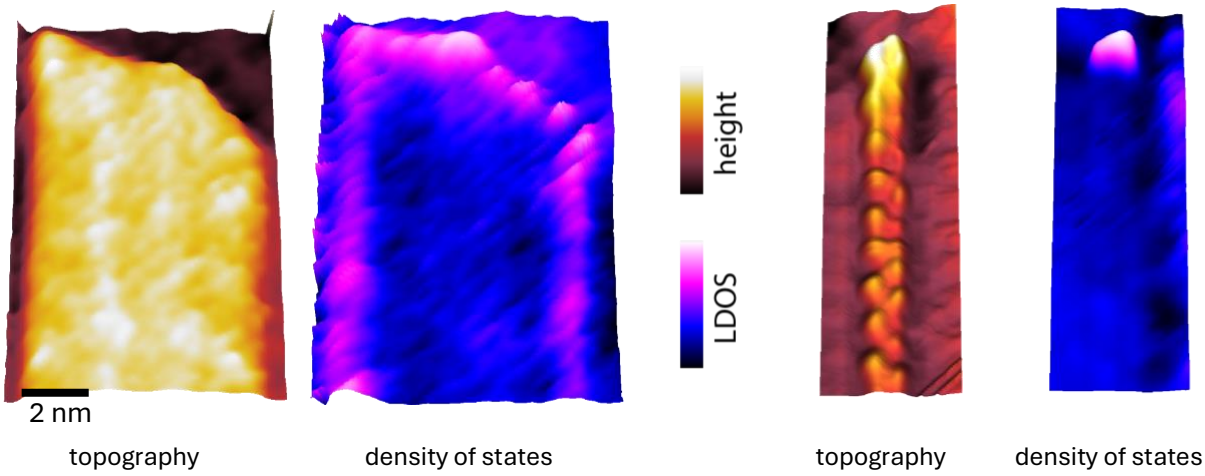

Fig. 1: Width-dependent evolution of electronic states in germanene nanoribbons. For wide nanoribbons (left), the low-energy states are localized along the ribbon edges. When the ribbon width is reduced to the very narrow limit (right), hybridization between opposite-edge states opens a gap, suppressing the extended edge modes and producing states localized at the ribbon ends.

Pb intercalation in epigraphene: Charge neutral graphene, 2D interlayer bands, and spin textures

Bharti Matta[1], Philipp Rosenzweig[1,2], Andres David Peña Unigarro[3], Craig Polley[4], Mats Leandersson[4], Sawani Datta[1], Philip Schädlich[3], Sibylle Gemming[3], Kathrin Küster[1], Ulrich Starke[1]

[1] Max-Planck-Institut für Festkörperforschung, Stuttgart, Germany
[2] Physikalisches Institut, Universität Stuttgart, Stuttgart, Germany
[3] Institut für Physik, Technische Universität Chemnitz, Chemnitz, Germany
[4] MAX IV Laboratory, Lund University, Lund, Sweden

Intercalation of epitaxial graphene is a robust approach for stabilizing two-dimensional (2D) interlayers confined at the graphene/SiC interface. Among the various elements explored as intercalants, Pb has attracted particular interest due to two key properties: it is a well-established superconductor, even in the form of ultrathin epitaxial films approaching the ultimate 2D limit [1], and it exhibits strong intrinsic spin-orbit coupling (SOC), with pronounced SOC effects persisting down to monolayer thickness [2,3]. These characteristics make Pb an excellent candidate for inducing both superconductivity and enhanced SOC in graphene via proximity coupling.

In this work, we present a detailed investigation of the electronic band structure of Pb-intercalated quasi-freestanding monolayer graphene (Pb-QFMLG) on SiC using angle-resolved photoelectron spectroscopy (ARPES). The graphene π bands show near charge-neutrality [4-6], involving a combined charge transfer from both the interlayer Pb and the SiC substrate [6]. The Pb-derived interlayer bands exhibit a metallic nature with a (1×1) registry with respect to the SiC substrate, corroborated by ARPES measurements within the repeated Brillouin zone of Pb [5,6]. Light polarization-dependent ARPES measurements reveal a predominantly out-of-plane orbital character for the Pb bands, suggesting potential interactions between the p_z orbitals of the interlayer Pb and graphene, potentially contributing to proximity-induced effects in graphene [6]. Density functional theory (DFT) calculations for a (1×1) Pb monolayer on SiC qualitatively agree with both the observed interlayer band structure and the light-polarization dependence [6].

Motivated by the prospect of SOC-driven effects, spin-resolved ARPES measurements were performed. These measurements reveal pronounced spin polarization in the Pb interlayer, reaching values up to about 50%, along with a tangential spin texture at the Fermi surface. Notably, the graphene π bands also exhibit measurable spin polarization, which may be attributed to Rashba-type spin splitting induced by the Pb interlayer. Spin-resolved DFT calculations support these findings.

References:
[1] T. Zhang et al., Nat. Phys. 6 (2010) 104-108.
[2] C. Brand et al., Phys. Rev. B 96 (2017) 035432.
[3] J. H. Dil et al., Phys. Rev. Lett. 101(2008) 266802.
[4] B. Matta et al., Phys. Rev. Research 4 (2022) 023250.
[5] P. Schädlich et al., Adv. Mater. Interfaces 10 (2023) 2300471.
[6] B. Matta et al., Phys. Rev. B 111 (2025) 155435.

Domain-resolved electronic structure of AgTe-intercalated graphene on SiC

V. Reddy[1], S. Datta[1], B. Matta[1], P. Rosenzweig[2], U. Starke[1], K. Küster[1]

[1] Max-Planck-Institut für Festkörperforschung, Heisenbergstraße 1, 70569 Stuttgart
[2] Universität Stuttgart, Pfaffenwaldring 57, 70569 Stuttgart

Intercalation at the interface of zero-layer graphene (ZLG) and SiC(0001) decouples the graphene from the SiC substrate, producing quasi-freestanding monolayer graphene (QFMLG). This enables tuning of graphene's electronic properties by controlling its charge carrier density and doping, while stabilizing novel intercalant-derived interfacial phases for both fundamental studies and potential device applications [1]. For instance, contrary to its bulk metallic nature, silver (Ag) intercalation stabilizes a two-dimensional (2D) Ag interlayer which is semiconducting due to quantum confinement [2]. Tellurium (Te) has an intrinsically chiral structure and exhibits topological features such as Weyl nodes [3]. Its intercalation offers tunable spin-orbit coupling (SOC) and thickness-dependent band-gap opening in graphene [4]. Studies of epitaxial AgTe monolayers on Ag(111) demonstrate that such interfacial alloy phases can host SOC manifested as orbital-driven Rashba-type spin-splitting [5], topologically non-trivial quantum spin Hall edge states and other emergent quantum phenomena [6]. AgTe intercalation could thus, combine these effects and produce a chemically and electronically rich interface with phase-dependent electronic properties that are protected under and potentially induced into graphene.

Competition between Ag and Te in a nominally AgTe-intercalated ZLG/SiC(0001) system currently stabilizes multiple intercalation regions, namely, Te-rich, AgTe alloy and Ag-rich intercalated domains, with distinct interlayer band dispersions and graphene doping levels. The Te-rich region exhibits semiconducting interlayer bands, and so does the Ag-rich region. However, the AgTe alloy region shows metallic interlayer bands. In different intercalation regions the graphene also exhibits different doping levels, with near charge-neutrality in the Te-rich region, moderate n-doping in the AgTe region and strong n-doping in the Ag-rich region (cf. Fig. 1). Collectively, these observations indicate that nominal AgTe intercalation produces a heterogeneous interface in which local stoichiometry critically determines both the interlayer electronic structure and the charge transfer into graphene. The coexistence of semiconducting and metallic interlayers, combined with spatially varying graphene doping underscores the pronounced sensitivity of the electronic properties of the system to subtle differences in intercalant composition and preparation parameters. Such phase-dependent electronic behavior establishes AgTe intercalation as a versatile platform for modulating electronic properties in graphene-based heterostructures, offering a route to design alloy interfaces with tailored quantum functionalities.

References:
[1] N. Briggs et al., Nanoscale 11 (2019) 15440.
[2] P. Rosenzweig and U. Starke, Phys. Rev. B 101 (2020) 201407.
[3] G. Qiu et al., npj 2D Mater. Appl. 6 (2022) 17.
[4] B. Muñiz Cano et al., Adv. Funct. Mater. 35 (2025) 2425154.
[5] M. Ünzelmann et al., Phys. Rev. Lett. 124 (2020) 176401.
[6] B. Liu et al., J. Phys. Chem. Lett. 10 (2019) 1866.

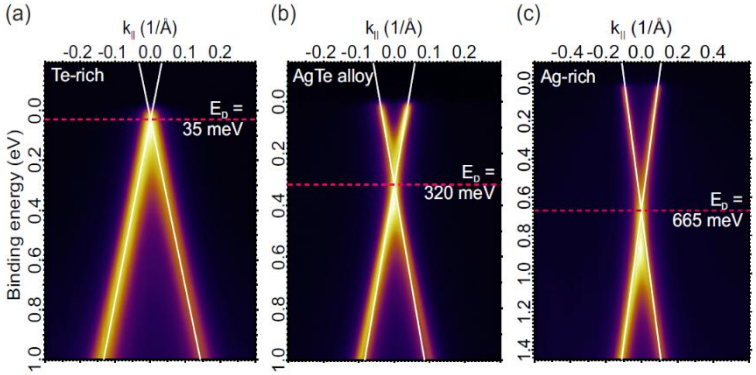

Fig. 1: Angle-resolved photoemission spectroscopy (ARPES) measurements of the graphene Dirac cone acquired (hv = 40 eV) at the $\overline{K}$-point perpendicular to the $\overline{\Gamma K}$ direction of the graphene Brillouin zone, in the (a) Te-rich, (b) AgTe alloy and (c) Ag-rich domains respectively.

Turning new “knobs” on Hamiltonians of 2D materials

Kirill I. Bolotin

[1] Freie Universität Berlin

We demonstrate new ways to use electric fields, mechanical strain, and twist-angle control to manipulate the properties of 2D materials and their heterostructures.

First, we demonstrate ultra-strong electric fields in 2D materials via "molecular gating" — sandwiching a 2D material between donor and acceptor molecular layers whose charge transfer generates fields exceeding 4 V/nm, the highest measured in a solid-state device. We show that these fields close the bandgap of bilayer semiconductors, driving a semiconductor-to-metal transition, lifting excitonic degeneracies, bringing distinct excitons into resonance, and giving rise to new excitonic states.

Second, we demonstrate in situ strain engineering of transition-metal dichalcogenides at cryogenic temperatures, including controlled uniaxial, biaxial, and spatially non-uniform strain distributions. Strain tunes transport, valley properties, and excitonic lifetimes and couplings. Using uniform strain, we realize a new excitonic state arising from the hybridization of long-lived dark free excitons with strongly coupled localized excitons — combining the advantages of both and making it uniquely suited for quantum information storage.

Finally, we describe a variant of the Quantum Twist Microscope that enables in-situ twist-angle control with simultaneous optical measurements. Using this platform, we demonstrate on-demand control of chiral polaritons in heterostructures of the anisotropic magnet CrSBr.

References:

[1] D. Yagodkin, K. Burfeindt, Z. A. Iakovlev, A. M. Kumar, A. Dewambrechies, O. Yücel, B. Höfer, C. Gahl, M. M. Glazov, and K. I. Bolotin, Fermi polarons under strain-induced pseudomagnetic fields, Nature Communications 16, 10232 (2025).

[2] S. Kovalchuk, K. Greben, A. M. Kumar, S. Pessel, J. Soyka, Q. Cao, K. Watanabe, T. Taniguchi, D. Christiansen, M. Selig, et al., *Revealing hidden interlayer excitons in 2D bilayers via hybrid molecular gating*, Nature Communications **16**, 9893 (2025).

[3] A. M. Kumar, D. Yagodkin, R. Rosati, D. J. Bock, C. Schattauer, S. Tobisch, J. Hagel, B. Höfer, J. N. Kirchhof, P. H. López, et al., Strain fingerprinting of exciton valley character in 2D semiconductors, Nature Communications 15, 7546 (2024).

Advanced Interfacial Engineering of Edge-Contacted Graphene Devices

J. Kunc[1], B. Morzhuk[1], V. Stará[2], D. Varshney[3], M. Shestopalov[1], K. Matějka[1], M. Rejhon[1], J. Novák[3], J. Čechal[2]

[1] Charles University, Faculty of Mathematics and Physics, Ke Karlovu 5, Prague, Czech Republic
[2] Central European Institute of Technology, Purkyňova 123, Brno, Czech Republic
[3] Masaryk University, Department of Condensed Matter Physics, Kotlářská 267, Brno, Czech Republic

The development of molecular quantum emulators is frequently hindered by polymer residues from lithography that disrupt molecular registry at 2D interfaces [1,2]. We present a modified post-fabrication purification protocol [3] that restores epitaxial graphene to UHV-equivalent purity within an edge-contacted graphene device [4]. This allows the graphene to act as a symmetry-breaking template, enforcing macroscopic long-range order in an overlayer of the organic semiconductor 2,3,6,7,10,11-hexamethoxytriphenylene (HMTP) [5]. By engineering this pristine interface, demonstrated by Low-Energy Electron Diffraction, we successfully resolve the Davydov-split excitonic manifold, Fig. 1, a hallmark of high-symmetry molecular crystals typically masked by disorder. We move beyond standard Franck-Condon models by implementing Herzberg-Teller corrections, accounting for non-Condon transitions where electronic states couple to specific vibrational modes. This approach allows for the experimental parameterization of the Holstein Hamiltonian in a functional hybrid architecture. Our findings are corroborated by Raman molecular dynamics simulations, which identify the specific vibrational modes leading to the observed excitonic phonon replicas. The results reveal a clear branching into bright and dark excitonic states, demonstrating that dark-exciton radiative channels dominate the low-energy regime. By bridging the gap between aggressive nanofabrication and high-precision surface science, this work establishes a scalable roadmap for exploring collective excitations and strong electron-phonon coupling in atomically clean molecular-2D heterostructures.

References:

[1] M. K. Huss-Hansen et al., Langmuir 36 (2020) 1898.
[2] T. Yager et al., APL 106 (2015) 063503.
[3] A. Tyagi et al., Nanoscale 14 (2022) 2167
[4] N. Shetty et al., ACS Applied Nano Materials 6 (2023) 6292.
[5] J. Kunc et al., Arxiv:2603.02301 (2026).

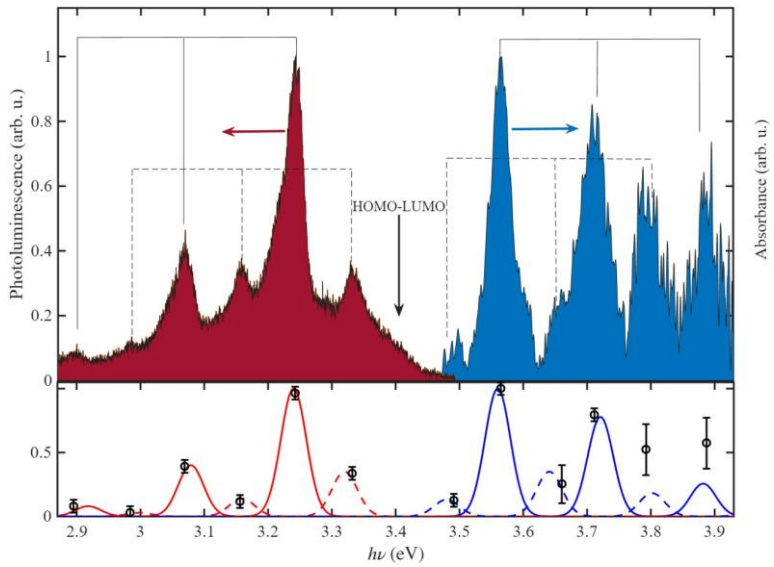

Fig. 1: Davydov-Split Excitonic Manifold in HMTP. Experimental PL and absorption spectra (top) compared with a theoretical model (bottom). The simulation incorporates a Franck-Condon mechanism with non-Condon Herzberg-Teller corrections, accurately capturing the dual sets of excitonic transitions.

Giant orbital Zeeman effects at the interface of graphene and Fe_3GeTe_2

T. Wichmann,[1,2,3] M. Sastges,[1,3,4] K. Jin,[1,2,3] J. Martinez-Castro,[1,2,3] T. G. Saunderson,[1,4] D. Go,[1,5] H. Boban,[1] S. Lounis,[10] L. Plucinski,[1] M. Ternes,[1,2,3] Y. Mokrousov,[1,4] F. S. Tautz[1,2,3], F. Lüpke[1,2,7]

[1] Peter Grünberg Institute, Forschungszentrum Jülich, 52425 Jülich, Germany
[2] Jülich Aachen Research Alliance (JARA-FIT), 52425 Jülich, Germany
[3] RWTH Aachen University, 52074 Aachen, Germany
[4] Institute of Physics, Johannes Gutenberg University, 55099 Mainz, Germany
[5] Department of Physics, Korea University, Seoul 02841, Republic of Korea
[6] Institute of Physics and Halle-Berlin-Regensburg Cluster of Excellence CCE, Martin-Luther-University Halle-Wittenberg, 06099 Halle, Germany
[7] Institute of Physics II, Universität zu Köln, Zülpicher Straße 77, 50937 Cologne, Germany

Van der Waals (vdW) heterostructures allow the engineering of electronic and magnetic properties by the stacking different two-dimensional vdW materials. For example, orbital hybridisation and charge transfer at a vdW interface may result in electric fields across the interface that give rise to Rashba spin-orbit coupling. In magnetic vdW heterostructures, this in turn can drive the Dzyaloshinskii-Moriya interaction which leads to a canting of local magnetic moments at the vdW interface and may thus stabilize novel 2D magnetic phases. While such emergent magnetic "interphases" offer a promising platform for spin-based electronics, direct spectroscopic evidence for them is still lacking. We report Zeeman effects with Landé *g*-factors up to ≈230 at the interface of graphene and the vdW ferromagnet Fe_3GeTe_2 [1]. They arise from a magnetic interphase in which local-moment canting and itinerant orbital moments generated by the non-trivial band topology of Fe_3GeTe_2 conspire to cause a giant asymmetric level splitting when a magnetic field is applied. Exploiting the inelastic phonon gap of graphene [2], we can directly access the buried vdW interface to the Fe_3GeTe_2 by scanning tunneling spectroscopy (STM). Systematically analyzing the Faraday-like screening of the tip electric field by the graphene, we demonstrate the tunability of the constitutional interface dipole, as well as the Zeeman effect, by tip gating. Our findings are supported by density functional theory and electrostatic modelling.

References

[1] T. Wichmann *et al.*, arXiv:2510.26662 (2025)
[2] Zhang *et al.*, Nat. Phys. 4, 627 (2008)

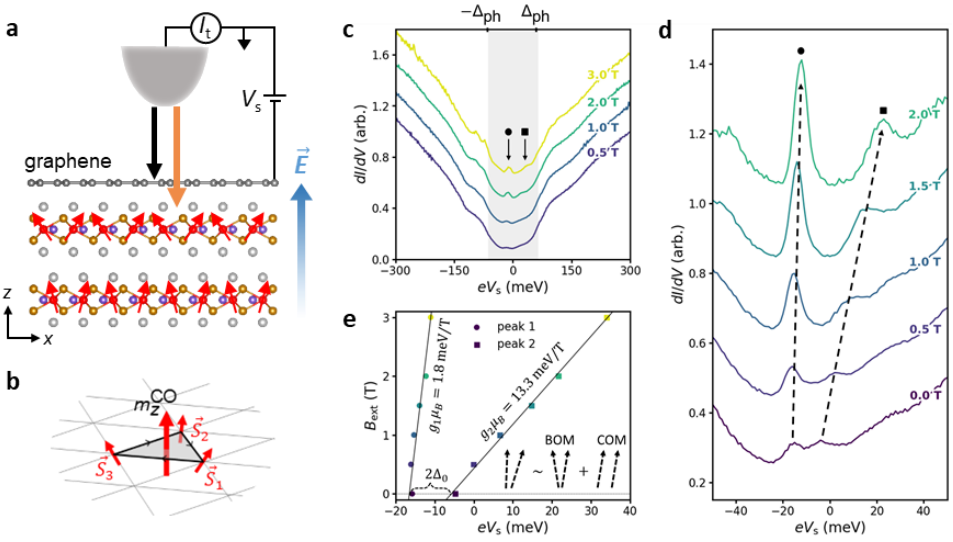

Fig 1. (a) Schematic side view of the sample and STM setup. (b) Schematic of non-collinear spin arrangement in the Fe sublattice, where a canting of localized spins results in a conical spin structure. (c) Tunneling spectra for different out-of-plane B fields. For clarity, curves are offset. In the inelastic gap of graphene (shaded region), two peaks emerge with increasing B field, as shown in detail in panel (d). (e) Peak positions as function of applied B field, corresponding to *g*-factors of ≈30 and ≈230, respectively.

Growth of hetero-epitaxial graphene and 2D materials on SiC

Wataru Norimatsu

Faculty of Science and Engineering, Waseda University, Tokyo, Japan

The graphene/SiC system is one of the ideal platforms for two-dimensional materials research because it has an atomically flat surface and allows us the production of large-area, single-orientation graphene. Using this graphene/SiC system, we can modulate the electronic state of graphene and fabricate new two-dimensional materials by introducing other substances. In this presentation, I will report on the fabrication of two-dimensional iron oxide with a structure not present in bulk at the graphene/SiC interface [1], and on graphene/NbC/SiC grown by thermal decomposition of NbC deposited on SiC.

For 2D-FeO growth, a buffer layer with a structure almost identical to graphene was formed on SiC, and then iron with a thickness of approximately 4 nm was deposited on top of it. The sample was exposed to air, and then re-introduced into a vacuum chamber and heated at 660ºC. Figure 1 shows a high-angle annular dark-field scanning transmission electron microscope (HAADF-STEM) image of the obtained sample. Three layers of bright spots are observed at the graphene/SiC interface. Our analysis revealed that these bright spots are 2D-FeO with a structure which was not present in nature.

On the other hand, when a thin NbC film with a thickness of approximately 10 nm was deposited on a SiC(000-1) substrate using pulsed laser deposition and then heated, graphene was formed on its surface. Angle-resolved photoemission spectroscopy measurements of the graphene/NbC/SiC sample revealed a linear band with a Dirac energy of about -0.4 eV at the K point of graphene in reciprocal space, as well as a Dirac-like band at about -3.0 eV. First-principles band structure calculation for graphene/NbC suggested that the former band is due to the uppermost graphene layer, while the latter is due to a carbon layer bonded to Nb on the surface of NbC. This is the similar situation to the electronic state of the buffer layer on the SiC(0001) surface.

In addition to these results, I will also present results for the fabrication of graphene/WC/SiC by thermal decomposition of WC deposited on SiC, WSe_2/WC/SiC by heating WC/SiC in a Se atmosphere, and WSe_2 on graphene/SiC using chemical vapor deposition [2].

References:
[1] R. Sakakibara, WN, et al., Small Methods 0, e01889 (2026).
[2] R. Sakakibara, WN, et al.. Nano Lett. 25, 12851 (2025).

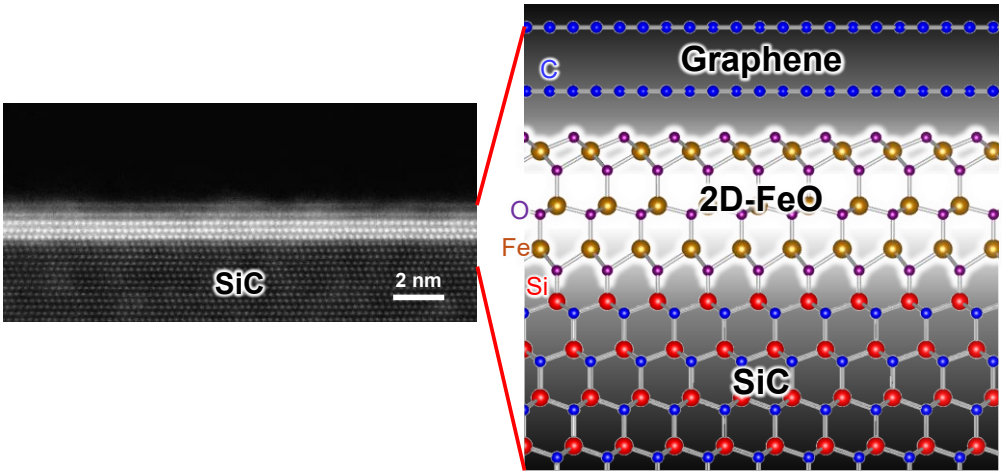

Fig. 1: HAADF-STEM image of graphene/2D-FeO/SiC together with its structural model.

Delamination and transfer of wafer-scale single-crystalline monolayer graphene from SiC substrate

J. Huhtasaari[1],J.J. Palakulam[1], A. Salha[1], P. Hyldgaard[1], E. Schröder[1],M.H. Berntsen[2], O. Tjernberg[2], M. Shah[3],R. Martinez-Duarte[3], H. He[4], J. Hofmann[5,6],T. Bauch[1], N. Shetty[1], S. Lara-Avila[1],

[1]Department of Microtechnology and Nanoscience, Chalmers University of Technology (Sweden)
[2]Department of Applied Physics, KTH Royal Institute of Technology (Sweden)
[3]Department of Mechanical Engineering, Clemson University (USA)
[4]RISE-Research Institutes of Sweden (Sweden)
[5]Department of Physics, Gothenburg University (Sweden)
[6]Nordita, Stockholm University and KTH Royal Institute of Technology (Sweden)

Producing large-area single-crystalline graphene is key to realizing its full potential in advanced applications, including twistronics. Yet, controlling graphene growth kinetics to avoid grain boundaries or multilayer growth remains challenging.

Here[1], we demonstrate single-crystalline graphene free from multilayer domains via one-step delamination of epitaxial graphene from silicon carbide(SiC).This is enabled by a specific surface reconstruction of 4H-SiC(0001) achieved in our growth conditions. High crystalline quality is confirmed by the observation of the half-integer quantum Hall effect – the hallmark of monolayer graphene– in near cm-sized crystals. The scalability of our process, explored with 4”-inch wafers, represents an advance toward large-scale integration of high-performance graphene applications.

References:
[1] Huhtasaari, J. *et al.* Wafer-Scale Single-Crystalline Monolayer Graphene. arXiv:2512.00394v1 (2025).

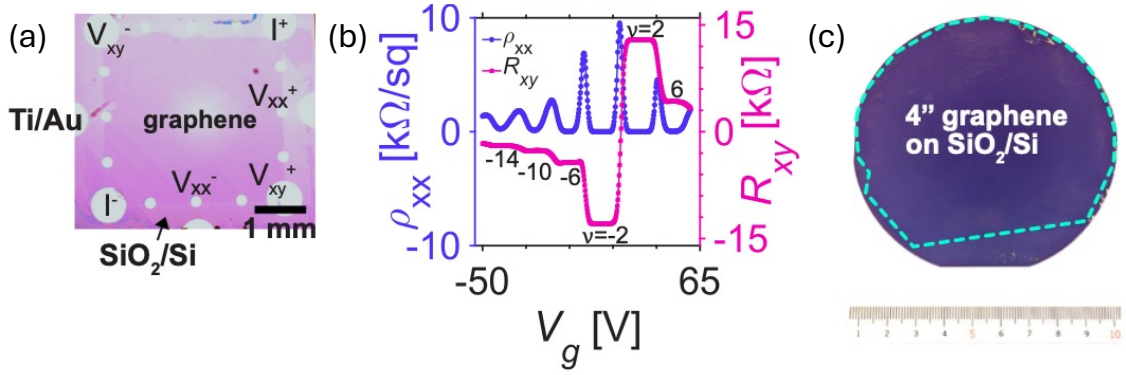

Fig. 1: Delamination and transfer of wafer-scale epitaxial graphene. (a) Large-area device with silver-transferred graphene on SiO2/Si.(b) Half-integer QHE at B=14 T, T=2 K in the large-area device. (c) 4-inch-sized graphene transferred from SiC to a 4 inch SiO_2/Si wafer.

Operando Monitoring of Epitaxial Graphene Growth using High Temperature Neutron Reflectometry

A. Pradeepkumar[1,2], D. Cortie[3], E. Smyth[3], A. P. Le Brun[3] and F. Iacopi[1,2]

[1]School of Electrical and Data Engineering, Faculty of Engineering and Information Technology, University of Technology Sydney, Australia.
[2]ARC Centre of Excellence for Transformative Meta-Optical Systems, University of Technology Sydney, Australia
[3]Australian Centre for Neutron Scattering, Australian Nuclear Science and Technology Organization, Australia.

Synthesis of epitaxial graphene (EG) on cubic silicon carbide (3C-SiC) on silicon offers an attractive route towards novel wafer-scale electronics and photonics integrated on silicon [1]. We have pioneered a unique way to achieve a controlled graphene growth on this challenging substrate by using a thin Ni/Cu alloy [2]. A detailed understanding of the epitaxial graphene growth mechanism, via operando characterization is critical to further optimize the process. In this work we report on the real-time epitaxial graphene growth mechanism on 3C-SiC/Si substrates using a unique setup of neutron reflectometry (NR) (up to 1100 °C, below 5×10^{-5} mbar and characterization [3,4], refer to Fig 1a) and b). We have conducted NR measurements during a controlled annealing on the Spatz time-of-flight neutron reflectometer at the 20 MW OPAL Multipurpose Reactor at the Australian Nuclear Science and Technology Organization (ANSTO, Lucas Heights, Australia). Spatz is a time-of-flight neutron reflectometer, which uses cold neutrons with wavelengths in the range of 2-20 Å. [5]

The advantages of using neutron beam are that it can penetrate through the walls of vacuum furnace to monitor the graphene formation at 1100 °C. In addition, due to the larger and distinct neutron scattering length of carbon, oxygen and silicon, these elements can be observed and differentiated under neutrons [6]. The use of standard X-ray reflectometry cannot achieve this due to two reasons: first, the X-rays cannot penetrate through the vacuum furnace walls and second, the X-ray scattering length for carbon, oxygen and silicon are relatively similar and smaller, making them less sensitive under X-rays.

The observations confirm formation of the metal silicide, which is the key player enabling the release of atomic carbon from SiC. Furthermore, the experiments also confirm the liquid phase nature of the epitaxial growth, which is the key reason for the uniform coverage of graphene on the substrate. It also illustrates formation of graphene layer as well as a thin silicate layer of ~20 Å between graphene and SiC. [3].

Through this work we unlock new avenues to use high temperature neutron reflectometry for the observation and optimization of epitaxial graphene growth and other 2D materials.

References:
[1] A. Pradeepkumar et al., ACS Appl. Nano Mater., (2019), 830–841.
[2] F. Iacopi, et al., J. Mater. Res 30.5 (2015).
[3] A. Pradeepkumar et al., RSC Adv., 14 (2024), 3232-3240
[4] A. Pradeepkumar et al., Neutron News 35(2) (2024) 9-11
[5] A. P. Le Brun et al., J. Appl. Crystallogr., 56 (2023) 18-25.
[6] S. Zheng et al., Sci. China Mater., 62 (2019) 1087-1095

a) b)

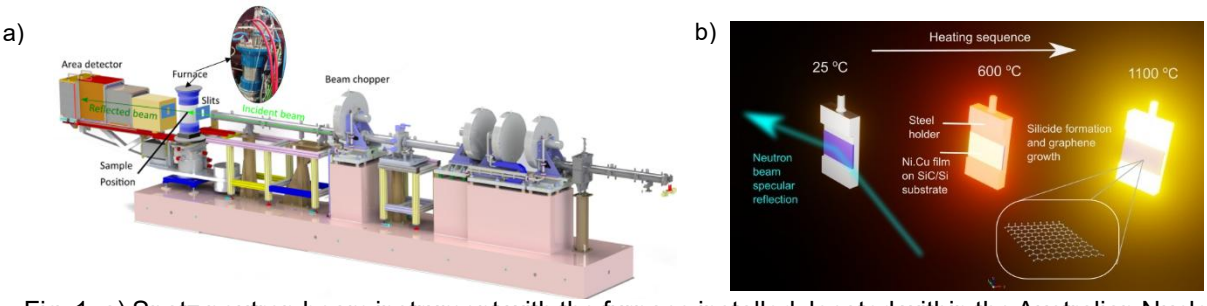

Fig. 1: a) Spatz neutron beam instrument with the furnace installed, located within the Australian Nuclear Science and Technology Organization (ANSTO), recreated from ref. 4 under creative commons license CC BY 4.0 DEED. b) Operando monitoring of EG synthesis using neutron reflectometry

Dynamics and Electron-Phonon Coupling in Graphene Heterostructures from Helium Atom Scattering

G. Benedek[1,2], J. R. Manson[3,2], S. Miret-Artès[4,2], M. M. Ùgeda[2]

[1]Dipartimento di Scienza dei Materiali, Università di Milano-Bicocca,
Via R. Cozzi 55, 20125 Milano, Italy
[2]Donostia International Physics Center (DIPC), Paseo M. de Lardizábal 4,
20018 Donostia/San Sebastián, Spain
[3]Department of Physics and Astronomy, Clemson University,
Clemson, SC 29634, USA
[4]Instituto de Fisica Fundamental, Consejo Superior de Investigaciones Cientificas,
Serrano 123, 28006 Madrid, Spain.

In Helium atom scattering (HAS) spectroscopy of conducting surfaces, the exchange of energy and momentum with surface and subsurface phonons occurs via the electron-phonon coupling (EPC). Thus, as shown by Sklyadneva *et al.* [1], inelastic HAS amplitudes from surface vibrational modes are proportional to the mode-selected EPC, while the temperature-dependent HAS Debye-Waller (DW) exponent was shown to bear information on the total EPC (mass-enhancement factor λ_{HAS}) [2]. In this talk, after a brief illustration of HAS spectroscopy and the main theoretical concepts, the application to graphene monolayers on different metal substrates is discussed. It is shown that the EPC, as derived experimentally from the DW exponent temperature dependence, increases by decreasing the graphene-substrate coupling force constant [3].

Further recent studies on more complex graphene heterostructures, like a bilayer graphene (BLG) on a 6H-SiC(0001) substrate, which is made quasi-freestanding via a carbon buffer layer, or an intercalated atomic hydrogen passivation, or a 2D polar gallium bilayer [4], provide evidence of an enhanced EPC in BLG systems (λ_{HAS} in the range 0.27−0.33), as compared to the above studies on single layer graphene samples on metal substrates.

A thorough study on the structure, phonon dynamics and EPC in 1ML-$NbSe_2$/BLG/SiC(0001) [5] demonstrates the power of high-resolution HAS spectroscopy, by revealing the 9x9 supercell of the $NbSe_2$ monolayer on BLG and the important role of moiré phonons. The specific effects of moiré phonons and of the BLG interfacing on the EPC and the superconductivity T_c of the $NbSe_2$ monolayer is finally discussed in some detail.

[1] I. Yu. Sklyadneva, G. Benedek, E. V. Chulkov, P. M. Echenique, R. Heid, K.-P. Bohnen, and J. P. Toennies, *Mode-Selected Electron-Phonon Coupling in Superconducting Pb Nanofilms Determined from He Atom Scattering*, Phys. Rev. Lett. 107 (2011) 095502.
[2] J. R. Manson, G. Benedek, S. Miret-Artés, *Atom scattering as a probe of the surface electron-phonon interaction at conducting surfaces*, Surface Science Reports 77 (2022)100552.
[3] G. Benedek, J. R. Manson, and S. Miret-Artés, *The Electron-Phonon Coupling Constant for Single-Layer Graphene on Metal Substrates Determined from He Atom Scattering*, PCCP, 23 (2021) 7553.
[4] N. J. Hourigan, Ph. Seiler, M. Wetherington, Ch. Dong, J. A. Robinson, G. Benedek, A. Tamtögl, *How does intercalation affect the structure and dynamics of bilayer graphene?*, Carbon 238 (2025) 120156.
[5] A. Al Taleb, W. Wan, G. Benedek, M. Ùgeda, and D. Farías, *Electron-phonon coupling and phonon dynamics in single-layer $NbSe_2$ on graphene: the role of moiré phonons*, ACSNano 19 (2025) 8895.

Ultrafast signatures of Dirac – flat-band hybrid states from time-resolved ARPES

Maria-Elisabeth Federl[1], Johannes Gradl[1], Franziska Bergmeier[1], Leonard Weigl[1], Lukas Bruckmeier[1,2,3], Theresa Glaser[1], Zamin Mamiyev[4], Christoph Tegenkamp[4], Niclas Tilgner[4,5], Thomas Seyller[4,5], Teresa Tschirner[6], Domenica Convertino[7], Stiven Forti[7], Camilla Coletti[7], Isabella Gierz[1]

[1] Department for Experimental and Applied Physics,
University of Regensburg, 93040 Regensburg
[2] Institut für Experimentelle und Angewandte Physik,
Christian-Albrechts-Universität zu Kiel, 24098 Kiel, Germany
[3] Ruprecht Haensel Laboratory, Deutsches Elektronen-Synchrotron
DESY, 22607 Hamburg, Germany
[4] Institute of Physics, Chemnitz University of Technology,
09126 Chemnitz, Germany
5 Research Center for Materials, Architectures and Integration of Nanomembranes (MAIN),
09126 Chemnitz, Germany
[6] Physikalisch-Technische Bundesanstalt,
38116 Braunschweig, Germany
[7] Center for Nanotechnology Innovation@NEST,
Instituto Italieno du Tecnologia, 56127 Pisa, Italy

Hybridization of highly itinerant Dirac electrons with localized flat-band states is predicted to yield emergent phenomena such as exotic heavy-fermion behaviour. Epitaxial graphene resting on a flat-band system at the graphene-SiC(0001) interface offers a promising platform, yet direct spectroscopic signatures - such as avoided crossings in equilibrium ARPES - have remained unresolved. We solved this problem using time-resolved ARPES where evidence of hybridization manifested in three key observations: (1) accelerated Dirac-carrier relaxation due to an increased scattering phase space, (2) transient charging of the Dirac cone enabled by direct optical excitation from the flat bands, and (3) ultrafast charge transfer back into the flat bands on timescales set by the interlayer coupling strength. We further demonstrate that the degree of hybridization can be tuned via the atomic number of the atoms intercalated at the graphene-SiC interface, establishing a controllable platform for investigating exotic correlated ground states. Our results thus provide a clear dynamical fingerprint of hybridization in a system where equilibrium probes have proven inconclusive.

Ultrafast dynamics of terahertz plasmons in in-plane periodic nanostructures of epitaxial graphene

A.Singh, B. Klusáková, H. Němec, R: Matuška, J. Kunc and P. Kužel

[1] Institute of Physics, Czech Academy of Sciences, Na Slovance 2, 18200 Prague 8, CZ
[2] Faculty of Mathematics and Physics, Charles University, Ke Karlovu 3, Prague 2 12116, CZ

In this paper we investigate THz plasmons in lithographically prepared nanoribbons and nanodots of epitaxial graphene and we demonstrate their ultrafast control by optical pulses using combined near-field and far-field THz spectroscopies.

We grew epitaxial graphene in Ar atmosphere by graphitization of 6H-SiC substrate both on its Si and C side. The layer on Si-face was submitted to the hydrogen intercalation process [1] leading quasi-free-standing single layer graphene (QFSLG) which is p-doped. The C-face of SiC hosts multilayer epitaxial graphene (MEG), where each layer exhibits electronic properties similar to isolated monolayer graphene as a result of twisted, non-Bernal stacking. The inner layers (close to the substrate) are usually significantly n-doped while outer layers are usually quasi-neutral (QN). After the growth we employed e-beam lithography followed by oxygen plasma etching to create graphene nanoribbon and nanodot plasmonic structures (see examples in Fig. 1a,b).

We determined the THz sheet conductivity spectra of the samples in the ground state as a function of temperature. Further we used optical pump – THz probe approach to assess picosecond dynamics of the THz plasmonic behavior after optical excitation. To these aims we used a combination of standard time-domain THz spectroscopy setup (0.15 – 3THz), THz air-based photonics setup (1 – 20 THz) and a THz local probe imaging device (THz-SNOM, Neaspec).

The studied structures feature a plasmonic resonance typically in the 1–4 THz spectral range depending on the lithographically fabricated pattern and its characteristic aspect ratios. The ultrafast dynamics of plasmons in optically excited graphene are entirely controlled by the Fermi level of laser-excited hot carriers through their temperature. The laser pulse heats the carriers up to about 5000 K and the carrier cooling occurs back to the lattice temperature occurs within a few picoseconds. The heating of carriers is accompanied by a weak plasmon redshift in (doped) QFSLG; the carrier mobility is $\sim 1700\ \mathrm{cm^2V^{-1}s^{-1}}$ and does not change significantly upon photoexcitation. In MEG, the doped and QN layers contribute approximately equally to the sheet conductivity in the ground state while the large amount of pexcited hot carriers occurring in QN layers upon the photoexcitation dominates the transient response and lead to a significant blueshift and broadening of the plasmon resonance (Fig. 1c,d). The carrier mobility of the doped layers is $\sim 2300\ \mathrm{cm^2V^{-1}s^{-1}}$, while in QN layers it reaches a value of $7.5 \times 10^5\ \mathrm{cm^2V^{-1}s^{-1}}$ at room temperature and shows a strong temperature dependence due to the variation of the chemical potential and carrier scattering time [2,3]. Peculiarities of the plasmon and electron dynamics will be discussed in the conference contribution.

References:
[1] C. Riedl et al, *Phys. Rev. Lett.* **103**, 246804 (2009).
[2] A. Singh et al., *Phys. Rev. Res.* **6**, 033063 (2024).
[3] A. Singh et al., *Phys. Rev. B* **113**, 115417 (2026).

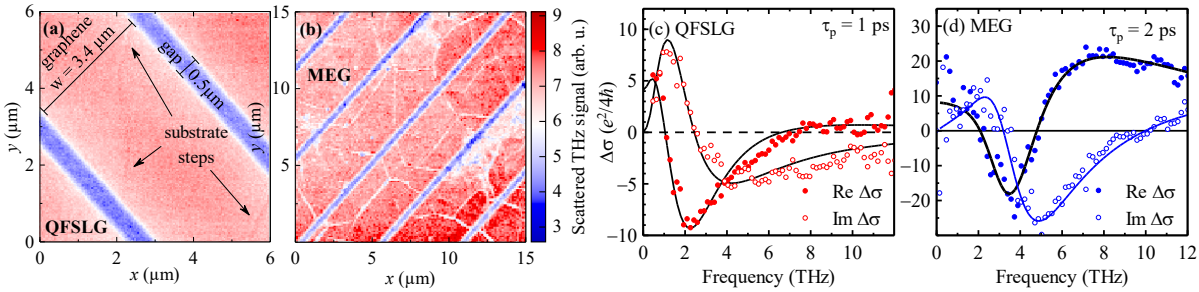

Fig. 1: Near-field THz conductivity image using THz-SNOM for graphene ribbons in (a) QFSLG and (b) MEG samples. Transient sheet photoconductivity spectra of (c) QFSLG and (d) MEG featuring plasmon resonance.

Influence of sulphur vacancies on ultrafast charge separation in WS_2-graphene heterostructures

J. Gradl[1], N. Hofmann[1], L. Weigl[1], S. Forti[2], N. Mishra[2,3], C. Coletti[2], R. Perea-Causin[4], E. Malic[5], and I. Gierz[1]

[1] Department for Experimental and Applied Physics, University of Regensburg, Regensburg, Germany
[2] Center for Nanotechnology Innovation@NEST, Istituto Italiano di Tecnologia, Pisa, Italy
[3] Graphene Labs, Istituto Italiano di Tecnologia, Genova, Italy
[4] Department of Physics, Stockholm University, AlbaNova University Center, Stockholm, Sweden
[5] Department of Physics, University of Marburg, Marburg, Germany

Ultrafast charge separation following photoexcitation, commonly observed in van der Waals heterostructures, is a key process for future optoelectronic devices that rely on the conversion of light into electricity. While electron and hole transfer rates are largely determined by band alignment and interlayer hybridization, recent experiments have revealed that defects critically affect the lifetime of the charge-separated state [1][2]. A microscopic understanding of defect-assisted charge transfer, however, remains elusive.

We disentangle the role of sulphur vacancies on ultrafast charge separation and recombination in WS_2-graphene heterostructures by (i) systematically increasing the defect density [3] and (ii) switching the defect-assisted charge transfer channel on and off.

Using time-resolved ARPES, we probe the resulting charge-transfer dynamics on ultrafast time scales directly in the band structure.

References:
[1] R. Krause et al., Phys. Rev. Lett. 127 (2021) 276401.
[2] S. Fu et al., Sci. Adv. 8 (2021) eabd9061.
[3] J. Gradl et al., arXiv:2603.16247 (2026)

Epitaxial growth of 2D Se-Ta-S Janus membranes on Au(111)

C. Grover[1], A. Bremerich[1], D. Wilks[1], T. Data[1], C. Busse[1], and T. Chagas[1]

[1] Department Physik, Universität Siegen, 57072 Siegen, Germany

2D transition metal chalcogenides (TMC) Janus membranes are asymmetric materials characterized by a transition metal layer (M) sandwiched between two different chalcogen layers (X and X'). Due to the intrinsic electric field generated by the differing partial charges of the chalcogens, they exhibit unique properties. For instance, breaking out-of-plane symmetry can lead to strong piezoelectric effects and Rashba spin splitting [1, 2].

Here, we report the controlled synthesis and atomic-scale characterization of Se-Ta-S Janus membrane grown on Au(111) under ultra-high vacuum. Tantalum is first deposited onto clean Au(111) and annealed in an H_2S atmosphere, resulting in tantalum monosulfide (TaS) under sulfur-poor conditions (Fig. 1a). From our previous works, we know that this phase can be further converted to TaS_2 by additional sulfurization (Fig. 1b) [3, 4]. Exploiting this layer-wise growth mechanism, we instead introduce selenium in a second step, enabling the formation of Se-Ta-S structures (Fig. 1c). Scanning tunneling microscopy reveals large-area, well-defined islands with atomic precision, providing strong evidence for the formation of Se-Ta-S Janus membranes. A similar growth behavior is observed in the TaSe system (Fig. 1d), where TaSe can be transformed into $TaSe_2$ (Fig. 1e), suggesting that our protocol can also enable Janus membranes with inverted polarity. Compared with existing approaches that rely on H_2 plasma stripping to introduce the second chalcogen, our method avoids this defect-inducing step, yielding more uniform, well-oriented samples. These results establish a reliable route for fabricating Janus TMCs with controlled composition and polarity.

References:
[1] A. Lu et al., Nat. Nanotechnol. 12 (2017) 744.
[2] L. Zhang et al., Nanoscale 11 (2019) 5666.
[3] D. Dombrowski et al., ACS Nano 15 (2021) 13516
[4] D. Dombrowski et al., 2D Mater. 10 (2023) 025005.

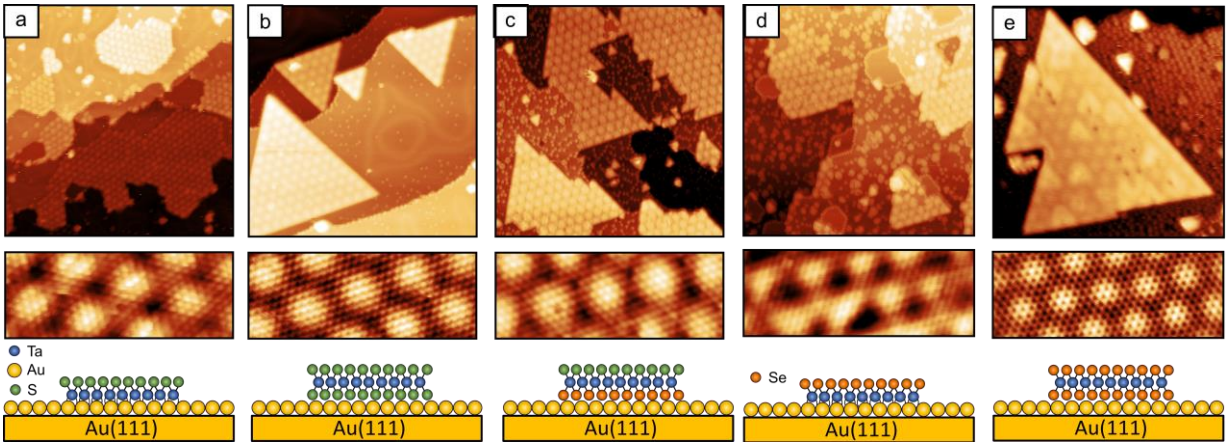

Fig. 1: STM images of (top) large-scale islands, (middle) their atomic and moiré resolution at a size 14.5 nm x 6.5 nm (bottom) corresponding model for (a) TaS, (b) TaS_2, (c) SeTaS, (d) TaSe and (e) $TaSe_2$. Image parameters: (a, top) V = -2.25 V, I = 0.01 nA, (a, middle) V = -0.91 V, I = 0.10 nA, (b, top) V = -0.83 V, I = 0.09 nA, (b, middle) V = -0.44 V, I = 3.80 nA,(c, top) V = -1.42 V, I = 0.17 nA, (c, middle) V = -0.30 V, I = 1.7 nA. (d, top) V = -1.66 V, I = 0.02 nA, (d, middle) V = -0.14 V, I = 0.14 nA, and (e, top) V = -0.35 V, I = 0.04 nA, (e, middle) V = -0.35 V, I = 0.58 nA, Image Sizes: (a, top) 21.5 nm × 21.5 nm, (b, top) 46.5 nm × 46.5 nm, (c, top) 49.0 nm × 49.0 nm, (d, top) 43.5 nm × 43.5 nm, and (e, top) 22.5 nm × 22.5 nm.

Surface reconstruction governs graphene epitaxy on sapphire

S. Forti[1,*], D. Acharya[2], D. Perilli[2], N. Mishra[1,†],
A. A. Zakharov[3], C. Di Valentin[2] and C. Coletti[1]

[1]Center for Nanotechnology Innovation, Istituto Italiano di Tecnologia,
Piazza San Silvestro 12, 56127 Pisa (IT)
[2]Department of Materials Science, University of Milano-Bicocca, via R. Cozzi 55, 20125 Milano, Italy
[†] Present address: CamGraPhiC Technologies, Pisa (IT)
[3] MAXIV Laboratory, Lund, Sweden

The direct growth of single-crystal graphene on dielectric substrates is highly appealing for semiconductor technologies, particularly in optoelectronics. Sapphire (α-Al_2O_3(0001), c-plane) is a platform holding great promise, yet graphene growth on this surface remains poorly understood and often results in rotational disorder and mosaicity [1,2]. A key source of ambiguity is that the role of the surface reconstruction, ubiquitous under growth conditions, is often overlooked. In this work, we provide experimental and theoretical results that clearly indicate how graphene epitaxy on sapphire is governed by the reconstructed interface [3,4,5]. Specifically, we show that two low-strain commensurate configurations of graphene on the most stable surface reconstruction under growth conditions, the ($\sqrt{31}\times\sqrt{31}$)R±9° phase, account for the majority of experimentally observed domains. We further suggest an alternative interpretation in which the frequently observed R30 orientation may emerge from the convolution of nearby commensurate diffraction spots, yielding a unified picture of graphene growth on sapphire. Our results highlight interface control as the key requirement for achieving flat, strain-free graphene with epitaxially constrained orientations on sapphire, and establish a consistent framework to interpret the commonly observed R30 feature and mosaicity.

References

[1] N. Mishra et al., Small **15**, 1904906 (2019).
[2] J. Hwang et al., ACS Nano **7**, 385 (2012).
[3] M. Gautier et al., J. Am. Ceram. Soc. **77**, 323 (1994)
[4] J. V. Lauritsen et al., Phys. Rev. Lett. **103**, 8 (2009)
[5] J. I. Hutner et al., Science **385**, 1241 (2024).

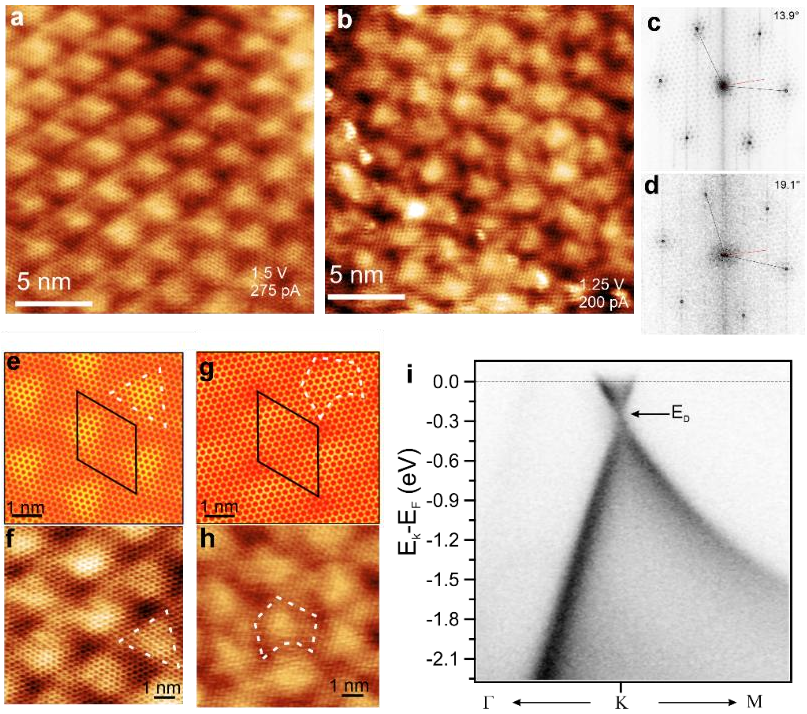

Fig. 1: **Structural and electronic properties of graphene/r31/sapphire. a** STM of r117. **b** STM on r112. **c** 2D-FFT of panel **a**. **d** 2D-FFT of panel **b**. **e** simulated pseudo-height map of r117. **f** measured STM on r117. **g** simulated pseudo-height map of r112. **h** measured STM on r112. **i** ARPES spectrum of Gr/r31/sapphire.

Controlled Partial Gallium Intercalation in Epitaxial Graphene Hall Bars A 2D Normal-Superconductor Junction

D. Höllmann[1], M. Bothe[1], S. Wundrack[1,2], J. C. Bayer[1], M. Gruschwitz[3], K. Pierz[1], A. Bakin[2], C. Tegenkamp[3], Rainer Stosch[1], H. W. Schumacher[1], and T. M. Tschirner[1]

[1] Physikalisch-Technische Bundesanstalt, Bundesallee 100, 38116 Braunschweig, Germany
[2]Institut für Halbleitertechnik, TU Braunschweig, Hans-Sommer-Str. 66, 38106 Braunschweig, Germany
[3]Institut für Physik, TU Chemnitz, Reichenhainer Str. 70, 09126 Chemnitz, Germany

Two-dimensional (2D) systems provide unique opportunities to tune electronic properties via proximity effects, allowing the controlled emergence of distinct electronic phases [1]. Intercalation of Gallium beneath epitaxial graphene on SiC forms a two-dimensional Gallium layer (2DGa) that induces superconductivity while decoupling the buffer layer from the substrate, converting it into quasi-freestanding bilayer graphene (QFBLG) [2]. The SiC/2DGa/QFBLG heterostructure has been shown to exhibit superconductivity with a critical onset temperature of $T_c \approx 3.5$ K, where the superconducting path is confined within the 2DGa layer [3]. High-quality samples are realized using polymer-assisted sublimation growth (PASG) [4], ensuring well-defined interfaces and reproducible electronic properties.

We introduce a device concept for the fabrication of Hall bar structures featuring a spatially defined normal-to-superconductor transition within a single 2D material system. The concept exploits the anisotropic diffusion of liquid gallium along SiC terrace directions, driven by the liquid metal intercalation technique (LiMIT) [3], to realize controlled partial intercalation of epitaxial graphene Hall bars. Orienting the Hall bar geometry perpendicular to the preferential $[1\bar{1}00]$ diffusion direction and controlling the intercalation process allows us to intercalate one half of the Hall bar, while leaving the other half as pristine epitaxial graphene. Consequently, a lateral junction forms at the boundary separating the 2DGa/QFBLG and monolayer epitaxial graphene region.

Precisely positioning and characterizing this interface yields a reproducible platform for investigating confined 2D superconductivity, proximity-induced effects at lateral junctions, possible Andreev reflection processes, and the interplay of structural inhomogeneity and electronic transport across the junction.

References:

[1] M. Bora and P. Deb, J. Phys. Mater **4**, 034014 (2021).
[2] S. Wundrack et al., Phys. Rev. Materials **5**, 024006 (2021).
[3] S. Wundrack et al., Adv. Mater. **38**, e11992 (2026).
[4] M. Kruskopf et al., 2D Mater. **3**, 041002 (2016).

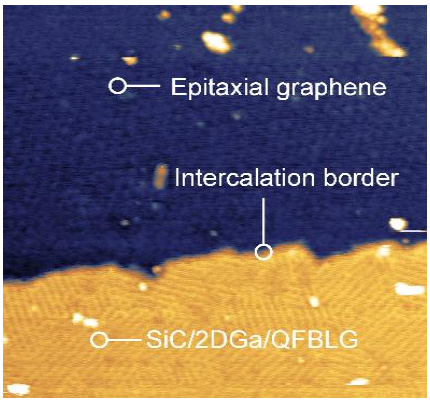

Fig. 1: Scanning tunneling microscopy (STM) image of the transition from Ga-intercalated QFBLG (yellow) to pristine epitaxial graphene (blue).

Graphene bolometers and calorimeters

Mikko Möttönen

QCD Labs, Aalto University

In this talk, I focus on our recent progress in ultrasensitive bolometers and calorimeters tailored for superconducting quantum circuits and fundamental radiation sensing. Thermal detectors have long been valued for their simplicity and absence of added quantum noise, and recent developments have pushed their performance into the regime required for circuit quantum electrodynamics [1].

We have recently demonstrated single-shot readout of a superconducting qubit using a nanobolometer, achieving a fidelity of 0.618 with a readout duration of 13.9 μs, mainly limited by qubit relaxation [2]. Removing relaxation errors indicates an intrinsic fidelity of 0.927, highlighting the strong potential of calorimetric qubit readout. In parallel, multiplexed operation of superconductor–normal-conductor–superconductor sensors has been realized with low cross-talk, paving the way toward scalable multi-qubit readout architectures [3].

A major recent milestone is our demonstration of zeptojoule calorimetry, where we resolve the energy of microwave pulses with a full-width-at-half-maximum resolution below 1 zJ [4]. This level of sensitivity opens a realistic path toward real-time single-photon detection in the 10 GHz range using graphene calorimeters [1] and enables new experiments in quantum thermodynamics, microwave quantum optics, and axion searches. Complementary measurements of microwave photon correlations using nanobolometers further confirm the photon-number resolving capability of thermal detectors at millikelvin temperatures [5].

Looking forward, graphene-based devices [1] are expected to further improve speed and energy resolution. I will present our latest progress toward graphene nanobolometers and discuss very recent, yet unpublished, results on epitaxial graphene devices.

References:
[1] R. Kokkoniemi et al., Nature 586 (2020) 47.
[2] A. M. Gunyhó et al., Nature Electronics 7 (2024) 288.
[3] P. Singh et al., arXiv:2411.12782 (2024).
[4] A. M. Gunyhó et al., arXiv:2412.14079 (2024).
[5] A. Keränen et al., arXiv:2407.05147 (2024).

Quantitative Photocurrent Decomposition in Epitaxial Graphene/6H-SiC Photodetectors

B. Morzhuk, T. Fridrišek, M. Shestopalov, V. Dědič, M. Rejhon, J. Kunc

Charles University, Faculty of Mathematics and Physics, Institute of Physics, Ke Karlovu 5, CZ-121 16, Prague 2, Czech Republic

Silicon carbide arises as promising material for ultraviolet (UV) photodetection in harsh environments—the wide bandgap (2.2-3.25 eV), high thermal conductivity, and chemical stability make it naturally suited for solar-blind UV sensing required in application ranging from combustion control and space-borne instruments to emerging quantum technologies [1]. The metal-semiconductor-metal (MSM) configuration is attractive for its fabrication simplicity and low parasitic capacitance, but conventional metal electrodes introduce optical shadowing that directly hampers quantum efficiency—a fundamental trade-off between field topology and optical access [2]. Epitaxial graphene (EG), grown on SiC by thermal decomposition, offers an alternative: it forms a Schottky contact with SiC without a prior transfer, absorbs only ~0.67% of incident broadband light and is thermally stable at wide range of temperatures. Despite these advantages, only a handful of EG/SiC MSM structures have been reported, and no experimental UV photodetector based on V-doped semiinsulating 6H-SiC with EG electrodes has been demonstrated to date.

We develop a Ramo–Shockley [3] simulation framework that quantitatively decomposes the spatially resolved photocurrent of EG/6H-SiC MSM photodetectors into bulk SiC (IQE ≈ 9 × 10^{-6}) and graphene IPE (~3%) contributions with a complete uncertainty budget (Fig. 1). Comparing graphene with simulated gold equivalents of identical field topology yields +-2-3 times signal gain from electrode transparency alone. At UV wavelengths, graphene IPE drops below 0.01% of total photocurrent, making EG a spectrally neutral transparent contact that decouples electrode design from optical shadowing

References:
[1] F. La Via et al., Micromachines 14 (2023) 1200
[2] S. Jang et al., J. Electrochem. Soc. 154 (2007) H830.
[3] Z. He, Nucl. Instrum. Methods Phys. Res. A 463 (2001) 250.

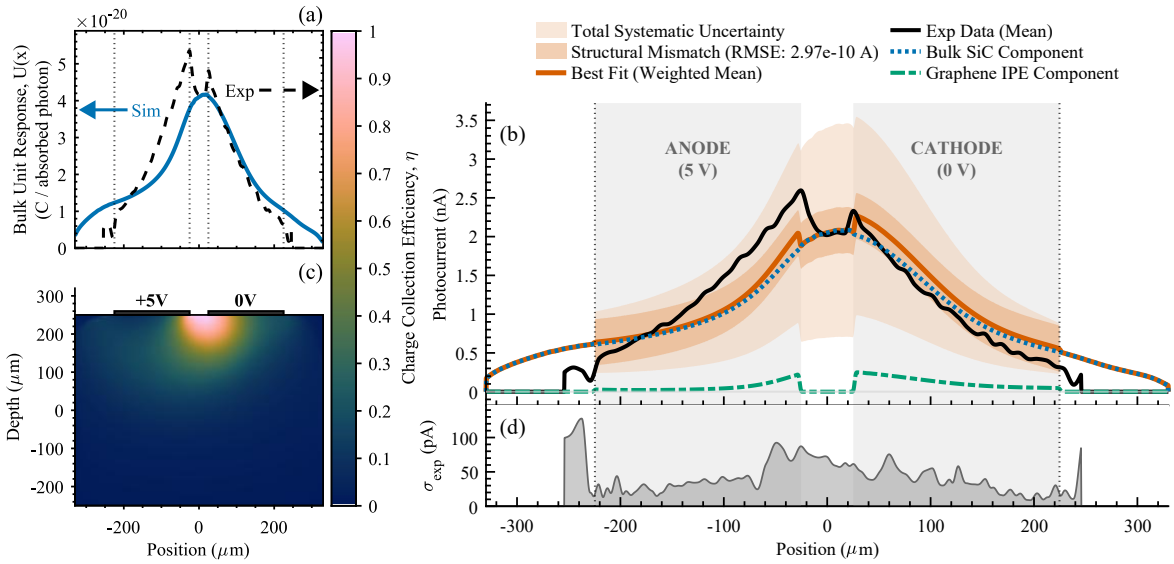

Fig. 1: Modeling of the device (200 μm electrode width, 100 μm gap, at 5 V bias, 532 nm excitation) and the photocurrent decomposition pipeline. (a)—overlay of the experimental photocurrent profile (black dashed, right axis) against the bulk unit response profile U(x) (solid blue, left axis), representing the expected induced charge per absorbed photon at position x; (b)—result (vermillion) of the U(x) scaled by incident laser flux and fitted to experiment (black), accompanied by shaded bands indicating structural mismatch (RMSE, darker) and total systematic uncertainty (lighter), and separate bulk SiC (blue dotted) and graphene IPE (bluish green dashed) contributions are shown; (c)—CCE map obtained via Shockley-Ramo trajectory tracking in a numerically solved Laplace field of photogenerated electron-hole pairs injected as spatial delta functions; (d)—the standard deviation of experimental photocurrent across the multiple scan lines at each spatial position x.

Quantitative imaging of surface potential: From molecules on metals towards charge density waves on 2D materials

S. Anchamkudy[1,2], J. Lorenz[1,3,4], H. Thake[5], A. Karimi[1], R. Temirov[1,2], R. J. Maurer[5,6,7], C. Wagner[1], F. S. Tautz[1,3,4], F. Lüpke[1,2,3]

[1] Peter Grünberg Institut (PGI-3), Forschungszentrum Jülich, Germany
[2] II Physikalisches Institut, University of Cologne, Germany
[3] Jülich Aachen Research Alliance (JARA), Germany
[4] Institut für Experimentalphysik IV A, RWTH Aachen University, Germany
[5] Department of Chemistry, University of Warwick, United Kingdom
[6] Department of Physics, University of Warwick, United Kingdom
[7] Faculty of Physics, University of Vienna, Austria

In this poster, I will discuss Scanning Quantum Dot Microscopy (SQDM) technique and its important results along with our recent advancements in broadening its application to 2D materials. SQDM is an extension of non-contact atomic force microscopy technique that uses charge state of a molecular quantum dot (perylene tetracarboxylic dianhydride (PTCDA)) attached to a tip to probe surface dipoles [1]. Developed at Peter-Grünberg-Institute (PGI-3) in Forschungszentrum Jülich, SQDM has been applied to molecular adsorbates, adatoms, defects, and atomic assemblies on the Ag surface [2,3] - and provided valuable benchmarks for theory where metal-organic hybrid systems are particularly challenging. Our recent results on measuring PTCDA molecules deposited on Ag (111) show the higher sensitivity of this technique. We could identify two preferred adsorption orientations (<1-10> and <11-2>) of PTCDA which differ by 30 degrees from each other showing distinctly different surface dipoles (-0.51 D and -0.65 D respectively). We also measured PTCDA deposited on Pb (111) and found that the PTCDA molecule has more than five times larger dipole when it is on Pb (111) compared to when it is on Ag (111). This difference can be attributed to significantly different charge transfer and adsorption height. Building on this established sensitivity of SQDM to surface potential, we extend the application of SQDM to investigate charge density waves (CDWs) in 2D materials. Although charge density variations with different CDWs in 2H-$NbSe_2$ and 1T-TaS_2 have already been imaged through scanning tunneling microscope, a quantitative mapping of surface potential variations by these CDWs are not done. On the way to this goal, we could already successfully deposit PTCDA molecules on $NbSe_2$ and our scanning tunneling experiments show clean PTCDA island with herringbone structure. Due to strong inter-molecular interactions, big islands are formed even with shorter deposition time. Currently we are optimizing the controlled picking up of PTCDA from the $NbSe_2$ surface to use it as the probe for executing SQDM technique.

References:
[1] C. Wagner, M. F. Green et al., Phys. Rev. Lett. 115, 026101 (2015).
[2] R. Bolat, J. M. Guevara et al., Nat Commun 15, 2259 (2024).
[3] C. Wagner, M. F. Green et al., Nat. Mater. 18, 853 (2019)

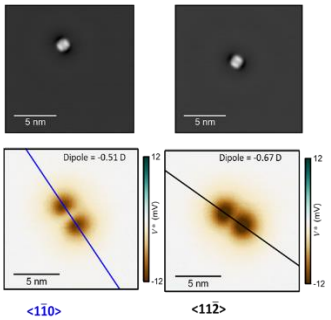

Fig. 1: SQDM results of PTCDA dipole on Ag (111) showing orientation dependence. Top two are the STM images of PTCDA molecules orienting in <1-10> and <11-2>. Bottom plots show the corresponding surface potential with the dipole values mentioned on the upper right corner.

Towards enhanced spin-orbit coupling in epitaxial graphene via Pb intercalation

M.Gruschwitz[1], S. Sologub[1,2], H. Jeon[3], S. Hus[3], A-P. Li[3], C. Tegenkamp[1]

[1] Institut für Physik, Technische Universität Chemnitz, Reichenhainer Str. 70, 09126 Chemnitz, Germany
[2] Institute of Physics, NAS of Ukraine, Nauki avenue 46, 03028 Kyiv, Ukraine
[3] Center for Nanophase Materials Sciences, Oak Ridge National Laboratory, Tennessee 37831, United States

The design of noval quantum phases by combining low dimensional materials poses the next evolution step of electronics. Intercalated epitaxial graphene on SiC embodies a van-der-Waals heterostack with well-defined lattice arrangement. Stabilizing monolayers of heavy elements in proximity to graphene, potentially enhances the spin-orbit interaction (SOI) in graphene. Using Pb as intercalant, we reliably decouple and neutralize graphene by minimizing the substrate influence. At the interface coexisting striped and hexagonal superstructures emerge from local strain and density variations in the Pb monolayer. [1] Multiprobe transport measurements, assisted by finite element simulations, revealed a temperature dependent resistance. This emergent behavior was attributed to a gap opening in graphene in the order of 3-5 meV. [2] Tip–sample spacing dependent spectroscopy supports this finding by a clearly reduced density of states at the Dirac point. The desired enhanced intrinsic SOI competes with Rashba-SOI and modulations of the sublattice potential by the Pb superstructure. Although the nature of this gap was not revealed yet, it has potential to stabilize a quantum spin Hall state.

References:
[1] M. Gruschwitz et al., Adv. Mater. Interfaces 12, 21 (2025) e00617
[2] M. Gruschwitz et al., Phys. Rev. B 109 (2024) 245430

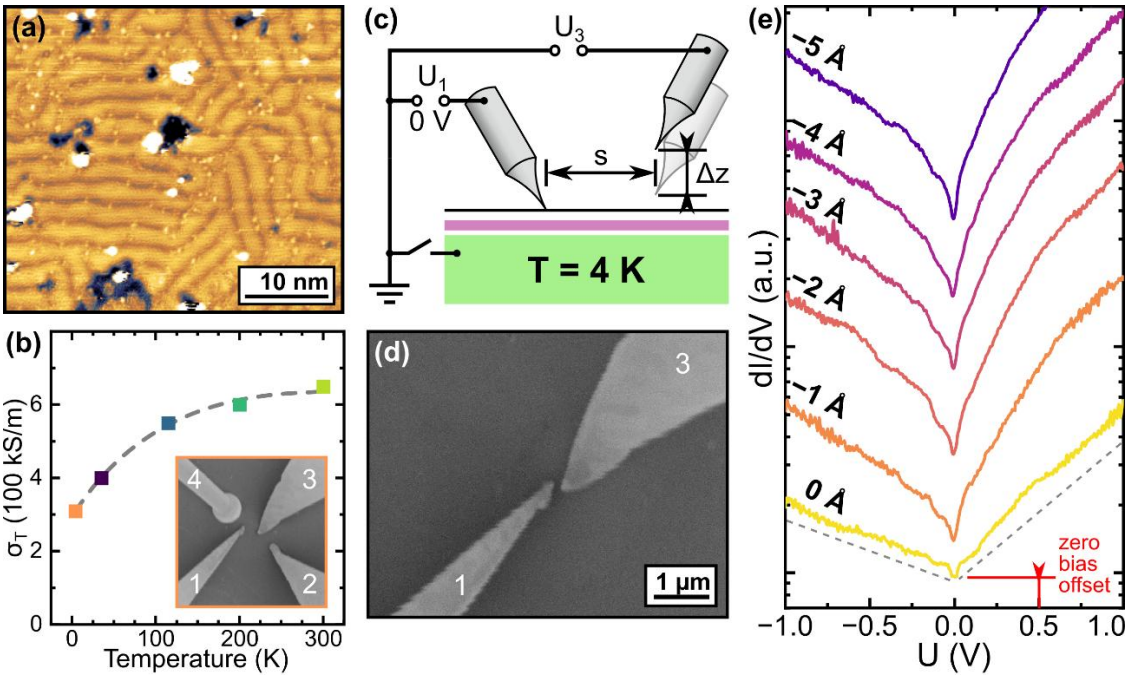

Fig. 1: Overview of transport measurements on Pb intercalated epitaxial graphene. Extended intercalated phases reveal a mixture of stripe and hexagonal Pb interface structures (a). (b) Temperature dependent local four-probe transport measurements indicated a small gap opening in the graphene layer. This gap opening was confirmed by tunneling spectroscopy (e) in a two probe setup with varied tunneling gap sizes (c). The second probe for local grounding suppresses non-local contributions in the tunneling spectra (d).

Shear-resistant topology and electrical anisotropy quasi-one-dimensional van der Waals material α-Bi_4Br_4

Jonathan K. Hofmann[1,2], Serhii Kovalchuk[1,3], Mingqian Zheng[4], Yuqi Zhang[4], Vasily Cherepanov[1], Timofey Balashov[1], Jin-Jian Zhou[4], Zhiwei Wang[4], Yugui Yao[4], Irek Morawski[3], F. Stefan Tautz[1,2], Felix Lüpke[1,5], and Bert Voigtländer[1,2]

[1] Peter Grünberg Institut (PGI-3), Forschungszentrum Jülich, Germany
[2] Experimentalphysik IV A, RWTH Aachen University, Germany
[3] Institute of Experimental Physics, University of Wrocław, Poland
[4] Key Laboratory of Advanced Optoelectronic Quantum Architecture and Measurement, Beijing Institute of Technology, China
[5] II. Physikalisches Institut, Universität zu Köln, Germany

α-Bi_4Br_4 is a quasi-one-dimensional material [see Fig. 1(a)]: covalently bonded Bi_4Br_4 chains are arranged in parallel, side-by-side and layer-by-layer, with van der Waals gaps in between [1,2,3]. Bulk α-Bi_4Br_4 is higher-order topological insulator [1]. At step edges on the (001) surface, quantum spin Hall (QSH) edge states are present [2], that can be observed up to room temperature [1].
Using a scanning tunneling microscope (STM), we analyzed a cleaved bulk crystal [3]. Fig. 1(b) shows STM topography of the (001) surface, showing a significant shift of the chains, relative to each other in crystallographic *b* direction [3]. We attribute this shift to shear stress arising from cleaving or gluing the crystal or from domain boundaries. Scanning tunneling spectroscopy [Fig. 1(c)] shows the bulk band gap on the terraces and a metallic density of states at step edges, which we attribute to the QSH edge states. Density functional theory (DFT) confirms that a strained monolayer of Bi_4Br_4 is a QSH insulator with $\mathbb{Z}_2 = 1$ [3].
Furthermore, we used a four-tip STM to disentangle the elements of the resistivity tensor of α-Bi_4Br_4 *in situ*. For this measurement, we prepared a bulk sample of α-Bi_4Br_4 to measure the anisotropy in the *ab*-plane [Fig. 1(d)] and a flake sample to measure the resistivity component ρ_b. Due to its crystal structure [Fig. 1(a)], α-Bi_4Br_4 tends to form long rectangular flakes. At room temperature, we find $\rho_b = 10(3)\ \mathrm{m\Omega cm}$ and an in-plane anisotropy of $A = 6.4(5)$. The out-of-plane component is much larger: $\rho_z = 11(3)\ \Omega\mathrm{cm}$. While the low resistivity along the chains (*b* direction) is expected from the crystal structure, the large difference between ρ_a and ρ_z is noteworthy. We attribute this marked difference in resistivity to the weak inter-layer coupling found by DFT [2].

References:
[1] Shumiya, N., *et al.*, *Nat. Mater.* **21**, 1111–1115 (2022).
[2] Zhou, J.-J., Y., *et al.*, *Nano Lett.* **14**, 4767–4771 (2014).
[3] Hofmann, J. K., *et al.*, *Phys. Rev. B* **111**, 245415 (2025).

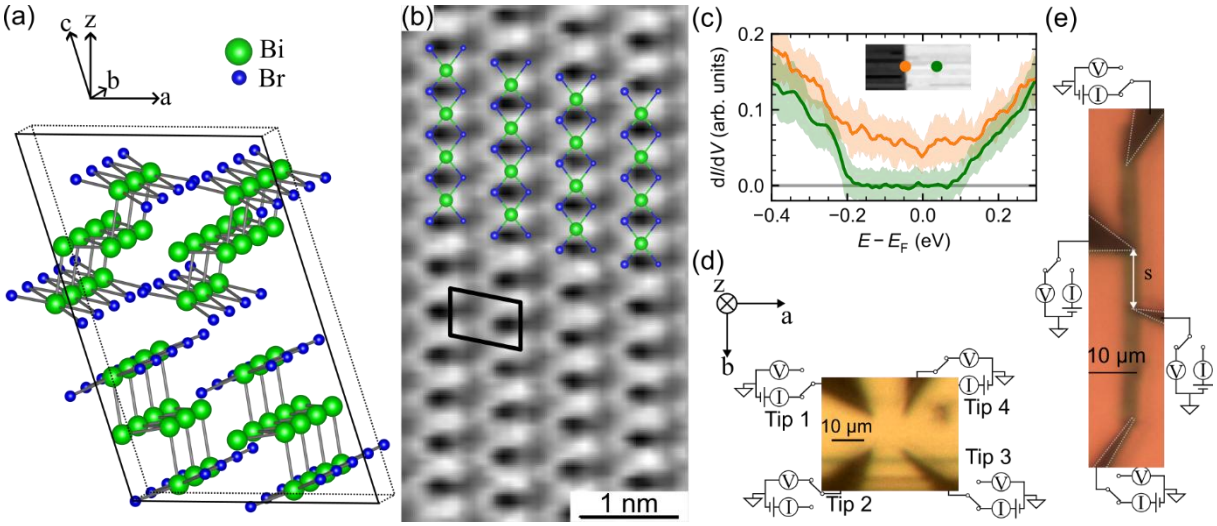

FIG. 1: (a) Model of the crystal structure of α-Bi_4Br_4. (b) STM topography of the α-Bi_4Br_4(001) surface showing the $^b/_3$ structure. A modified crystal model has been overlayed. (c) STS showing the bulk band gap visible on the (001) surface and metallic DOS present at a step edge. (d) Transport measurements in a square geometry on a bulk sample. (e) Linear transport measurements on an exfoliated flake.

Growth of carbon nanotubes on the surface of SiC powder by controlling pressure and gas atmosphere

Shuri Inagaki, Wataru Norimatsu

Faculty of Science and Engineering, Waseda University

Carbon nanotube (CNT) is a material with cylindrical structure of graphene, and has high thermal conductivity, electrical conductivity and large specific surface area. Closely-packed CNTs thin film can be produced by the thermal decomposition of SiC [1]. The nanometer-scale structure after thermal decomposition of SiC varies depending on the heating atmosphere, such as pressure and oxygen concentration. CNT/SiC composite particles have large specific area, so they are promising candidates for use to support catalyst in them. In this study, we optimized the CNT growth conditions from the SiC particles.

Averaged diameter of the SiC particles was about 2 μm. As a pretreatment, the powder was ground with a mortar and pestle. It was then introduced into a rotating container and was heated to 1500℃. The powder was heated under either N_2 : O_2 = 79 : 21 or pure O_2 atmosphere, with the flow rate of 0.05 sccm. The pressure during heating was maintained to 10^0, 10^1, 10^2, or 10^3 Pa. To ensure continuous exposure of the surface to gas, the container was rotated with the speed of 6 rpm, in the temperature range from 1200 to 1400 ℃. The samples were observed by JEM-2100-type transmission electron microscope (TEM).

Figure 1 shows TEM images of the sample which were heated under N_2/O_2 gas at 10^0 or 10^2 Pa. Under both conditions, linear contrast parallel to the surface of the particle was observed, indicating the formation of graphite covering the SiC particle. According to the previous studies, it is due to the lack of oxygen needed for CNT growth [2,3]. Figure 2 shows TEM images of the samples which were heated under pure O_2 gas at 10^0 or 10^2 Pa. In the sample which was heated at 10^0 Pa, linear contrast parallel to the surface of the particle was observed, similar to those in Figure 1, indicating the formation of graphite covering the SiC particle. This is also attributed to the insufficient oxygen supply. In contrast, in the sample which was heated at 10^2 Pa, linear contrasts perpendicular to the surface of particle was observed, indicating the growth of CNTs. However, their orientation was poor. These results suggest that appropriate control of the oxygen supply is necessary for the formation of highly orientated CNTs.

[1]M. Kusunoki, *et al*., Chem Phys. Lett. **366**, 458(2002).
[2]W. Norimatsu, *et al*., Chem Phys. Lett. **468**, 52(2009).
[3]M. Kusunoki, *et al*., Appl. Phys. Lett. **77**, 531(2000).

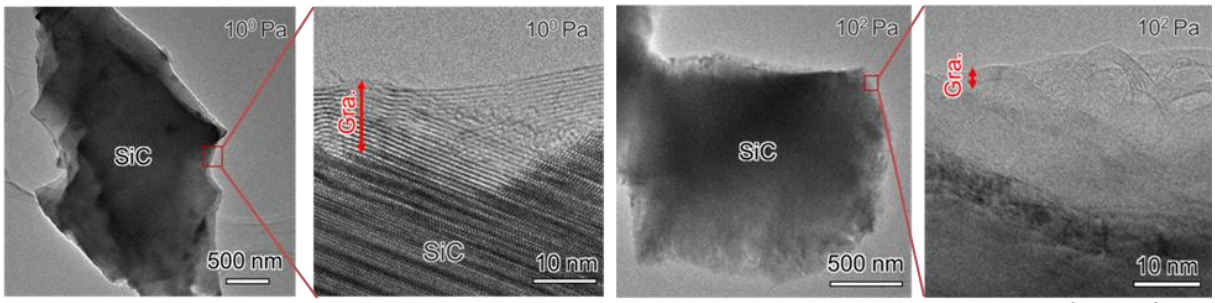

Fig. 1 TEM images of the samples which were heated under N_2/O_2 mixed gas at 10^0 or 10^2 Pa.

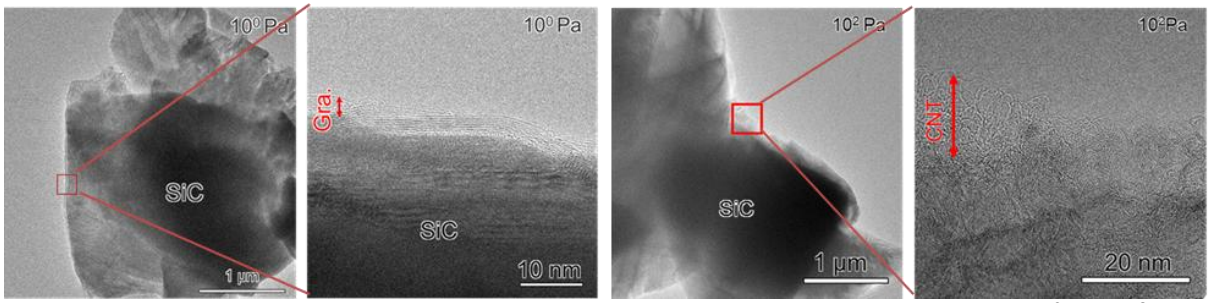

Fig 2 TEM images of the samples which were heated under pure O_2 gas at 10^0 or 10^2 Pa.

Fabrication of graphene/Mo_2C/SiC heterostructure and its electrical states

Takuya Kamimura[1], Takahiro Ito[2], Akinobu Kanda[3], Hiroki Hibino[4],Wataru Norimatsu[1]

[1] Faculty of Science and Engineering, Waseda University, Japan
[2] Nagoya University Synchrotron Radiation Research Center (NUSR), Nagoya University, Japan
[3] Department of Physics, Faculty of Pure and Applied Sciences, University of Tsukuba, Japan
[4] School of Engineering, Kwansei Gakuin University, Japan

Graphene/superconductor interfaces are expected to host unique quantum phenomena, such as proximity-induced superconductivity in graphene. In this study, we focus on hexagonal Mo_2C, which exhibits a superconducting transition at approximately 3.2 K [1] and has also been proposed as a candidate of a topological superconductor because of its fourfold-degenerate nodal line crossing the Fermi level. Since the lattice constant of hexagonal Mo_2C (a = 3.01 Å) is close to that of 4H-SiC (a = 3.08 Å), epitaxial growth of Mo_2C on SiC is expected. In our previous studies, TiC and B_4C thin films were formed on SiC substrates, and graphene was subsequently synthesized on their surfaces by thermal decomposition of the carbides [2,3]. Based on these backgrounds, we grew a Mo_2C thin film on a 4H-SiC single-crystal substrate, followed by graphene growth by thermal decomposition of Mo_2C. We then investigated the surface electronic structure of the graphene/Mo_2C/SiC heterostructure.

Mo_2C thin film was deposited on the 4H-SiC(000$\bar{1}$) substrate by the pulsed laser deposition technique. The substrate was then heated at 1650°C under vacuum (2×10^{-5} Pa) to fabricate a graphene/Mo_2C/SiC heterostructure. The samples were characterized by atomic force microscopy (AFM), reflection high-energy electron diffraction (RHEED), low-energy electron diffraction (LEED), low-energy electron microscopy (LEEM), and angle-resolved photoemission spectroscopy (ARPES).

Our analysis revealed that the orientation relation between Mo_2C and SiC was $(0001)_{Mo2C}//(000\bar{1})_{SiC}$, $[11\bar{2}0]_{Mo2C}//[11\bar{2}0]_{SiC}$. Graphene was grown with multiple orientations of 0°, 15°, 30°, and 45° with respect to the SiC substrate. Figure 1 is the ARPES image of the graphene/Mo_2C/SiC sample. The E-k image exhibited a clear Dirac cone near the K point of graphene, with the Dirac point located approximately 0.4 eV below the Fermi level, indicating electron doping in graphene. It includes multiple Dirac cones due to different graphene orientations. In addition to the bands due to graphene, some bands convex downward were observed around the Γ point, which can be explained by the band structure of Mo_2C.

References:
[1] T. Shang *et al.*, Phys. Rev. B **110**, 064510 (2024).
[2] K. Kimura *et al.*, Phys. Rev. B **87**, 075431 (2013).
[3] W. Norimatsu *et al.*, Nanotechnol. **31**, 145711 (2020).

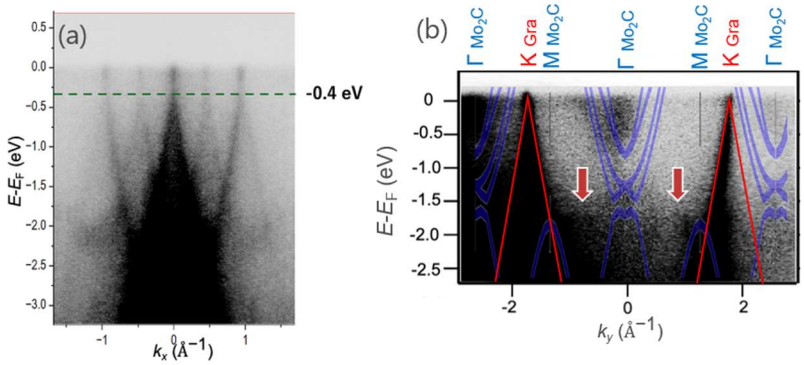

Fig. 1: ARPES images of the graphene/Mo_2C/SiC sample. (a) E-k_x image near the K point of graphene. (b) E-k_y image along the K-Γ-K line of graphene. The band structures of graphene and the Mo_2C(0001) surface, obtained by first-principles calculations, are overlaid by red and blue lines, respectively. The red arrows indicate bands that do not belong to either Mo_2C or graphene.

Functionalization of epitaxial graphene by proximity to heavy metals and TMDs

J. Koch[1], S. Sologub[1,2], N. Jentzsch[1], C. Ghosal[1], C. Tegenkamp[1]

[1] Institut für Physik, Technische Universität Chemnitz, Reichenhainerstr. 70, 09126 Chemnitz, Germany
[2] Institute of Physics, National Academy of Sciences of Ukraine, Nauki avenue 46, 03028 Kyiv, Ukraine

The proximity effect allows for the functionalization of graphene by introducing properties into it that are not inherent to it. In this study, heavy metals and transition-metal dichalcogenides (TMDs) are brought into contact with monolayer graphene (MLG)/SiC(0001) with the aim of increasing graphene's negligible spin-orbit interaction, and investigated by magneto transport, electron diffraction and scanning tunneling microscopy.

Bi deposited at 300 K on MLG/SiC forms of a majority of needle-like Bi(110) islands elongated in the Bi(110) zig-zag direction, which are aligned with the MLG armchair direction except for a small misalignment angle of about 1.75°. Additionally, we observed a minority of needle-like Bi(110) islands orientated roughly orthogonal to the majority structure, whose concentration significantly increased after an annealing step at 410 K. This minority structure has four sub-domains, which we attribute to the formation of mirror twin boundaries, resulting in two potential alignments of Bi(110) majority and minority domains with respect to each other, in addition to two possible alignments of the majority domain with respect to graphene (see figure). The carrier concentration determined from the SdH oscillations remains at $1 \times 10^{13}\ \mathrm{cm}^{-1}$independent of the Bi coverage. In contrast, photoemission spectroscopy shows a strong doping of the graphene by Bi [1], indicating that the carrier concentration is highly anisotropic. This is confirmed by a positive, temperature independent contribution to the magneto resistivity, which indicates that the Bi covered regions are electrically dead zones causing the electrons to scatter at the boundaries. This reduces the mobility from around $2250\ \mathrm{cm}^2/(\mathrm{Vs})$ for MLG to $1920\ \mathrm{cm}^2/(\mathrm{Vs})$ at 2.4 BL Bi, a decrease of approximately 14%. [2,3]

Additionally, single layer MoS_2 flakes and epitaxial WS_2, which are expected to introduce strong spin-orbit coupling in graphene due to their inherent spin structure [3], were brought into contact with MLG/SiC. The influence of the SiC substrate results in TMD states intersecting the Fermi level and therefore contributing to the transport. Sondheimer oscillations were observed in the magneto resistance, indicating a hybridization of the TMD layer with the graphene.

References:
[1] I. Gierz et al., Nano Lett. 8, 12 (2008) 4603
[2] J. Koch et al., J. Phys.: Condens. Matter 36 (2024) 065701.
[3] J. Koch et al., Phys. Rev. B 109 (2024) 235107.
[4] M. Gmitra and J. Fabian, Phys. Rev. B 95 (2015) 155403.

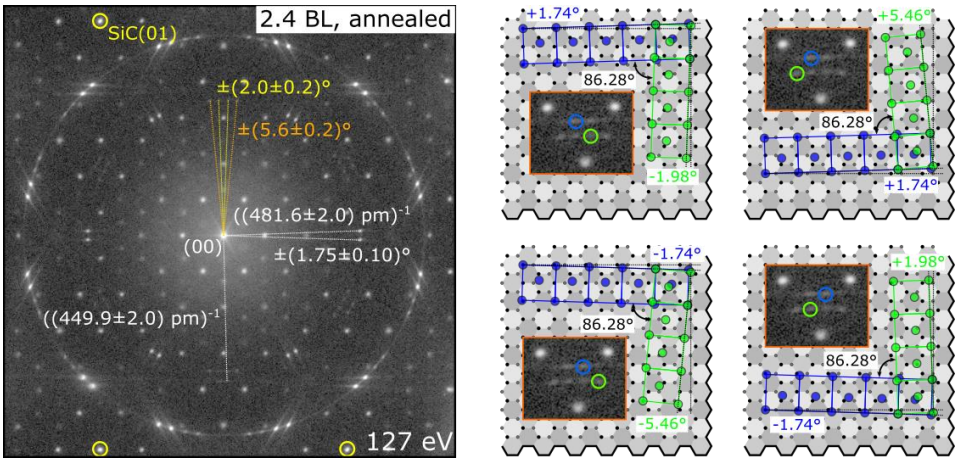

Fig. 1: LEED image of MLG with a Bi coverage of 2.4 BL after annealing at 410 K for 30 min recorded at 127 eV (left). Alignment of the Bi(110) majority (blue) and minority (green) islands with respect to graphene (right). [1]

Intercalation of graphene on SiC: tuning the electronic structure of graphene by proximity coupling and inducing novel 2D interlayer band structures

K. Küster, B. Matta, V. Reddy, S. Datta, U. Starke

Max Planck Institute for Solid State Research, 70569 Stuttgart, Germany

Epitaxial graphene grown on silicon carbide (SiC) has proven to be a suitable candidate for carbon-based electronics [1] as it is directly prepared on a wide band gap semiconductor, thus avoiding cumbersome and size-restricting flake exfoliation or transfer procedures. Homogeneous graphene layers can be fabricated with defined atomic thickness on a wafer scale by using sublimation growth under argon atmosphere [2]. The first carbon layer that is grown is still partially covalently bound to the SiC substrate and is usually called buffer-layer or zero-layer graphene (ZLG). A second layer of carbon can be grown underneath the first one, decoupling it from the substrate, which is referred to as monolayer graphene (MLG). Alternatively, intercalation – a technique used to insert foreign atomic species between the SiC surface and the ZLG – can be used to saturate the dangling bonds of SiC thereby decoupling the carbon layer leading to so-called quasi-freestanding monolayer graphene (QFMLG) as first demonstrated with hydrogen [3].

Intercalation can be used to tune the doping of graphene ranging from the hole regime through charge neutrality to strong n-doping thereby reaching or even going beyond the van Hove singularity (VHS) of graphene's π*-bands. Besides the precise tuning of the doping level of graphene, intercalation can also be used to stabilize otherwise unstable 2D layers underneath the graphene. Those interlayers often exhibit electronic properties strongly deviating from those of their bulk counterpart.

In this poster, we summarize the research highlights of our group within the DFG funded research unit FOR5242. We will demonstrate that the intercalation of Tb can dope graphene beyond the VHS, with a flat band scenario emerging along the $\overline{KMK'}$ direction of the Brillouin zone, residing 70 meV below the Fermi level. This strong n-doping is theoretically predicted to induce d-wave superconductivity with a critical temperature in the range of 300 – 600 mK [4]. Furthermore, we show that the confinement of metallic materials like Ag and Te leads to the development of semiconducting 2D interlayer bands: In the case of Ag the atomic structure of the interlayer and in consequence its band structure as well as the graphene doping and electron-plasmon coupling can be steered by the amount of intercalant by defect engineering of the ZLG. [5] We will also show the first example of an intercalated transition metal alloy, namely AgTe. The possibility to intercalate alloys gives rise to completely new aspects in the field of intercalation and expands the possibilities to tune the band structure of graphene as well as that of the interlayer. Interestingly, the AgTe interface band is metallic in nature, in contrast to the pure Ag and Te interlayers which are semiconducting. Last but not least, we have extensively studied the intercalation of Pb [6-8], which not only shows a pronounced momentum-space spin texture in the Pb layer itself, but also tends to induce a noticeable spin-polarization in the graphene π-bands via proximity coupling.

References:
[1] C. Berger et al., J. Phys. Chem. B 108 (2004) 19912
[2] K. Emtsev et al., Nat. Materials 8 (2009) 203.
[3] C. Riedl et al., Phys. Rev. Lett. 103 (2009) 246804.
[4] S. A. Herrera et al., ACS Nano 18 (2024) 34842.
[5] A. Jain et al., arXiv:2511.07151.
[6] B. Matta et al., Phys. Rev. Res. 4 (2022) 023250.
[7] P. Schädlich et al., Adv. Mater. Interfaces 10 (2023) 2300471.
[8] B. Matta et al., Phys. Rev. B 111 (2025) 155435.

Polymer assisted sublimation graphene growth on 4º off SiC(0001)

Takuto Nishina and Wataru Norimatsu

Faculty of Science and Engineering, Waseda University, Tokyo, Japan

Homogeneous graphene can be grown using a polymer as a carbon source, when the polymer is pre-coated onto a SiC(0001) substrate and then heated. This technique is called polymer-assisted sublimation growth (PASG) and enables graphene growth with suppressed step bunching [1,2]. While 4º off SiC substrates are commonly used in SiC-based power devices, there are no reports of graphene growth on off-axis SiC substrates using the PASG method. In this study, we investigated the effects of off-angle and polymer concentration on graphene growth using the PASG method.

Polymer solutions were spin-coated onto 4H-SiC(0001) substrates with off-angles of 0.0, 0.2, 0.5, 1.0, 2.0, and 4.0º along the [1-100] direction. We used photoresist polymer AZ-5214E dissolved in isopropanol solvent at concentrations of 2000, 3000, 4000, 5000, 6000, 7000, 8000, and 10000 ppm. Graphene samples were grown by heating these substrates in an Ar atmosphere at the temperature optimized for each off-angle.

Figure 1 shows atomic force microscope (AFM) images of samples at different polymer concentrations on a 4.0º off-axis SiC substrate. Compared to 0 ppm, step bunching was effectively suppressed at 5000 ppm. However, at 10000 ppm, numerous substances adhere to the surface, suggesting the presence of excess polymer. Figure 2 shows the averaged step height on the substrate surface at various off-angles and polymer concentrations. It was found that the averaged step height decreased with increasing polymer concentration in all off-angle samples. It was also found that the polymer concentration required to suppress step bunching increased with increasing off-angle. This suggests a correlation between the density of steps where graphene nucleation occurs and the amount of polymer required as a carbon source.

References:
[1] M. Kruskopf, et al., 2D Mater. 3, 041002 (2016).
[2] D. M. Pakdehi, et al., ACS Appl. Mater. Interfaces 10, 6039-6045 (2018).

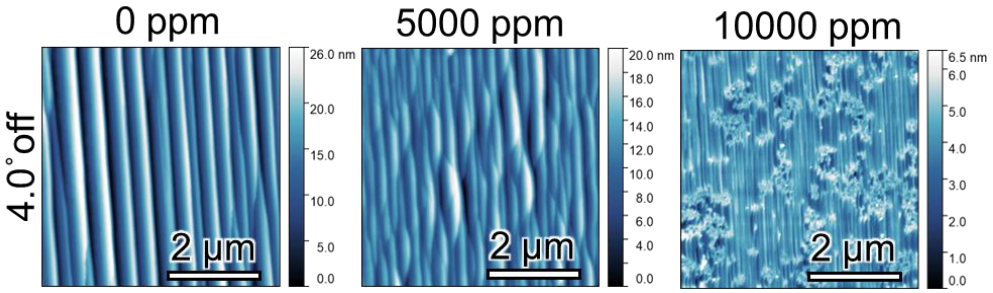

Fig. 1: AFM topography images of the graphene/SiC samples with different polymer concentrations.

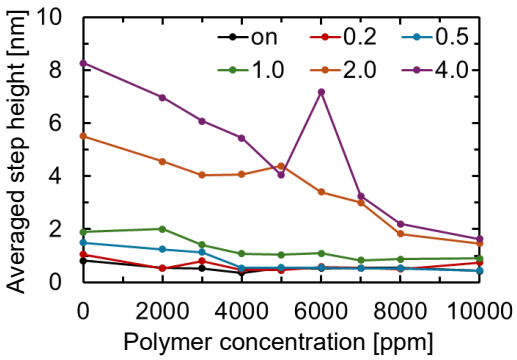

Fig. 2: Averaged step height with different off-axes and polymer concentrations.

Effect of gas flow on carbon nanotubes growth on SiC

F. Onodera, W. Norimatsu

Faculty of Science and Engineering, Waseda University, Tokyo, Japan

Carbon nanotubes (CNTs) can be grown by the SiC surface decomposition method [1]. Contrary to graphene growth from SiC, CNT growth requires heating the SiC(000-1) substrate under vacuum with a little amount of oxygen. Previous studies have shown that heating the SiC(000-1) substrate at 1600°C for 30 minutes in a vacuum of about 1×10^{-2} Pa can form high-density, highly oriented CNTs with a length of about 120 nm [1,2]. In these studies, CNT thin film was grown using a large furnace with graphite insulation which emits oxygen during heating. In this furnace, oxygen emission is hard to control. Therefore, in this study, we grow CNTs using a tabletop tubular furnace under controlled introduction of oxygen into a vacuum. In particular, we investigated the effect of gas flow in the vicinity of the substrate surface.

In this study, a substrate cut from a 4H-SiC(000$\bar{1}$) single crystal wafer manufactured by TanKeBlue, with a thickness of about 400 μm, was used. After cleaning, the substrate was placed on a sample stage and introduced into the center of the furnace tube. The temperature was raised from room temperature to 1500°C at a rate of 7.5°C/min and kept at 1500°C for 2 hours. A nitrogen-oxygen mixed gas (N_2:O_2 = 80:20) was introduced at a flow rate of 0.020 sccm when the temperature reached 1100°C, and the pressure during heating was controlled to be approximately 1.0×10^{-2} Pa. The feature of the CNT film was observed by a transmission electron microscope (TEM).

First, we investigated the characteristics of the CNTs formed when the sample stage arrangement was changed, without gas introduction. When any gas was not introduced, air introduced into the furnace by leakage is the main species in vacuum. Figure 1 shows a schematic diagram of the sample stage and TEM images of the CNT film. In sample #1, non-uniform CNTs with a length of approximately 30 nm were formed. In sample #2, CNTs of uniform length of approximately 70 nm were formed. In these cases, the interface between the CNT film and the SiC substrate was flat. On the other hand, when N_2:O_2 gas was introduced, the interface was different from the above results. In sample #3, long CNTs of approximately 100 nm in length were formed, but their interface was rough. These results suggest that the CNT film was thicker when the gas flow velocity near the substrate surface is high, and that some gas molecules other than N_2/O_2 affect the smoothness of the interface.

References:
[1] M. Kusunoki, *et al.*, Chem. Phys. Lett. 366, 458 (2002).
[2] K. Matsuda, *et al.*, J. Appl. Phys. 123, 045104 (2018).

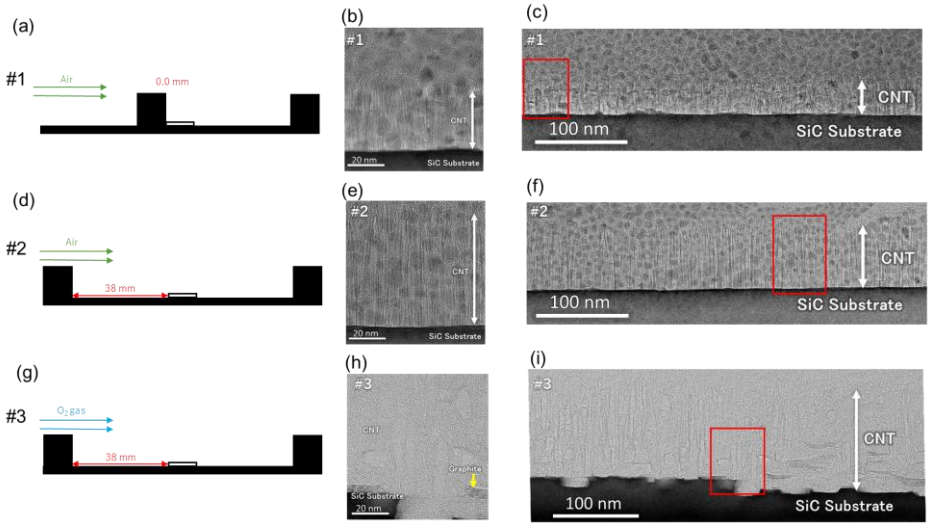

Fig. 1: Schematic diagrams of the sample stage configurations (a) #1, (d) #2, and (g) #3. Low-magnification TEM images of the samples #1, #2, and #3 are shown in (b), (e), and (h), and the corresponding high-resolution TEM images are shown in (c), (f), and (i), respectively.

Reversible transition between (10×10) and (11×11) phases of Pb intercalated EG on 6H-SiC(0001)

S. Sologub[1,2], M. Gruschwitz[1], B. Matta[3], A.D.P. Unigarro[1], P. Rosenzweig[3], S. Gemming[1], K. Küster[3], U. Starke[3], and C. Tegenkamp[1]

[1] Institut für Physik, TU Chemnitz, Chemnitz
[2] Institute of Physics, NAS of Ukraine, Kyiv
[3] Max-Planck-Institut für Festkörperforschung, Stuttgart

The intercalation of metals beneath graphene offers a powerful route to stabilizing and protecting novel 2D phases. Epitaxial graphene (EG) obtained by intercalation of a buffer layer on 6H-SiC(0001) with Pb atoms is the subject of intensive experimental [1,2] and theoretical studies [3] due to its charge neutrality, the band gap opening and proximity superconductivity. We performed a detailed intercalation study of Pb beneath the ZLG on SiC(0001) using low-energy electron diffraction (at the temperatures from 70 K to 600 K, Fig. 1) as well as scanning electron, dark field imaging photoemission electron and tunneling microscopy [4]. Importantly, the degree and ease of intercalation strongly depended on the defect density of the initial buffer layer.

Our analysis revealed the formation of different 2D Pb monolayer phases, such as stripes and hexagons, which emerge due to the interplay between substrate pinning and strain within the Pb layer, depending on local coverage. The interface reconstruction of Pb can be *reversibly* tuned by varying the details of the intercalation protocol within the periodicity range from $(9\times9)_{Gr}$ to $(13\times13)_{Gr}$.

Based on our experiments combined with recent simulations [5], an intercalation model, accounting for the different periodicities observed in the interface layer, was proposed. These findings provide new insights into the strain-driven stabilization of intercalated metal layers and highlight the potential of graphene as a versatile platform for engineering low-dimensional materials.

References:
[1] A. Vera et al., ACS Nano 18 (2024) 21985.
[2] P. Schädlich et al., Adv. Mater. Interfaces 10 (2023) 2300471.
[3] Z. Han et al., Phys. Rev. Mat. 10 (2024) 044002.
[4] M. Gruschwitz et al., Adv. Mater. Interfaces 12 (2025) e00617.
[5] L.-L. Wang et al., Appl. Surf. Sci. 681 (2025) 161572.

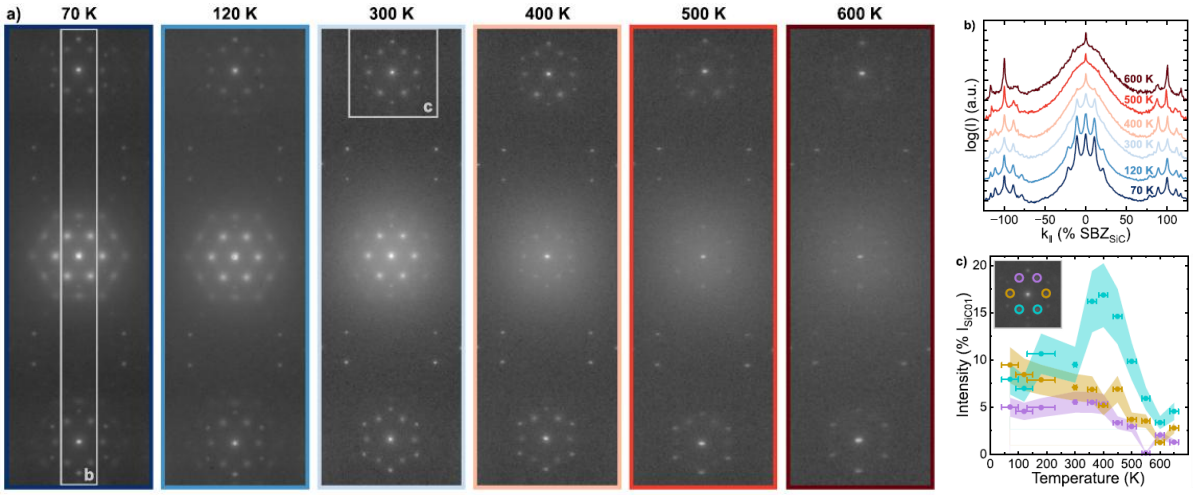

Fig. 1: a) Section of normalized SPA-LEED images along $k_{||,SiC}$ taken at E = 168 eV at various temperatures. The box in the 70 K measurement marks the direction and averaging width of the extracted line profiles plotted in b). A constant offset is added for better visibility. While the quasi-$(10 \times 10)_{Gr}$ reflexes completely vanish at 500 K, two Pb diffraction spots reach maximum intensity relative to the SiC(10) reflex at 400 K. The intensity plot in c) reveals a significant difference in the temperature dependence of the Pb spots around SiC(10). The intensity maxima can be associated with first-order diffraction spots of one α-Pb domain rotated by 3.7° w.r.t. $k_{||,SiC}$.

Selenium intercalation of graphene on SiC(0001)

Susanne Wolff[1,2], Philip, Schädlich[2,3], Thomas Seyller[2,3], Christian Kumpf[1,4]

[1] Peter Grünberg Institute (PGI-3), Forschungszentrum Jülich, Jülich, Germany, and Jülich-Aachen Research Alliance (JARA), Fundamentals of Future Information Technology
[2] Institute of Physics, Chemnitz University of Technology, Chemnitz, Germany
[3] Research Center for Materials, Architectures and Integration of Nanomembranes (MAIN), Chemnitz University of Technology, Chemnitz, Germany
[4] Experimentalphysik IV A, RWTH Aachen University, Aachen, Germany

Intercalation of different atomic species is a powerful method of stabilising a thin layer of material at the interface of graphene and SiC. A variety of elements have already been successfully intercalated, with each of them influencing the electronic properties of the decoupled graphene. For example, the intercalation of hydrogen results in a p-type doping of the graphene [1], whereas decoupling with copper leads to electron doped graphene [2]. Depending on the number of atoms present at the interface, the intercalation with gold [3] or bismuth [4,5] can lead to n-type or p-type doping of the graphene.

However, intercalation not only manipulates the properties of graphene, but also enables the synthesis of novel phases of two-dimensional (2D) materials that would otherwise be unstable. For example, a 2D lead layer can form at the interface where the intercalated atoms arrange in either (1×1) [6] or (10×10) [7–9] periodicity. In both cases, the intercalant compensates the spontaneous polarisation of the SiC substrate, resulting in a doping of the lead layer and charge neutrality of the decoupled graphene layer above.

In this project we investigated the intercalation of selenium at the interface between the zeroth layer graphene (ZLG) and the SiC. The intercalation process was carried out in a two-zone tube furnace containing two individually heatable zones, with $SnSe_2$ acting as the selenium precursor. X-ray photoelectron spectroscopy (XPS) and angle-resolved photoelectron spectroscopy (ARPES) revealed the successful formation of a p-doped quasi-freestanding graphene with selenium atoms present at the interface as well as on top of the non-intercalated ZLG. Similar observations were made for the intercalation of sulfur [10]. However, in contrast to sulfur-intercalated graphene, an additional annealing in UHV at elevated temperatures caused the selenium atoms to evaporate from the surface without further decoupling of the ZLG. Upon annealing, a new component Se* appeared in the Se core levels (see Fig. 1), corresponding to atoms at the graphene/ SiC interface, and the hole doping of the decoupled graphene layer was increased. Low-energy electron microscopy (LEEM) could potentially help to elucidate the origin of the two different selenium intercalation species.

References:
[1] C. Riedl et al., Phys. Rev. Lett. 103 (2009) 246804.
[2] S. Forti et al., 2D Mat. 3 (2016) 035003.
[3] I. Gierz et al., Phys. Rev. B 81 (2010) 235408.
[4] Y. Sohn et al., J. Korean Phys. Soc. 78 (2021) 157.
[5] S. Wolff et al., New J. Phys. 26 (2024) 103009.
[6] F. Schölzel et al., Small Struct. 6 (2025) 2400338.
[7] A. Yurtsever et al., Small 12 (2016) 3956.
[8] M. Gruschwitz et al., Materials 4 (2021) 7706.
[9] B. Matta et al., Phys. Rev. Res. 4 (2022) 023250.
[10] S. Wolff et al., Adv. Mater. Interfaces 11 (2024) 2300725.

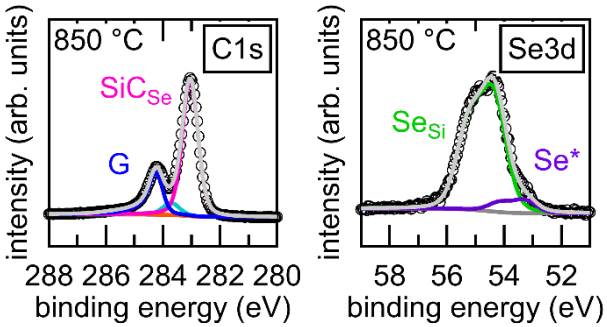

Fig. 1: C1s and Se3d core level of a partially intercalated ZLG sample after annealing at 850°C in UHV

Mechanism of step unbunching phenomenon on 4° off-axis 4H-SiC (0001) surface

M. Yokose, W. Norimatsu

Faculty of Science and Engineering, Waseda University, Tokyo, Japan

In the graphene growth process by thermal decomposition of SiC, step bunching of the SiC surface occurs. The higher step height, the greater the electrical resistance of the graphene covering the step[1]. Therefore, it is necessary to maintain a flat surface with low steps. Recently, a stap unbunching phenomenon was discovered on on-axis 4H-SiC (0001) surfaces, in which steps that had once become high due to step bunching separated into lower steps by the subsequent heating at the lower temperature[2]. On the other hand, weather or not the step unbunching phenomenon occurs on 4° off-axis substrates, which have much high step density, and its mechanism remains unclear. Thus, in this study we aimed to elucidate the mechanism of step unbunching on 4° off-axis 4H-SiC (0001) substrates.

First, the 4° off-axis 4H-SiC (0001) substrates were heated at 1650°C under atmospheric pressure of Ar/H_2 (vol.%) in order to obtain high steps. Then, the sample temperature was directly lowered to 1400°C, and kept at this temperature for 4~20 minutes. The surface morphology of the samples was observed by an atomic force microscope (AFM).

Figure 1 shows the AFM topographic images and the corresponding height profiles of the samples heated (a) at 1650°C for 10 minutes, and (b) at 1650°C for 10 minutes followed by holding at 1400°C for 20 minutes. In (a), steps with a height of approximately 20-50 nm were observed. In (b), the number of high steps decreased and broad facets of approximately 2 μm were formed, which suggest step unbunching, as indicated by red arrows in the figure. In addition, surface irregularities as shown by blue arrows, which were not b=observed on on-axis substrates, were found on some facets. These results suggest that the step ubunching on 4° off-axis substrates proceeds via a different mechanism form on-axis substrates.

References:

[1] H. Watanabe and T. Hosoi, Intech 9 (2012) 235-150.

[2] R. Sakakibara, J. Bao, K. Yuhara, K. Matsuda, T. Terasawa, M. Kusunoki and W. Norimatsu, Appl. Phys. Lett. 123 (2023) 031603.

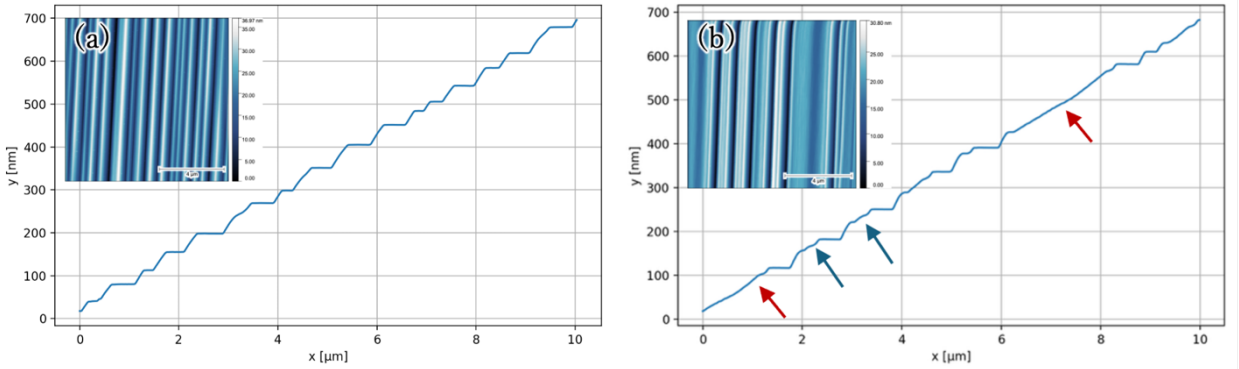

Fig: AFM topographic images and corresponding height profiles of samples (a) held at 1650°C for 10 minutes and (b) subsequently held at 1400°C for 20 minutes.

Vapor-Controlled Growth of Semiconducting Epitaxial Graphene

Ziceng ZHANG[1],Yu FENG[1], Chenxi LIU[1], Junchi SONG[1], Chengxin JIANG[1,2], Qiujuan SUN[2], Ziqiang KONG[1], Zijian WANG[1], Yihui QU[1], Shengda GAO[3], Jian FENG[4],and Haomin WANG[1,2]

[1]State Key Laboratory of Materials for Integrated Circuits, Shanghai Institute of Microsystem and Information Technology, Chinese Academy of Sciences, Shanghai, 200050, China
[2]Shanghai Grapheneflag Technology Co., Ltd., Building 49, No. 6999 Chuansha Road, Pudong New Area, Shanghai, 201202, China
[3]School of Advanced Technology, Xi'an Jiaotong-Liverpool University, Suzhou, 215123, China
[4]Shanghai Institute of Measurement and Testing Technology, Shanghai Key Laboratory of On-line Testing and Control Technology, Shanghai, 201203, China

Semiconducting epitaxial graphene (SEG) formed on the Si-terminated face of silicon carbide (SiC) has emerged as a highly promising 2D semiconductor, exhibiting a well-defined bandgap and ultrahigh room-temperature mobility [1]. However, achieving macroscopic homogeneity remains a critical challenge due to the complex and often non-equilibrium silicon sublimation dynamics in conventional confinement-controlled sublimation (CCS) [2]. In this work, we demonstrate that the morphology and structural order of SEG can be deterministically regulated by controlling the local silicon vapor pressure during high-temperature annealing. We systematically investigated the surface reconstruction dynamics of SiC(0001) using two distinct quasi-equilibrium growth configurations: the face-to-face (FTF) and face-to-graphite (FTG) methods. Our experimental results reveal that the FTF configuration establishes a highly confined micro-environment with a saturated Si vapor pressure, which thermodynamically drives extensive and sequential step bunching [3]. This dynamic coalescence of underlying substrate steps yields macroscopic, wide, and atomically flat terraces, allowing for the continuous nucleation and growth of large-area SEG [4]. Conversely, the FTG method alters the local mass transport, leading to a different Si vapor environment where substrate steps remain unmerged and narrow, consequently restricting the continuous growth area of the SEG domains [5]. Surface characterizations, including cryogenic scanning tunneling microscopy and Raman mapping, confirm that the SEG grown on the wide terraces in the FTF setup is structurally pristine and phase-pure. These findings highlight that modulating Si vapor pressure to intentionally induce step bunching is a deterministic mechanism for synthesizing wafer-scale, high-quality SEG, paving the way for next-generation 2D nanoelectronics.

References:
[1] M. Nair et al., Nano Lett. 17 (2017) 2681.
[2] W. A. de Heer et al., Proc. Natl. Acad. Sci. 108 (2011) 16900.
[3] J. Bao et al., Appl. Phys. Lett. 109 (2016) 081602.
[4] J. Zhao et al., Nature 625 (2024) 60.
[5] M. Kruskopf et al., 2D Mater. 3 (2016) 041002.

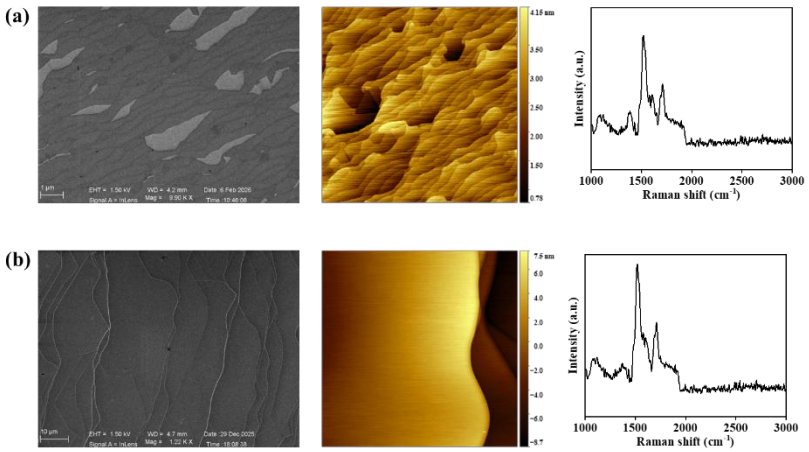

Fig. 1 Morphology and structural characterization of the fabricated samples. (a) SEM image, AFM topography map, and Raman spectrum of the sample fabricated via FTF; (b) SEM image, AFM topography map, and Raman spectrum of the sample fabricated via FTG.

Beneath the Moiré: Decoupling Intrinsic and Graphene-Induced Properties in Intercalated 2D Films

J. Erhardt[1,2], C. Schmitt[1,2], L. Gehrig[1,2], B. Liu[1,2], J. Schäfer[1,2], S. Moser[1,2,3], R. Claessen[1,2]

[1] 1Physikalisches Institut, Universität Würzburg, D-97074 Würzburg, Germany
[2] Würzburg-Dresden Cluster of Excellence ctd.qmat, Universität Würzburg, D-97074 Würzburg,Germany
[3]Ruhr-Universität Bochum, Experimentalphysik IV - AG Oberflächen, D-44801 Bochum, Germany

Intercalation of epitaxial graphene on silicon carbide has opened a powerful route to atomically thin films that remain stable under ambient conditions, protected by a van der Waals–bound graphene capping layer. This platform offers a dual advantage: it enables controlled tuning of graphene's electronic properties via proximity effects, while granting access to a rich spectrum of emergent 2D phenomena within the intercalated layer itself, including quantum spin Hall insulators (QSHI) and superconductors [1-6].

However, a central challenge in this field is disentangling the intrinsic structural and electronic properties of the intercalant from those arising due to the presence of the graphene capping layer, evident, for example, in the moiré structures commonly observed in scanning tunneling microscopy (STM) (Fig. 1**a**) [3].

In this talk, I will elucidate the influence of graphene on intercalated 2D films through a direct comparison with their pristine, graphene-free counterparts. Using indenene and bismuthene as case examples – indium and bismuth realizations of the QSHI phase on SiC(0001) – I first examine the growth with and without graphene, using STM and angle-resolved photoemission spectroscopy (ARPES). I then address their electronic properties, highlighting significant charge transfer to graphene and demonstrating orbital-selective tunneling that allows minimizing the moiré modulation in STM images, as evidenced by bias-dependent imaging of the indenene and graphene lattices (Fig. 1**b**,**c**). These results provide direct access to the intrinsic structure of the intercalated films and enable a sophisticated assessment of graphene–intercalant coupling.

References:
[1] C. Schmitt and J. Erhardt et al., Nat. Commun. 15 (2024) 1486
[2] J. Erhardt et al., Nat. Commun. 16 (2025) 8209
[3] L. Gehrig, et al., Adv. Mater. 37 (2025) 2502412
[4] N. Tilgner et al., Nat. Commun. (2025) 16 6171
[5] N. Briggs et al., Nat. Mater. 19 (2020) 637–643
[6] M. Gruschwitz et al., Materials 14 (2021) 1–11

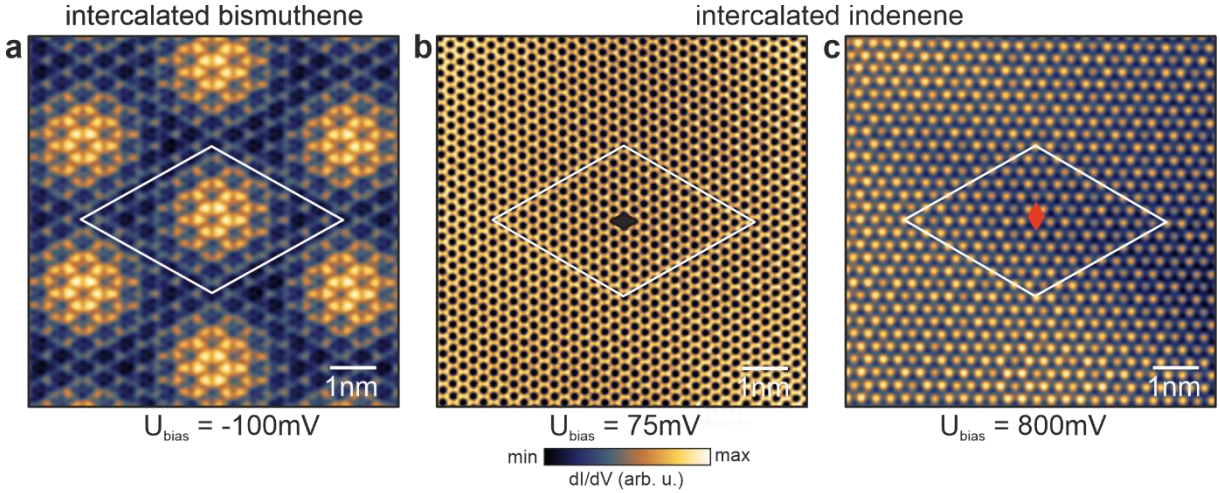

Fig. 1: STM lock-in dI/dV maps taken in constant height mode showing **a** the pronounced moiré unit cell (white rhombus) of intercalated bismuthene and **b**,**c** the bias-selective tunneling into either **b** graphene p_z-orbitals (black unit cell), or **c** indium p_z-orbitals in the case of intercalated indenene (red unit cell).

Engineering Bismuthene via Confinement Heteroepitaxy: Hydrogen-Controlled Structure and Spin Texture

N. Tilgner[1], S. Wolff[1], A. D. Peña Unigarro[1], S. Soubatch[2], T.-L. Lee[3], M. Leandersson[4], S. Gemming[1], F. S. Tautz[2], T. Seyller[1], C. Kumpf[2], P. Schädlich[1]

[1] Institute of Physics, Chemnitz University of Technology, Chemnitz, Germany
[2] Peter Grünberg Institute (PGI-3), Forschungszentrum Jülich, Jülich, Germany
[3] Diamond Light Source Ltd, Harwell Science and Innovation Campus, Didcot, United Kingdom
[4] MAX IV Laboratory, Lund University, Lund, Sweden

Confinement heteroepitaxy, which describes the intercalation of species beneath epitaxial graphene on SiC, has emerged as a versatile approach for synthesizing environmentally protected two-dimensional materials at well-defined interfaces [1]. Recently, considerable attention focused on Bi-intercalation of the graphene zero layer because it was reported to form a ($\sqrt{3}\times\sqrt{3}$) reconstructed β phase [2,3] that can be reversibly transformed – by hydrogenation or dehydrogenation – into the large-gap quantum spin Hall insulator bismuthene [4,5].

Using a combination of normal incidence X-ray standing wave imaging, spin- and angle-resolved photoelectron spectroscopy, and density functional theory, we demonstrate an H-induced change of the Bi adsorption site, which is accompanied by a contraction of the Bi layer. The atoms of the β phase occupy T_4 hollow sites with 1/3 monolayer coverage – a configuration that prohibits bismuthene formation. Partial H-passivation of the SiC interface contracts the lattice to a honeycomb structure with 2/3 monolayer coverage and shifts the atoms to the T_1 on top position. This allows for Bi-Bi hybridization, which, together with the remaining Bi-Si bond, establishes the orbital composition around the Fermi level required for the formation of bismuthene's Dirac-like band structure (see Fig. 1 (a)).

Due to the covalent bonding to the substrate, both Bi-rich structures are prone to strong mirror symmetry breaking, which leads to Rashba splitting of the valence bands. For the β and bismuthene phases, we demonstrate the lifting of the spin degeneracy, as well as the expected Rashba-type spin-momentum locking. Figs. 1 (b) and (d) show the in-plane polarizations of an exemplary energy distribution curve (EDC) that cuts through the bismuthene valence bands close to the K point (see black rectangle in (a)). In both directions, we observe significant polarization of the photocurrent that changes sign along the energy axis. This gives rise to two oppositely polarized components of the EDC, as shown in (c) and (e), which are attributed to bismuthene's spin-split valence bands.

References:
[1] N. Briggs et al., Nat. Mater. 19 (2020) 637.
[2] Y. Sohn et al., J. Korean Phys. Soc. 78 (2021) 157.
[3] S. Wolff et al., New J. Phys. 26 (2024) 103009.
[4] L. Gehrig et al., Adv. Mater. 37 (2025) 2502412.
[5] N. Tilgner et al., Nat. Commun. 16 (2025) 6171.

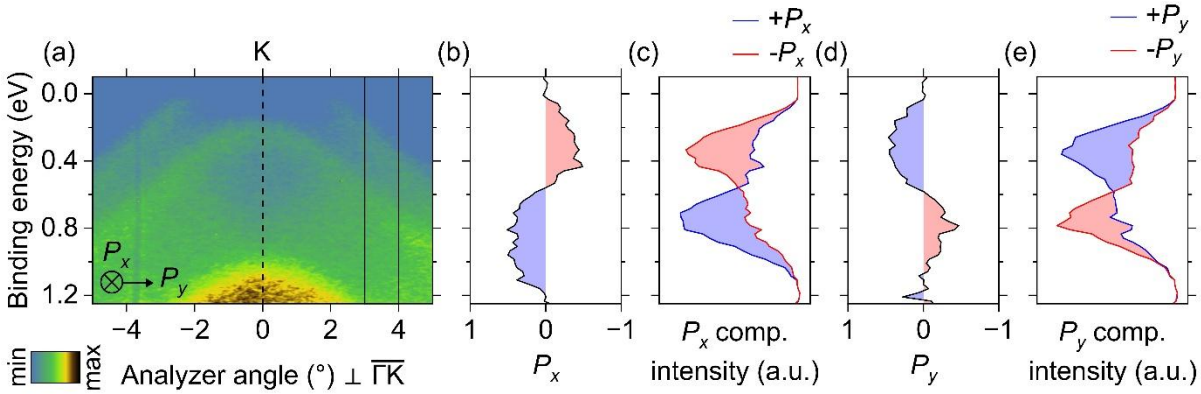

Fig. 1: (a) Energy-angle map of bismuthene at K, perpendicular to the $\overline{\Gamma K}$ direction. The black rectangle indicates the region from which the spin-resolved EDC was extracted. (b) and (d) show the respective polarizations in the two in-plane directions: $P_x \parallel \overline{\Gamma K}$, and $P_y \perp \overline{\Gamma K}$. (c) and (e) display the corresponding EDC component intensities. Red and blue colors denote negative and positive polarization, respectively.

Solving the Phase Problem of Diffraction: X-Ray Standing Waves Imaging on Bismuthene / SiC(0001)

Niclas Tilgner [1], Susanne Wolff [1], Serguei Soubatch [2], Tien-Lin Lee [3], Fabian Göhler [1], F. Stefan Tautz [2,4], Thomas Seyller [1], Philip Schädlich [1], and Christian Kumpf [2,4]

[1] Institute of Physics, Chemnitz University of Technology, Chemnitz, Germany
[2] Peter Grünberg Institute (PGI-3), Forschungszentrum Jülich, Jülich, Germany, and Jülich-Aachen Research Alliance (JARA), Fundamentals of Future Information Technology
[3] Diamond Light Source Ltd., Didcot, Oxfordshire, United Kingdom
[4] Experimentalphysik IV A, RWTH Aachen University, Aachen, Germany

Over the decades, a variety of diffraction-based techniques for determining the structure of materials at an atomic level has been developed and employed. These techniques have contributed significantly to our understanding of the properties and functionalities of physical systems and devices in many fields, particularly in surface and interface science. However, a fundamental limitation of such methods is the so-called 'phase problem', as diffraction techniques can only measure intensities (i.e., the squared magnitudes of the complex scattering factors), while their phases remain inaccessible in an experiment. If both amplitudes and phases of the structure factors were available, it would be straightforward to use an inverse Fourier transform to reconstruct the three-dimensional atomic density distribution. One way to overcome this limitation is to exploit the direct relationship between the phase of the structure factor and the phase of the X-ray standing wave (XSW) generated by a Bragg reflection from a crystalline substrate. This technique, known as XSW imaging, was first proposed 40 years ago [1], but its application has remained limited due to the demanding experimental requirements involved.

In this study, we demonstrate the potential of XSW imaging to reveal atomic-scale processes and structural transformations on surfaces. As a case study, we investigated bismuthene, a quantum spin Hall insulator prepared by intercalating Bi between a graphene layer and a silicon carbide substrate [2,3]. The electronic, spintronic, and topological properties of the bismuthene layer are discussed in the contribution by N. Tilgner. Here, we focus on the structural properties, in particular on the mechanism driving the reversible phase transition between the bismuthene phase and its topologically trivial precursor phase (the so called ***β*** phase). Using several Bragg reflections, we identified the position of the Bi atoms in both phases and, as a reference, those of the Si and C bulk species in the unit cell of the 4H-SiC crystal. The key finding is that the adsorption site of the Bi atoms changed during the phase transition [2]. This is accompanied by a reorganization of chemical bonds at the interface, resulting in the formation of the distinctive electronic band structure characteristic of two-dimensional bismuthene.

References:
[1] M.J. Bedzyk and G. Materlik, Phys. Rev. B **32**, 6456 (1985).
[2] N. Tilgner et al., 2D Materials **12**, 045020 (2025)
[3] N. Tilgner et al., Nature Commun. **16**, 6171 (2025)

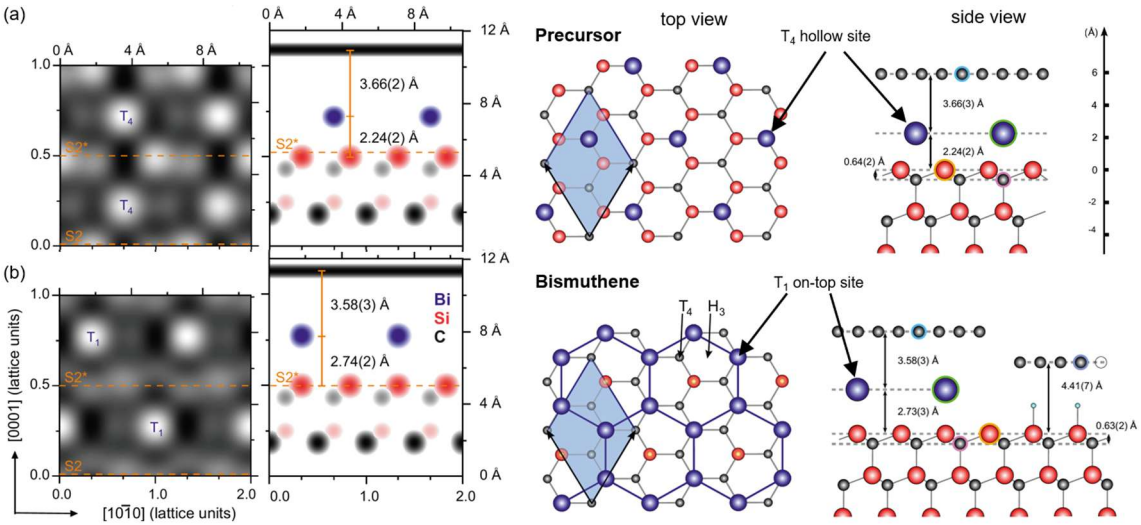

Fig. 1: Atomic densities, as obtained from XSW imaging, and atomic models (top- and side view) for (a) the topologically inactive precursor phase (***β*** phase) and (b) the bismuthene phase.

Epitaxial Graphene Devices for Quantum Electrical Metrology

Dong-Hun Chae

Korea Research Institute of Standard and Science, Daejeon, Republic of Korea

Quantum electrical metrology is an important application area of collective states of matter. One prominent example is the quantum Hall condensate for the realization of the resistance unit, the ohm. Compared with two-dimensional electrons with finite effective masses at the interface of semiconducting heterostructures, the linear energy-momentum dispersion of quasiparticles in graphene allows for a practical realization of the quantum Hall resistance standard under easily accessible experimental conditions of temperature and magnetic field. The metrology community has focused on epitaxial graphene, which was observed at least five decades ago [1], as a scalable platform to develop a practically accessible quantum resistance standard for more than a decade and a half. Technology has become mature enough that epitaxial graphene is now gradually deployed at national metrology institutes. Epitaxial graphene devices are formally accepted by the metrology community as an attractive alternative to the traditional semiconducting devices along with a formal guideline [2], which was approved by the Consultative Committee for Electricity and Magnetism. Here, we present the latest advances of graphene-based electrical metrology [3]. These include advancements in device fabrication, the long-term stability, the practical realization of graphene-based resistance quantum standards, graphene-based impedance quantum standards, and graphene-based current metrology at direct and alternating currents.

References:

[1] A.J.J. Van Bommel, J.E. Crombeen and A. Van Tooren Surf. Sci. 48 (1975) 463.

[2] *Companion Guide to the Revised Technical Guidelines for Reliable dc Measurements of the Quantized Hall Resistance for Graphene-Based Devices* (to be published)

[3] D.-H. Chae, H. He and M. Kruskopf, Meas. Sci. Technol. (2026) https://doi.org/10.1088/1361-6501/ae57c8

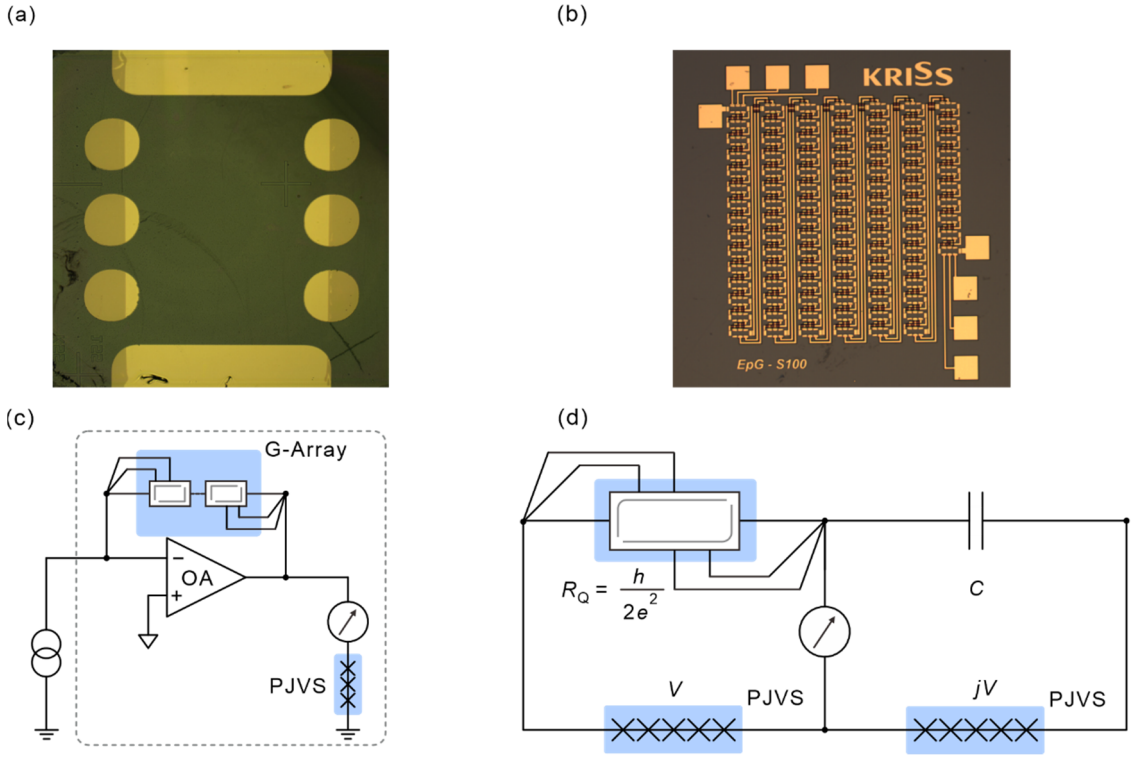

Fig. 1: (a) Centimeter scale graphene device for quantum resistance metrology. (b) Graphene-based array. (c) Graphene-based quantum mechanical ammeter. (d) Graphene-based impedance quantum standard.

Magneto-Transport Investigation of PASG-grown Graphene/van der Waals Heterostructures

M. Bothe[1], D. Höllmann[1], S. Wundrack[1], K. Jin[2], J. C. Bayer[1], V. Labracherie[1], S. Anchamkudy[2], H. W. Schumacher[1], F. Lüpke[2], T. M. Tschirner[1]

[1] Physikalisch-Technische Bundesanstalt, Bundesallee 100, 38116 Braunschweig, Germany
[2] Peter Grunberg Institute (PGI-3), Forschungszentrum Jülich, 52425 Jülich, Germany

Graphene is the most promising candidate for the next generation of DC electrical resistance standards based on the quantum Hall effect (QHE). To date, only epitaxial graphene (EG) grown on SiC by Si sublimation meets the necessary metrological requirements. In particular, the use of the polymer-assisted sublimation growth (PASG) technique enables large-scale, highly reproducible, and homogeneous graphene growth [1]. For metrological standards, both high measurement precision and relaxed operating conditions, such as reduced magnetic fields and higher temperatures, are important criteria. These characteristics can be further improved through targeted optimization of EG properties.

A key requirement for implementing PASG-grown EG as a QHE resistance standard is precise control of the charge carrier density, which can be achieved by doping the EG. So far this has been investigated with molecular dopants such as F4-TCNQ [2] or via proximity induced doping effects through metal intercalation [3]. In this work we explore an alternative strategy for tailoring EG properties by stacking a variety of layered two-dimensional materials on top of the EG, including hBN and transition-metal dichalcogenides such as MoS_2, WSe_2 and $NbSe_2$. To characterize the resulting van der Waals heterostructures, Hall bar devices are fabricated from PASG-grown graphene using electron beam lithography. Subsequently, the 2D materials are exfoliated from bulk crystals and suitably large and homogeneous flakes are transferred onto the completed Hall bars using a polymer-based stamp technique [4] (see Fig. 1). By establishing a direct interfacial contact between the exfoliated flakes and the EG, we aim to induce proximity effects that modify the electronic properties of the EG, including carrier mobility enhancement, doping contributions and spin-orbit coupling [5-7]. These effects are investigated using low-temperature magneto-transport measurements and Raman spectroscopy.

References:

[1] M. Kruskopf et al., 2D Mater. 3 (2016) 041002
[2] Y. Yin et al., Adv. Phys. Res. 1 (2022) 2200015
[3] S. Wundrack et al., Adv. Mater. 38 (2026) e11992
[4] M. Onodera and T. Machida, Sens. Mater. 35 (2023) 3299
[5] A. Geim and I. Grigorieva, Nature 499 (2013) 12385
[6] S. Subramanian et al., npj 2D Mater Appl 4 (2020) s41699-020-0144-0
[7] J. D. Gerber et al., Nano Lett. 25 (2025) 5c02309

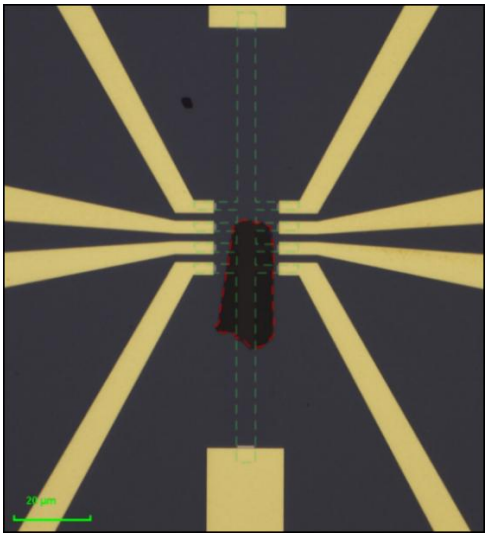

Fig. 1: Optical microscope image of a lithographically structured graphene Hall bar fabricated with gold contacts and with an hBN flake stacked on top. The graphene area is highlighted by a green dashed outline and the flake area by a red dashed outline. The Hall bar dimensions are 5 µm × 100 µm.

High-precision quantum resistance metrology based on epitaxial graphene and all-graphene-based multi-parameter quantum metrology devices

Xiaodong Fan[1]

[1] Department of Physics, University of Science and Technology of China

In recent years, the quality of epitaxial graphene on silicon carbide has been continuously improved. Coupled with its compatibility with semiconductor processes, it exhibits great potential for the development of functional devices and monolithic integration applications. On the other hand, its distinctive interface pinning effect provides significant advantages for quantum resistance metrology under relaxed experimental conditions.

Traditional quantum resistance metrology generally employs n-type doped epitaxial graphene, yet the understanding of how doping type affects quantum metrology performance remains insufficient. We systematically compared the quantum Hall effect behaviors of epitaxial graphene with different doping types and concentrations, and analyzed the influence of scattering mechanisms on the robustness of the quantum Hall effect via quantum interference effects. This work provides an important reference for the design of quantum resistance metrology devices [1]. Based on relevant experience, we fabricated high-quality quantum resistance metrology devices using epitaxial graphene. Through comparison with the national primary standard, it is confirmed that a relative standard uncertainty of resistance value at the 10^{-9} level can be achieved under relatively relaxed experimental conditions (4.4 K, 5.8 T).

In addition, graphene shows the potential for the simultaneous quantum realization of the three basic electrical units: volt, ohm, and ampere. Drawing on our experience in constructing complex graphene functional devices [2], we designed multi-electrical-parameter quantum metrology devices [3]: we achieved quantum voltage output at liquid helium temperatures in graphene-based Josephson junctions through in situ modulation of the superconducting dissipation mechanism; we fabricated high-quality graphene double quantum dot devices, enabling quantum current output at pumping frequencies exceeding 1 GHz; and we developed quantum resistance devices based on graphene heterostructures that operate at extremely low magnetic fields. These advances lay the foundation for realizing an electrical quantum metrology multimeter based on a unified material system in the future.

References:
[1] Xinyi Wan, **Xiaodong Fan*** et al. Chin. Phys. Lett. 40 (2023) 107201.
[2] Shuai Wang, Zhen Zhan, **Xiaodong Fan*** et al., Phys. Rev. Lett. 133 (2024) 066302.
[3] In preparation.

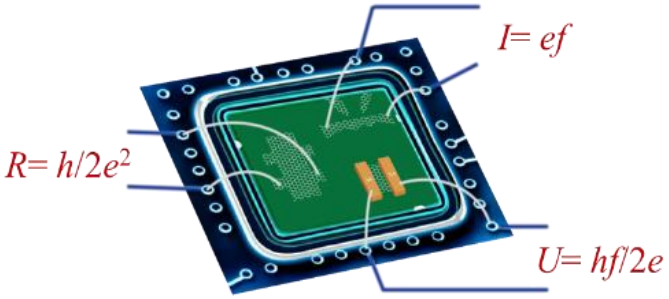

Fig. 1: Schematic of all-graphene-based multi-electrical-parameter quantum metrology devices.

Pronounced scale-dependent charge carrier density in graphene quantum Hall devices

Yu FENG[1], Ziceng ZHANG[1], Chenxi LIU[1], Junchi SONG[1], Chengxin JIANG[1,2], Qiujuan SUN[2], Ziqiang KONG[1], Zijian WANG[1], Yihui QU[1], Shengda GAO[3], Jian FENG[4],and Haomin WANG[1,2]

[1]State Key Laboratory of Materials for Integrated Circuits, Shanghai Institute of Microsystem and Information Technology, Chinese Academy of Sciences, Shanghai, 200050, China
[2]Shanghai Grapheneflag Technology Co., Ltd., Building 49, No. 6999 Chuansha Road, Pudong New Area, Shanghai, 201202, China
[3]School of Advanced Technology, Xi'an Jiaotong-Liverpool University, Suzhou, 215123, China
[4]Shanghai Institute of Measurement and Testing Technology, Shanghai Key Laboratory of On-line Testing and Control Technology, Shanghai, 201203, China

Abstract: The miniaturization of quantum Hall resistance standards (QHRS) using epitaxial graphene on silicon carbide (SiC) necessitates understanding how device dimensions impact performance. This study reveals a pronounced scale-dependent carrier density in graphene Hall devices: under electron doping, carrier density decreases with increasing channel width (Wd), while the opposite occurs under hole doping. This phenomenon, most significant for Wd ≤ 400 μm, directly influences the onset of magnetic field required for quantization. Fermi velocity measurements and angle-resolved photoemission spectroscopy (ARPES) analysis indicate that band structure modifications and electron-electron interactions underlie this size dependence. Utilizing machine learning with limited data, we optimized the device geometry, identifying a channel width of ~360 μm as the optimal balance between resistance uncertainty and on-chip integration density. This work provides key insights for designing high-performance, miniaturized graphene-based QHRS arrays.

References:

[1] L. Chen, H. Wang, Z. Kong, et al., "Gaseous catalyst assisted growth of graphene on silicon carbide for quantum Hall resistance standard device," Adv. Mater. Technol., vol. 8, no. 2, [2023] 2201127.
[2] Z. Kong, Y. Feng, H. Gao, et al., "Pronounced scale-dependent charge carrier density in graphene quantum Hall devices," Mater. Today Phys., vol. 51, [2025] 101928.

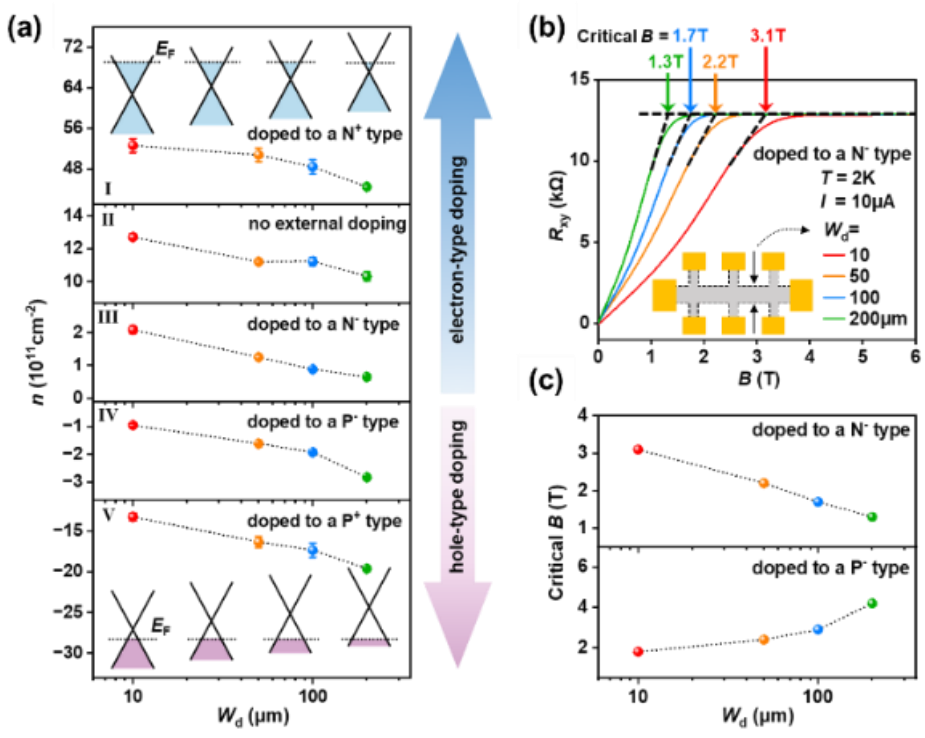

Fig. 1. Scale-Dependent Carrier Density and Device Optimization Scale-dependent carrier density. (a) Carrier density n as a function of channel width Wd under different doping conditions (N^+, undoped, N^-, P^-, P^+). Insets illustrate the shift of Fermi level with Wd. (b) and (c) showing the variation of the onset of magnetic field (*B*) for entering quantized Hall pleteaus as a function of Wd in N^- and P^- type.

Understanding local electronic properties in epitaxial graphene heterostructures by scanning tunneling microscopy and spectroscopy

M. Kolmer[1,2]

[1] Division of Materials Sciences and Engineering, Ames National Laboratory, Ames, 50011 IA, USA
[2] Department of Physics and Astronomy, Iowa State University, Ames, Iowa 50011, USA

Despite long-standing efforts to understand the interface between epitaxial graphene and the Si-terminated silicon carbide (0001) substrate, the exact atomic-scale structure, its complex bonding configurations, and the resulting electronic properties of the first epitaxial graphene carbon layer (C_{buffer}) remain open problems. In the first part of the talk, we will present how to control the local structure of the epitaxial graphene-SiC interface with a low-temperature scanning tunneling microscope (STM) [1]. We will show that the covalent bonds between C_{buffer} and the SiC substrate may be reversibly broken and restored using the polarity of the electric field from the STM tip, generating protrusions at the interface of slightly higher amplitude. This buried interface manipulation enabled us to pattern epitaxial graphene with lateral precision, reaching the scale of a single 1.8 nm unit cell of the graphene-SiC interface (6×6)SiC moiré lattice. We propose applying this local patterning of the epitaxial graphene heterostructures at the bottom interface to synthesize metastable interface configurations by controlling the location of the nanoprotrusions. The decoupled interface could be locally arranged in ordered superstructures, creating a new 2D template with a long-range periodic potential for the Dirac electrons in graphene to tune its electronic properties. This strategy will be similar to the templates currently used in the artificially arranged atomic or molecular adsorbates.

However, the STM manipulation experiments also provide direct evidence of silicon vacancies at the topmost reconstructed SiC(0001) layers [2]. Bias-voltage- and epitaxial graphene thickness-dependent characterization of the collective C_{buffer}-SiC interface showed that 'Si' vacancy sites exhibit stable, non-switching behavior under STM electric fields. Moreover, vacancies introduce localized electronic states below the Fermi level. Our experimental results directly elucidate the atomic-scale interface and the influence of atomic and bonding configurations on the local density of states for graphene of different thicknesses on SiC(0001).

In the second part of the talk, we will present the methodology for identifying the intrinsic electronic density of states of unoccupied bands above the vacuum level as a function of pristine graphene thickness and intercalated metal phases under graphene, using high-bias scanning tunneling spectroscopy. The low-temperature STM operating at high sample bias voltages up to ~40 V was used to study the interaction between graphene interface states within the unoccupied electronic band regime and the high-bias field emission resonances formed within the triangular potential in the tip-sample gap. The systems studied include C_{buffer}, monolayer, bilayer, and trilayer graphene prepared on a SiC(0001) surface, as well as intercalated phases of gadolinium and dysprosium. With increasing tunneling current for the same tip-sample voltage, the potential well becomes progressively steeper and narrower, and the confined energy levels of the resonances shift. The alignment between the resonance's energy and the intrinsic interface electronic states is a unique way to map the unoccupied bands in the different types of heterostructures and selectively study the characteristic interface states.

Acknowledgements: This work was supported by the U.S. Department of Energy (DOE), Office of Science, Basic Energy Sciences, Materials Science and Engineering Division through a DOE Early Career Project at the Ames National Laboratory, which is operated for the U.S. DOE by Iowa State University under contract # DE-AC02-07CH11358. Part of the research was performed as a User Project at the Center for Nanophase Materials Sciences, which is a DOE Office of Science User Facility.

References:

[1] M. Kolmer, J. Hall, S. Chen, S. Roberts, Z. Fei, Y. Han, and M. C. Tringides, Atomic-scale manipulation of buried graphene–silicon carbide interface by local electric field, Communications Physics, 7, 16 (2024).
[2] U. Thupakula, S. Chen, Y. Han, M. C. Tringides, and M. Kolmer, Subsurface Interface Structure Controlling Local Electronic Properties of Epitaxial Graphene on SiC(0001), The Journal of Physical Chemistry Letters, 16, 10487−10498 (2025).

Electronic properties of epitaxial graphene-Mn_5Ge_3-Ge interfaces

Yuriy Dedkov[1], Elena Voloshina[2]

[1] CALT, Institute of Physics, 10000 Zagreb, Croatia
[2] Division of Theoretical Physics, Ruđer Bošković Institute, 10000 Zagreb, Croatia

Recently, much of experimental and theoretical efforts were dedicated to the investigation of the structural, electronic and transport properties of graphene-based systems, where it is interfaced with other two-dimensional materials, with metals, and with semiconducting materials, like gr/Ge(001) or gr/Ge(110) [1]. Particularly, the interfaces of graphene (and other 2D materials) with ferromagnetic (FM) materials are interesting, as in perspective they can lead to the implementation of these 2D layers in the spintronics applications as spin-filters or effective conductors for the spin-polarized electrons.

Very recently an elegant new approach for realization of the gr/FM interface with linear energy dispersion for electrons in graphene was proposed (Fig. 1) [2]. As was theoretically found, the strong exchange splitting in Mn_5Ge_3 leads to the appearance of the large exchange splitting for the graphene π bands. As a consequence of this effect, the linear dispersion is preserved for spin-up electrons that makes this gr/FM-Mn_5Ge_3 system perspective for spintronics applications.

In our recent work we study the electronic and magnetic properties of the gr/FM-Mn_5Ge_3 interfaces formed via and during intercalation of Mn in two epitaxial interfaces, gr/Ge(110) and gr/Ge(111) [3]. The protective properties of graphene allowed to perform the systematic studies of the crystallographic structure and ordering in the obtained epitaxial intercalation systems using different in situ and ex situ methods. At the same time the magnetic measurements confirm the strong FM ordering in the system with Curie temperature close to room temperature. Despite the expected small distance between graphene and FM-Mn_5Ge_3 and relatively strong interaction at the gr/FM-Mn_5Ge_3 interface in both epitaxial systems, our systematic ARPES experiments confirm E(k) dependence in the vicinity of the Fermi level for the carriers in graphene. Considering all experimental observations supported by the results of the previous DFT calculations we discuss the possible applications of the obtained gr/FM-Mn_5Ge_3/Ge heterosystems in spintronics and electronics.

References:
[1] Y. Dedkov and E. Voloshina, Nanoscale 12 (2020) 11416.
[2] E. Voloshina and Y. Dedkov, J. Phys. Chem. Lett. 10 (2019) 3212.
[3] Y. Dedkov et al., ACS Appl. Mater. Interfaces 15 (2023) 26190.

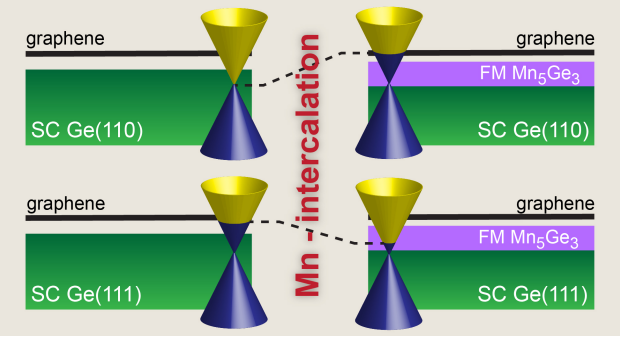

Fig. 1: Schematic presentation of the doping level change in graphene upon Mn intercalation and formation of Mn_5Ge_3 at the gr/Ge interfaces.

Reconstruction of 2D silver at the interface between graphene and SiC

V. D Pham[1], B. Zheng[2], A. Jain[2], C. Dong[2], L-S. Lu[4], Z. W. Henshaw[3], W. H. Blades[3], J. A. Robinson[2], V. H. Crespi[2], A. Trampert[1], R. Engel-Herbert[1]

[1] Paul-Drude-Institut für Festkörperelektronik, Leibniz-Institut im Forschungsverbund Berlin e. V., Hausvogteiplatz 5–7, 10117 Berlin, Germany
[2] Department of Physics, The Pennsylvania State University, University Park, Pennsylvania 16802, USA
[3] Department of Physics and Engineering Physics, Juniata College, Huntingdon, Pennsylvania 16652, USA

Atomically thin metals confined between graphene and SiC represent a compelling materials platform. In this reduced-dimensionality environment, 2D metals can exhibit exotic physical properties with potential relevance to electronic devices and quantum technology. Despite this promise, the structural behavior of metals confined to this nanospace has remained largely unexplored.

In this work, we shed new light on this problem. Focusing on monolayer silver epitaxially grown on SiC (0001), we show how strain at the silver-SiC interface drives the formation of a non-ideal silver structure, specifically a one-dimensional reconstruction known as a Frenkel-Kontorova domain. This strain arises from competing interactions between silver-SiC bonding and silver-silver interatomic forces, producing a long-range structural modulation and a characteristic electronic state at 0.75 eV above the Fermi level. The findings were obtained using cryogenic scanning tunneling microscopy, supported by first-principles density functional theory (DFT) calculations.

The results uncover the interplay between atomic structure and electronic properties in this confined system and open new pathways for engineering 2D metals at the nanoscale. The work has been published in Physical Review Materials and selected as an Editor's Suggestion [1].

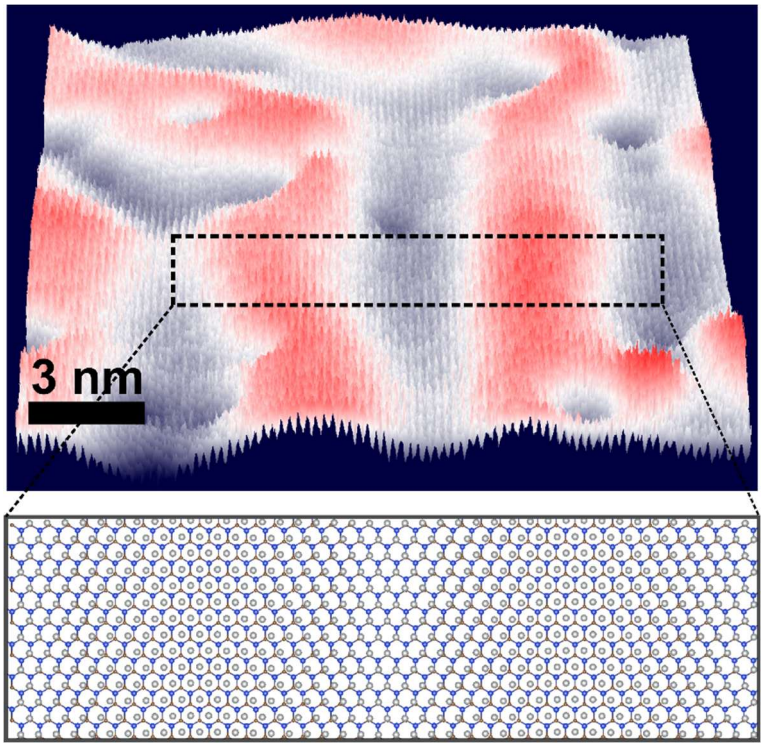

Fig. 1: High-resolution STM image and calculated DFT of the reconstructed monolayer of silver under graphene.

References:

[1] V. D Pham[1,*,†], B. Zheng[2*], A. Jain[3], C. Dong[2], L-S. Lu[4], Z. W. Henshaw[6], W. H. Blades[6], J. A. Robinson[2,3], V. H. Crespi[2], A. Trampert[1], R. Engel-Herbert[1]. Phys. Rev. Materials **10** (2026), 034003.

Epitaxial Graphene Interfaces: From Atomistic Understanding to Band Structure Control

E. Voloshina[1]

[1] Division of Theoretical Physics, Ruđer Bošković Institute, 10000 Zagreb, Croatia

The burgeoning field of two-dimensional (2D) materials offers exciting opportunities for fundamental research and nanoscale applications. However, the development of next-generation devices is intrinsically linked to our ability to precisely control their electronic landscapes. This talk focuses on graphene, which remains at the forefront of 2D research due to its behavior of graphene-derived π-states near the Fermi level, which exhibit linear dispersion around the K-points of the Brillouin zone. While these attributes enable excellent charge and spin transport, they also present significant challenges for device integration [1].

To address these challenges, interface engineering between graphene and functional substrates has emerged as a powerful tool for band-structure manipulation [2,3]. Crucially, this interaction is reciprocal: while the substrate can induce novel phases in graphene, graphene itself can significantly modify the electronic properties of the underlying material. A persistent challenge in these heterostructures is engineering the interface to achieve desired functionalities without destroying the characteristic Dirac cones.

In this talk, I will discuss several representative examples – from a theoretical perspective – that illustrate how the graphene's interaction with various substrates impacts the properties of the resulting system. Particular attention will be given to recent findings regarding interface effects in complex heterostructures [4,5], highlighting how atomistic insights can guide the design of stable, high-performance 2D interfaces.

References:
[1] A. K. Sood et al., Int. J. Eng. Res. 8 (2015) 125.
[2] Y. Dedkov and E. Voloshina, J. Phys.: Condens. Matter 27 (2015) 303002.
[3] E. Voloshina and Y. Dedkov, NPG Asia Mater. (2026). https://doi.org/10.1038/s41427-026-00633-y
[4] Y. Guo et al., Carbon 234 (2025) 119974.
[5] J. Zhang et al., J. Mater. Chem. C 13 (2025) 11789.

Investigation of the Heterogeneity and Temperature Dependence of Bilayer Gallium Intercalated at the Epitaxial Graphene/Silicon Carbide Interface with Cryogenic Spectroscopic Imaging Ellipsometry

J. Henz[1], U. Limberg[2], S. Rajabpour[2], A. Vera[2], A. Jain[2], J. A. Robinson[2], S. Y. Quek[3] and U. Wurstbauer[1]

[1] Institute of Physics, University of Münster, Germany
[2] MatSE; Center for 2DLM, PennState University, USA
[3] Centre for Advanced 2D Materials, NUS, Singapore

Metal intercalation at the interface of epitaxial graphene and silicon carbide (SiC) offers a powerful route for the stabilization of novel covalently bonded 2D phases. One method, confinement heteroepitaxial growth (CHet), results in large area, environmentally stable, mono- to fewlayer films [1]. Due to the bonding gradient along the out-of-plane direction ranging from covalent over metallic forces to a vdW interaction within only a few Angstroms, these systems have been dubbed 2D polar metals [2]. These materials systems feature a wide range of electronic and optical properties, from the tunable plasmonic resonances in binary In:Ga alloys [3] to a two phase system of semiconducting Ag monolayers [4].

Here, we focus primarily on 2D polar Ga, which stabilizes as metallic bi- and trilayer films. The material features interesting properties, including a thickness dependent plasmonic resonance [5], giant second-order susceptibilities approaching 10 nm V^{-1} [2] and a superconducting phase transition below 3 K [1].

To uncover the relation between light-matter interaction, temperature and structural changes, bilayer 2D gallium is studied by temperature dependent spectroscopic imaging ellipsometry.
Spectroscopic Imaging Ellipsometry (SIE) is a powerful optical measurement technique, combining the ability of an ellipsometer to determine layer thicknesses and optical properties of thin film samples to the monolayer limit with the lateral resolution of a microscope. The resolution enables the investigation of the dielectric response on the micrometer scale, allowing us to study the homogeneity of the terrace structure in 2D polar metals [4].
In combination with a cryostat with free beam optical access, we explore the temperature-dependence of the local dielectric function of 2D polar Ga, from room temperature down to 5 K. We show a change in the local dielectric response of the material from homogenous behavior at room temperature to a heterogenous regime at low temperatures, characterized by two absorption peaks localized to distinct surface areas on the sample [6]. We interpret this change to indicate a structural phase transition in the material.

References:
[1] N. Briggs et al., Nat. Mater. 19 (2020) 637.
[2] M. Steves et al., Nano Lett. 20 (2020) 8312-8318.
[3] S. Rajabpour et al., Adv. Mater. 33.44 (2021) 2104265.
[4] A. Jain et al., arXiv preprint, (2025) arXiv:2511.07151
[5] K. Nisi et al., Adv. Funct. Mater. 31 (2021) 2005977.
[6] J. Henz et al., in preparation

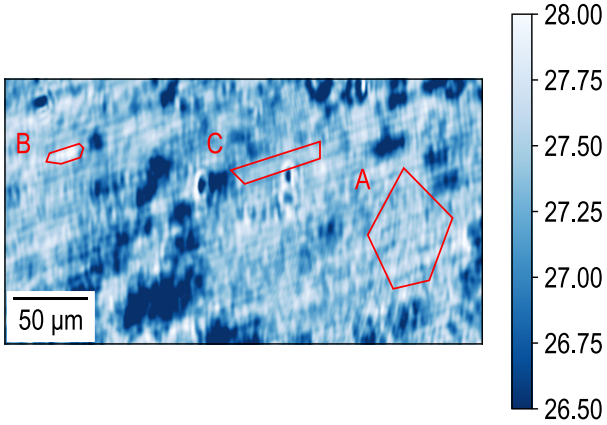

Fig. 1: Ellipsometric Ψ-map of bilayer 2D Ga at 575nm, at measured temperature 4K, showcasing terrace dependent optical behavior.

Metals under confinement: Unlocking room temperature intercalation of indium in epitaxial graphene

S. Wundrack[1,2,3], N. M. Savadkouhi[1], M. Bothe[1], K. Küster[5], M. Gruschwitz[4], P. Schädlich[4], T. Tschirner[1], B. Matta[5], S. Datta[5], T. Seyller[4], U. Starke[5], K. Pierz[1], H. W. Schumacher[1], T. Seyller[4], C. Tegenkamp[4], R. Stosch[1], A. Bakin[2,3]

[1] Physikalisch-Technische Bundesanstalt, Bundesallee 100, 38116 Braunschweig, Germany
[2] Institut für Halbleitertechnik, TU Braunschweig, Hans-Sommer-Str. 66, 38106 Braunschweig, Germany
[3] Laboratory of Emerging Nanometrology (LENA) der Technischen Universität Braunschweig, Langer Kamp 6 a/b, 38106 Braunschweig, Germany
[4] Institut für Physik, TU Chemnitz, Reichenhainer Str. 70, 09126 Chemnitz, Germany
[5] Max-Planck-Institut für Festkörperforschung, Heisenbergstraße 1, 70569 Stuttgart, Germany

Intercalation of foreign species into two-dimensional van der Waals materials provides a route to tailor interfacial coupling and electronic structure. In epitaxial graphene on SiC(0001), metal intercalation induces decoupling of the covalently bonded graphene zero-layer from the substrate, while the resulting confinement at the graphene–SiC interface stabilizes metallic phases with structural and electronic properties distinct from those of their bulk counterparts [1-3].

Here, we show that indium intercalation beneath epitaxial graphene already occurs at room temperature, despite the bulk melting point of indium being 157 °C. Time-resolved microscopy reveals a laterally propagating intercalation front that follows the SiC terrace morphology, consistent with gallium intercalation [4], and strongly evidences anisotropic mass transport. SPA-LEED, Raman, and ARPES indicate the formation of a structurally ordered confined indium phase and the conversion of epitaxial graphene into quasi-freestanding bilayer graphene (QFBLG). Our observations can be described within a thickness-dependent thermodynamic framework, in which both the chemical potential of confined indium, driven by relaxation of epitaxial graphene, and the imbalance between the In/SiC and In/graphene interfacial energies promote intercalation.

References:
[1] S. Forti et al., Nat. Commun. 11, 2236 (2020).
[2] C. Ghosal et al., Phys. Rev. Lett. 129, 116802 (2022).
[3] C. Schmitt et al., Nat. Commun. 15, 1486 (2024).
[4] S. Wundrack et al., Phys. Rev. Materials 5, 024006 (2021).

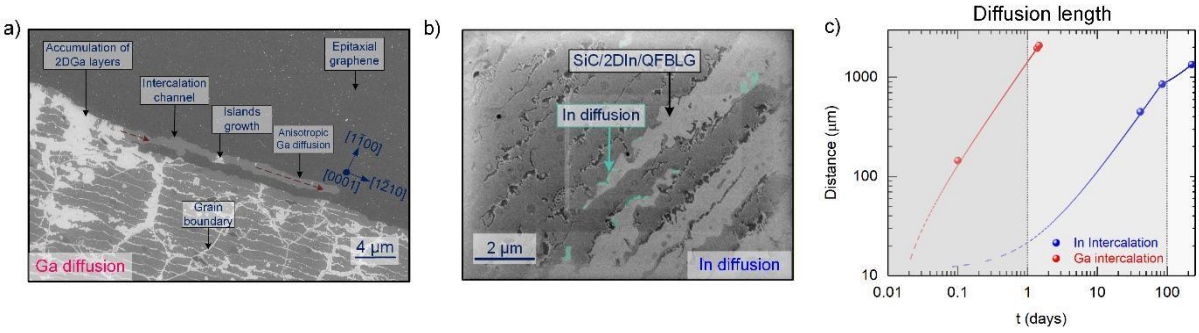

Fig. 1: Time-resolved microscopy of room-temperature metal intercalation beneath epitaxial graphene on SiC(0001). **a, b)** Microscopy images showing anisotropic lateral propagation of the intercalation front along the SiC terraces for Ga and In, respectively. **c)** Time-dependent evolution of the diffusion length, highlighting the distinct intercalation behavior of indium compared to gallium.

The CISS effect: spin transport phenomena through chiral molecules proximitized to surfaces

C. Tegenkamp[1]

[1] Institut für Physik, Technische Universität Chemnitz, Reichenhainer Str. 70, 09126 Chemnitz, Germany

The transmission properties of electrons through chiral systems are currently attracting significant attention. In DNA and polypeptides, the so-called chiral-induced spin selectivity (CISS) effect describes the emergence of extraordinarily high spin polarizations during long-range electron transfer. Moreover, strong spin polarizations have also been reported in chiral carbon nanotubes. This is surprising, as heavy atoms are absent in these carbon-based systems. It has been shown that even in systems with weak spin–orbit coupling, spin transmission can be strongly amplified by molecular helicity.

We performed local transport experiments using scanning tunneling microscopy (STM) on lysine-doped and cysteine-terminated single helical polyalanine (PA) molecules adsorbed on magnetic Al_2O_3/Pt/Au/Co/Au nanostructures with perpendicular anisotropy. The highest CISS magnetoresistance values were observed for ordered self-assembled monolayers with well-defined chemical coupling between the molecules and the magnetic substrate.

In recent experiments, the same molecules were inverted, for example by adsorption onto the Au tip or by functionalization of the opposite terminus. Surprisingly, high electron transmission required opposite orientations of the Co layer magnetization. This result clearly demonstrates that the molecular orientation plays a decisive role. The approximately point-symmetric behavior of the I–V curves can be understood in terms of a “spinterface,” defined by the helicity and electric dipole orientation of the molecule at the interface. In this sense, the helical system does not act as a simple spin filter or polarizer.

Raman Spectroscopy of Intercalated Epitaxial Graphene on SiC(0001)

Z. Mamiyev, N. O. Balayeva, D. R.T. Zahn, C. Tegenkamp

Institute of Physics, Chemnitz University of Technology

Raman spectroscopy provides a powerful and non-destructive probe of graphene, offering rich information on its structural, electronic, and vibrational properties, including strain, doping, and electron-phonon interactions.[1] In this work, we employ resonance Raman spectroscopy to investigate epitaxial graphene on SiC(0001) achieved by intercalation with different species, including hydrogen (H), indium (In), and tin (Sn) into the zeroth layer of graphene (ZLG), as well as the as-grown monolayer graphene (MLG) system.

Epitaxial graphene on SiC offers a scalable and stable platform, while intercalation enables precise control over the graphene-substrate interaction, allowing both the decoupling of graphene into quasi-free-standing layers and the formation of novel interfacial phases beneath graphene.[2,3] Through systematic Raman analysis, we examine the evolution of strain and charge doping across these systems, revealing distinct signatures associated with each intercalant and interface configuration. In particular, we demonstrate the formation of a metallic triangular Sn(1×1) phase beneath graphene, which, together with an on-surface plasmonic Sn nanoantenna, gives rise to enhanced light-matter interaction via gap-mode plasmonic effects.[4] This results in more than two orders of magnitude enhancement of the graphene Raman response, accompanied by modified selection rules and intrinsic electron-phonon coupling.[5] Furthermore, we investigate the thermomechanical behavior of these systems and show that the properties of the graphene layer are strongly governed by the nature of the interfacial coupling.

Our results establish Raman spectroscopy as a versatile tool to characterize intercalated epitaxial graphene systems and provide insight into the interplay between graphene and engineered buried interfaces, with implications for tunable electronic, plasmonic, and optoelectronic applications.

[1] A.C. Ferrari et al., Nature Nanotechnology 8 (2013) 235-246
[2] K. V. Emtsev et al., Nature Materials 8 (2009) 203-207
[3] Z. Mamiyev et.al., Carbon 234 (2025) 120002
[4] Z. Mamiyev et.al., arXiv:2602.16451 (2026)
[5] Z. Mamiyev et.al., Advanced Optical Materials 13 (2025) e00979

Strain introduction into graphene via Pd intercalation

Ayato Yamane[1], Tomo-o Terasawa[2], Takahiro Ito[3], and Wataru Norimatsu[1]

[1] Faculty of Science and Engineering, Waseda University, 3-4-1, Okubo, Shinjuku-ku, Tokyo 169-8555, Japan

[2] Advanced Science Research Center, Japan Atomic Energy Agency, 2-4 Shirakata, Tokai, Ibaraki 319-1195, Japan

[3] Nagoya University Synchrotron Radiation Research Center (NUSR), Nagoya University, Furo-cho, Chikusa, Nagoya 464-8603, Japan

e-mail: ayt1129@akane.waseda.jp

Graphene, a one-atom-thin carbon material, can be grown by thermal decomposition of SiC. When the SiC single-crystal substrate is heated, the buffer layer is formed prior to graphene growth. Carbon atoms in this buffer layer have covalent bonds with the silicon atoms in SiC. Foreign elements can be intercalated into the interface between the buffer layer and SiC, which transforms the buffer layer into quasi-free-standing monolayer graphene. In this study, we attempted Pd intercalation. Pd intercalation is expected to induce strain in graphene due to its strong interaction with carbon. In this study, we investigated the spatially distributed strain in graphene by Pd intercalation.

The buffer layer samples were prepared by heating the SiC single-crystal substrate at 1580°C for 3 min. Pd was deposited by a molecular beam epitaxy technique at room temperature on a buffer layer, and then the substrate was heated to 400-900°C for intercalation. The samples were characterized by atomic force microscopy (AFM), Raman spectroscopy, and angle-resolved photoemission spectroscopy (ARPES).

From the Raman spectra before and after the intercalation treatment, we found that the buffer layer was converted into graphene by Pd intercalation. Figure 1 shows the Raman spectra of a sample in which Pd intercalation was attempted by annealing at 900 °C after depositing Pd with the thickness of 1 nm. Peak positions of the G and 2D band in the spectra exhibited a significant redshift as shown by a red line. Figure 2 shows the relation between the G and 2D band peak positions and strain, indicating that the Pd-intercalated graphene was subjected to tensile strain of approximately 0.8–1.2%. In the AFM and Raman mapping images, intercalated and non-intercalated regions were alternately arranged in a striped pattern.

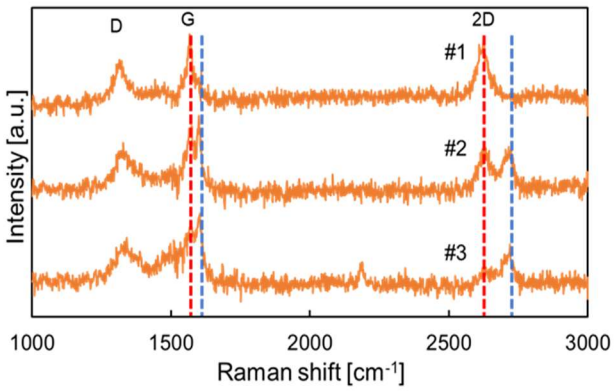

Fig. 1 Raman spectra of a sample after Pd-treatment measured at three different points (#1-#3).

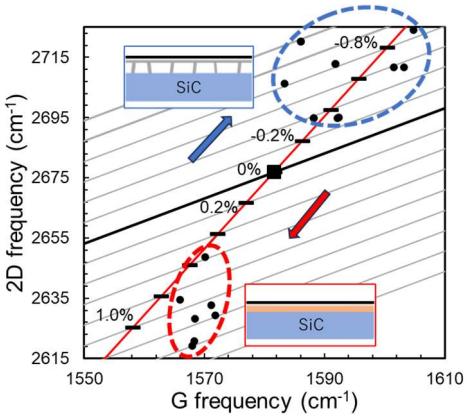

Fig. 2 Relation between G and 2D band peaks and strain of Pd-intercalated (red) and epitaxial graphene on SiC (blue).

Exploring the electronic structure of topology-protected surface states by advanced angle-resolved photoemission

F. Göhler[1], A. C. Mathisen[1], S. S. Brinkman[1], X. L. Tan[1], Ø. Finnseth[2], K. Mæland[3], C.-H. Min[1], J. Buck[4,5], K. Rossnagel[4,5], G. Shipunov[6], A. Isaeva[6], J. I. Facio[7], H. Bentmann[1]

[1] Center for Quantum Spintronics, Department of Physics, NTNU, Trondheim, Norway
[2] Department of Materials Science and Engineering, NTNU, Trondheim, Norway
[3] Institute for Theoretical Physics and Astrophysics, University of Würzburg, Germany
[4] Institute of Experimental and Applied Physics, Kiel University, Germany
[5] Ruprecht Haensel Laboratory, DESY, Hamburg, Germany
[6] Institute of Physics, University of Amsterdam, The Netherlands
[7] Instituto Balseiro, National University of Cuyo, Argentina

Novel quantum materials, characterized by different forms of strongly correlated electrons in solids, may pave the way towards next generation applications such as dissipationless quantum transport or quantum computing. A key feature of some of these materials are non-spin degenerate electronic bands, such as in the recently discovered altermagnets [1]. For example, topological insulators and topological Weyl semimetals host topology-protected, spin-polarized surface states. A full experimental characterization of these states thus requires measurements of the electron spin over wide regions in momentum space.

In the first part of this talk, I will present first results from our recently established spin-resolved momentum microscope setup at NTNU Trondheim (Fig. 1(a)), which gives the photoelectron momentum distribution over the full half-sphere above the sample surface. When combined with a 2D imaging spin filter, this allows parallel measurement of the in-plane spin polarization for full constant energy cuts $E(k_x, k_y)$ (Fig. 1(b)). The second part of the talk will focus on our results on the layered topological Weyl semimetal $PtBi_2$. In this material, bulk Weyl nodes – the emergence of which is commonly attributed to accidental crossings between non-degenerate valence and conduction bands – are connected on the surface by Fermi arcs. Recent reports indicate that these Fermi arcs host unconventional superconductivity at elevated temperatures [2, 3, 4]. We have performed a comprehensive analysis of the two inequivalent surface terminations of $PtBi_2$ by means of spin- and angle-resolved VUV photoemission at the BLOCH Beamline of the MAX IV Synchrotron in Lund, Sweden, complemented by bulk-sensitive soft-X-ray ARPES experiments at the ASPHERE III end station at the variable polarization XUV beamline P04 of the PETRA III storage ring at DESY (Fig. 1(c, d)).

References:
[1] L. Šmejkal et al., Phys. Rev. X 12 (2022) 031042.
[2] A. Kuibarov et al., Nature 626 (2024) 294.
[3] S. Changdar et al., Nature 647 (2025) 613.
[4] K. Mæland et al., Phys. Rev. B 112 (2025) 104507.

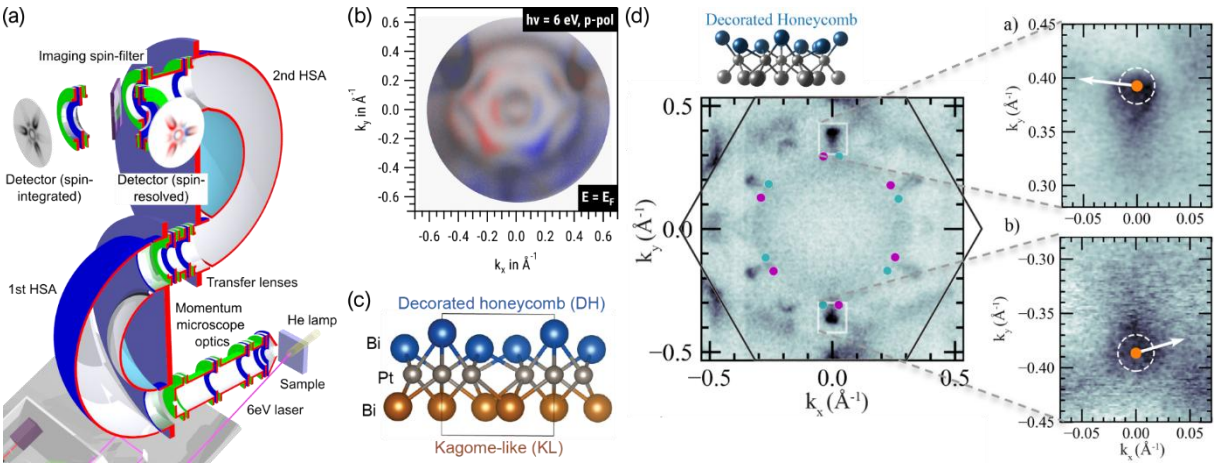

Fig. 1: (a) Sketch of the spin-resolved momentum microscope setup at NTNU Trondheim. (b) Spin-resolved momentum map of a $BiCu_2$ surface alloy. (c) Layer structure of $PtBi_2$. (d) Spin-integrated momentum map of DH-terminated $PtBi_2$ (insets: in-plane spin orientation of the Fermi arcs).

Phase-controlled two-dimensional Ag intercalation at the graphene/SiC interface

Sawani Datta[1], Boyang Zheng[2], Arpit Jain[2], Kathrin Küster[1],
Joshua A. Robinson[2], Vincent H. Crespi[2], and Ulrich Starke[1]

[1] Max-Planck-Institut für Festkörperforschung, Heisenbergstrase 1, 70569 Stuttgart, Germany
[2] The Pennsylvania State University, University Park, PA 16802, USA

Intercalation at the graphene/SiC interface offers a controlled route to stabilize atomically thin phases while maintaining a clean, encapsulated environment: the SiC substrate provides structural templating, and the graphene overlayer acts as an inert cap [1]. In the intercalation method, the defect density of the initial substrate plays an important role. As recently shown using the confinement heteroepitaxy method, Ag intercalation at the graphene/SiC interface can yield two distinct phases: the $Ag_{(1)}$ phase, which adopts a triangular lattice in registry with the SiC substrate, and the denser $Ag_{(2)}$ phase, which exhibits a more complex epitaxial relationship with the substrate [2]. Under ultra-high-vacuum (UHV) conditions, conventional intercalation starting from the zero-layer graphene (ZLG) substrate has been reported to produce $Ag_{(1)}$ [3, 4]. In this study, we demonstrate an in situ UHV preparation route that stabilizes the dense $Ag_{(2)}$ phase at the graphene/SiC interface and compare the structural and electronic properties of $Ag_{(1)}$ and $Ag_{(2)}$ using low-energy electron diffraction (LEED) and angle-resolved photoemission spectroscopy (ARPES).

In UHV, $Ag_{(2)}$ is prepared using the conventional method (deposition of Ag and annealing), starting from a Pb intercalated–quasi-free-standing monolayer graphene (QFMLG) substrate [5, 6, 7], taking advantage of the fact that Pb intercalation can introduce more vacancy and boundary defects. LEED identifies the structural fingerprints of $Ag_{(2)}$: the Ag lattice is rotated by 30° relative to SiC unitcell and forms superstructures with the adjacent layers, including an approximately (6×6) periodicity with respect to graphene and a (5×5) periodicity with respect to SiC (Fig. 1(a)).

High-resolution ARPES shows that $Ag_{(2)}$ is semiconducting and exhibits a more complex valence-band structure than $Ag_{(1)}$, with multiple branches near the $\overline{K}_{SiC}$-point (Fig. 1(b)) and reduced hexagonal warping in constant-energy contours (CECs) (Fig. 1(c)), indicating a weaker imprint of the SiC periodic potential. Density-functional-theory (DFT) calculations based on a structural model for $Ag_{(2)}$ reproduce the main experimental dispersions and show that the redistribution of the valence-band partial charge density plays an important role in the band dispersion of the second Ag phase.

Finally, we show that the intercalated Ag phase tunes the electronic response of the overlying quasi-free-standing graphene. Compared with $Ag_{(1)}$-QFMLG, $Ag_{(2)}$-QFMLG exhibits stronger n-type doping and enhanced electron–plasmon coupling in the graphene layer, consistent with reduced effective screening at the interface. We also observe Dirac-cone replica pockets that directly reflect the formation of the $Ag_{(2)}$/graphene supercell. These results demonstrate defect-enabled access to different confined-2D-Ag phases with distinct electronic structure and phase-dependent proximity coupling to graphene.

References:
[1] C. Riedl et al., Phys. Rev. Lett. 103 (2009) 246804.
[2] A. Jain et al., arXiv:2511.07151.
[3] P. Rosenzweig and U. Starke, Phys. Rev. B 101 (2020) 201407.
[4] P. Rosenzweig et al., Phys. Rev. B 105 (2022) 235428.
[5] B. Matta et al., Phys. Rev. Res. 4 (2022) 023250.
[6] P. Schädlich et al., Adv. Mater. Interfaces 10 (2023) 2300471.
[7] B. Matta et al., Phys. Rev. B 111 (2025) 155435.

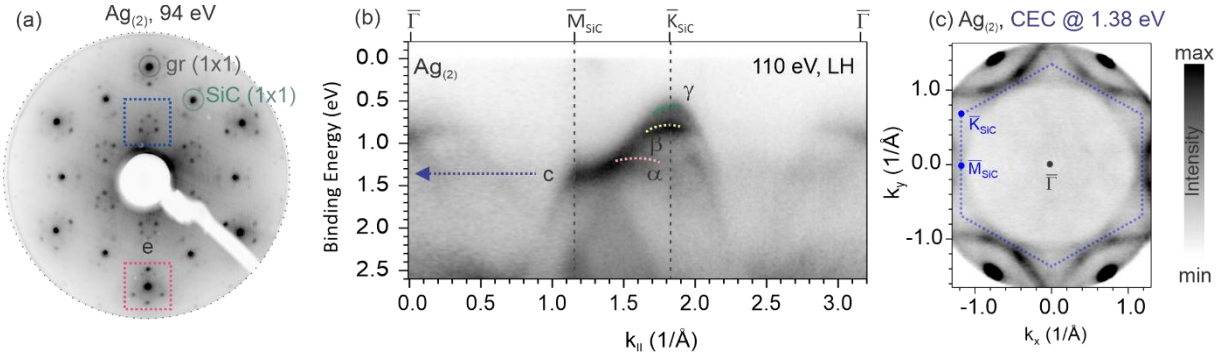

Fig. 1: (a) LEED of $Ag_{(2)}$-QFMLG shows the superstructure spots inside the pink and blue square, (b) ARPES data of $Ag_{(2)}$-QFMLG along $\overline{\Gamma M_{SiC}} \overline{K_{SiC}} \overline{\Gamma}$ direction , (c) CEC of $Ag_{(2)}$ at 1.38 eV binding energy.

Calcium intercalation of epitaxial graphene

L. Mahdi Syed[1], N. Tilgner[1], P. Schädlich[1,2], Th. Seyller[1,2]

[1] Institut für Physik, Technische Universität Chemnitz
[2] Research Center for Materials, Architecture and Integration of Nanomembranes (MAIN), Technische Universität Chemnitz

Realizing proximity-induced correlation effects, such as superconductivity, in graphene is a major challenge in the field of research on two-dimensional (2D) materials. Among the graphite intercalation compounds (GICs), the Ca-GICs exhibit the highest critical temperature with T_c=11.5 K, where the electron doping from the Ca atoms may be a crucial factor.

Hence, expanding this superconducting phase into the 2D limit of epitaxial monolayer graphene (EMLG) on SiC(0001) requires precise control over the arrangement of the intercalated Ca atoms. However, several structural models have been proposed for Ca-intercalated EMLG, and in particular, the vertical position - i.e., the gallery - in which Ca resides remains unresolved [1,2].

Here, we investigate Ca-intercalation into EMLG and zero-layer graphene (ZLG) grown by polymer-assisted sublimation growth. Using x-ray and angle-resolved photoemission spectroscopy, we monitor the intercalation process and quantify the doping level. Our results indicate the saturation of the SiC interface by Ca. We observe the low-energy bands of the resulting intercalated bilayer graphene (see Figure 1, left), and more interestingly regarding the superconducting state, a highly doped graphene π-band (Figure 1, right), which may point towards the presence of calcium in the upper gallery. In the case of ZLG, Ca intercalation leads to decoupling from the substrate and, consequently, to the formation of a graphene π band. We also observe strong electron doping for this band, comparable to the result obtained for the EMLG system. Based on these results, this contribution will discuss possible scenarios for the structural model of this system.

References:
[1] S. Ichinokura et al., ACS Nano 10 (2016) 2761.
[2] J. C. Kotsakidis et al., Chem. Mater. 32 (2020) 6464.

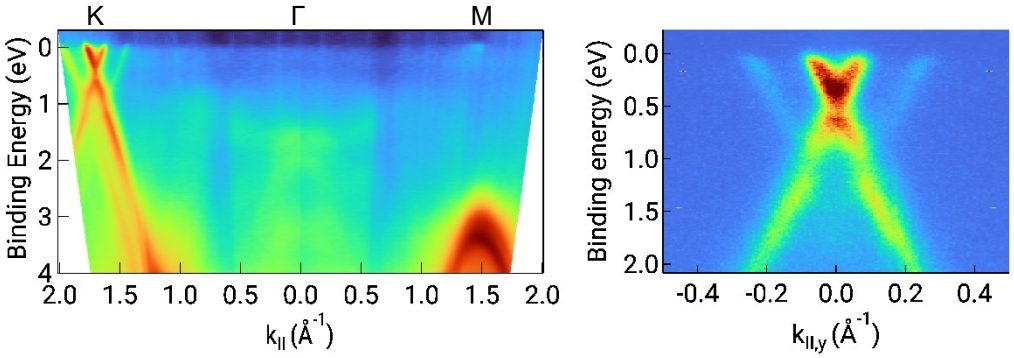

Fig. 1: ARPES map of Ca-intercalated EMLG along the ΓK and ΓM high symmetry directions of graphene (left) and in the vicinity of the graphene K point (right).